



**Sudan University of Science
and Technology
College of Graduate Studies**



**Verification of Statistical Physics and Thermodynamics Properties
of (Al, Fe, and Cu) Irradiated by Gamma Rays for Non-Equilibrium
States**

التحقق من خصائص الفيزياء الإحصائية والديناميكا الحرارية لـ (الألمونيوم والحديد والنحاس) مشععة بواسطة أشعة جاما في حالة عدم الإتزان

**A thesis Submitted for the Fulfillment of the degree of Doctor of
Philosophy in Physics**

By:

Sufyan Babiker Elhag Abdalla

Supervisor: Prof. Mubarak Dirar Abdallah

Co-Supervisor: Dr. Hoda Mohamed Kamal

November 2021



**Sudan University of Science
and Technology
College of Graduate Studies**



**Verification of Statistical Physics and Thermodynamics Properties
of (Al, Fe, and Cu) Irradiated by Gamma Rays for Non-Equilibrium
States**

التحقق من خصائص الفيزياء الإحصائية والديناميكا الحرارية لـ (الألمونيوم، الحديد، والنحاس) مشععة بواسطة أشعة جاما في حالة عدم الإتزان

**A thesis Submitted for the Fulfillment of the degree of Doctor of
Philosophy in Physics**

By:

Sufyan Babiker Elhag Abdalla

Supervisor: Prof. Mubarak Dirar Abdallah

Co-Supervisor: Dr. Hoda Mohamed Kamal

November 2021

Ayah

الآية

(أنزل من السماء ماء فسالت أودية بقدرها فاحتمل السيل زبدا رابيا وما
يوقرون عليه في النار ابتغاء حلية أو متاع زبد مثله كذلك يضرب الله الحق
والباطل فاما الزبد فيذهب جفا، وأما ما ينفع الناس فيمكث في الأرض
كذلك يضرب الله الأمثال)

قرآن كريم- سورة الرعد - الآية (١٧)

(He sends down water from the skies, and the channels flow, each according to its measure: But the torrent bears away to foam that mounts up to the surface. Even so, from that (ore) which they heat in the fire, to make ornaments or utensils therewith, there is a scum likewise. Thus doth Allah (by parables) show forth Truth and Vanity. For the scum disappears like froth cast out; while that which is for the good of mankind remains on the earth. Thus doth Allah set forth parables).

Holly Quraan – Surat Ar-Ra'd – Ayah(17)

DEDICATION

I dedicate my thesis work to my family and many friends. A special feeling of gratitude to my loving parents, Babiker and Zeinabia whose words of encouragement and push for tenacity ring in my ears.

I dedicate to my sisters and brothers have never left my side and are very special. I also dedicate this dissertation to my wife, who has supported me throughout the process.

I also want to remember many beloved people who have meant and continue to mean so much to me.

Finally, I dedicate this work to fellow professionals holding embroidery and burning to show the way for generations

ACKNOWLEDGEMENTS

First and foremost, praises and thanks to the Allah, the Almighty, my creator, my strong pillar, my source of inspiration, wisdom, knowledge and understanding. He has been the source of my strength throughout this program and on His wings only have I soared, throughout my research work to complete the research successfully.

I would like to express my deep and sincere gratitude to my research supervisor, Professor Mubarak Dirar Abdallah and Dr. Hoda Mohamed Kamal for giving me the opportunity to do research and providing invaluable guidance throughout this research. Their dynamism, vision, sincerity and motivation have deeply inspired me. They have taught me the methodology to carry out the research and to present the research works as clearly as possible. It was a great privilege and honor to work and study under their guidance. I am extremely grateful for what they have offered me.

I am extremely grateful to my parents for their love, prayers, caring and sacrifices for educating and preparing me for my future. Also I express my thanks to my sister Sahar for her support.

I am extending my thanks to the Yarmouk Industrial Complex especially to Eng. Hashim Adam, and Eng. Hamad Jumaa for their support to do this work.

I would like to say thanks to my friends Dr. Ahamed Mohamed Salih, and Dr. Farah Abuzaid Saboun for their standing beside me during the experimental work.

Finally, my thanks go to all the people who have supported me to complete the research work directly or indirectly.

Sufyan Babiker Elhag

ABSTRACT

The aim of this work is to study the behavior of attenuation coefficient for gamma rays under thermal non-equilibrium statistical conditions. To do this, 18 samples from Al, Fe, and Cu were prepared. Six samples from each material were prepared in the form of pellets. First, samples from Al, Fe, and Cu left without being exposed to heat, and after that the samples are heated to (24, 40, 50, 60, and 70)⁰C, then exposed to gamma radiation. The thickness of each mineral were changed to be (5, 10, 15, 20, 25, and 30) mm for Al, (4, 8, 12, 16, 20, and 24) mm for Fe, and (3, 6, 9, 12, 15, and 18) mm for Cu, and they also exposed to gamma rays. The transmitted beam intensity was measured using GM counter. To see the effect of heating in evaporating gases and light elements FTIR spectrometer was used.

Copper and Iron samples analyzed by X-Ray Fluorescence (XRF) and we found that the sample of iron contains (99% of Fe and 1% Ti), and the sample of Copper contains (61% Cu, 31% Zn, 5%Pb, and 3% Fe)

The results obtained shows that the transmitted intensity in general decreases upon increasing both temperature and thickness. These two effects are related to thermal collision and thermal expansion which changes thickness. The temperature increase and heat flow are related to non-thermal equilibrium and entropy increase. The non-thermal equilibrium is described by non-equilibrium statistical laws. The empirical relations of these effects can be easily described using non-equilibrium statistical laws derived from plasma and quantum laws for resistive media. These laws describe non-thermal equilibrium statistical states and are related to entropy and thermal internal heat energy. The attenuation coefficient increases first with temperature then shows gentle decrease. The initial increase may result from the fact that initial heating evaporate light elements, which causes the density to increase. This evaporation results from thermal agitation and the heat energy thermal mass transfer. Further heating cause samples to expand, thus increasing its volume which decreases the density. The expansion results from increase of thermal vibration rate which increases amplitude. Thus the attenuation coefficient decreases. The increase of thickness decreases attenuation coefficient which may be related to the re emission process, in which atomic nuclei emit rays. Thus the decrease of attenuation coefficient can be described by non-equilibrium statistical laws.

مستخلص

يهدف هذا البحث لدراسة سلوك معامل التوهين لأشعة جاما تحت تأثير ظروف عدم التوازن الحراري الإحصائي. للقيام بذلك حضرت 18 عينة من كل من الألمونيوم (Al) و الحديد (Fe) والنحاس (Cu). أعدت ست عينات من كل مادة في شكل حبيبات. أولاً، تُركت عينات من العناصر الثلاثة دون تعريضها للحرارة، وبعد ذلك سُخنت العينات إلى درجات الحرارة (24، 40، 50، 60، 70) درجة مئوية، ثم تم تعريضها لإشعاع جاما. تم تغيير سمك كل معدن ليكون (5، 10، 15، 20، 25، و 30) مم للألمونيوم ، (4، 8، 12، 16، 20 و 24) مم للحديد و (3 و 6 و 9 و 12 و 15 و 18) ملم بالنسبة إلى النحاس ، وتم تعريضها لأشعة جاما. تم قياس شدة الإشعاع النافذ من كل عينة باستخدام عداد جايجر - مولر . ولمعرفة أثر التسخين على الغازات المتبخرة وفي العناصر الضوئية، تمّ استخدام مقياس طيف FTIR.

عينات النحاس والحديد التي تم تحليلها بواسطة الأشعة السينية الفلورية (XRF) ووجدنا أن عينة الحديد تحتوي على (99% من الحديد Fe و 1% من التيتانيوم Ti) ، وعينة النحاس تحتوي على (61% من النحاس Cu و 31% من الزنك Zn و 5% من الرصاص Pb و 3% من الحديد Fe). وتبين النتائج التي تم الحصول عليها أن الكثافة المنتقلة تنخفض بصفة عامة عند زيادة درجة الحرارة وسماكتها على حد سواء. ويتعلق هذان المؤثران بالتصادم الحراري والتمدد الحراري اللذان يغيران في السُمك. ويرتبط ارتفاع درجة الحرارة وتدفق الحرارة بالتوازن غير الحراري وزيادة الإنتروبيا. ويرد وصف التوازن غير الحراري في القوانين الإحصائية غير المتعلقة بالتوازن. ويمكن وصف العلاقات التجريبية لهذه الآثار بسهولة باستخدام قوانين إحصائية غير متوازنة مستمدة من قوانين البلازما والكم من أجل الوسائط الدافعة. وتصف هذه القوانين الحالة الإحصائية للتوازن غير الحراري ، وهي تتعلق بالإنتروبيا وطاقة الحرارة الداخلية الحرارية. ويزداد معامل التخفيف أولاً مع انخفاض درجة الحرارة ثم يظهر انخفاض طفيف. وقد تنجم الزيادة الأولية عن أن التسخين الأولي يتبخر العناصر الخفيفة ، مما يتسبب في زيادة الكثافة. وينتج هذا التبخر عن الإثارة الحرارية ونقل الكتلة الحرارية للطاقة الحرارية. ويؤدي المزيد من التسخين إلى توسيع العينات ، مما يزيد من حجمها مما يقلل من الكثافة. وينتج التمدد عن زيادة معدل الاهتزاز الحراري الذي يزيد من الاتساع. وهكذا ينخفض معامل التخفيف. وتنقص الزيادة في السماكة معامل التوهين الذي قد يكون مرتبطاً بعملية إعادة الانبعاث ، التي تصدر فيها النواة الذرية أشعة. وبالتالي يمكن وصف انخفاض معامل التوهين بقوانين إحصائية غير متزنة. ويزداد معامل التوهين أولاً مع انخفاض درجة الحرارة ثم يظهر انخفاض طفيف. وقد تنجم الزيادة الأولية عن أن التسخين الأولي يبخر العناصر الخفيفة ، مما يتسبب في زيادة الكثافة. وينتج هذا التبخر عن الإثارة الحرارية ونقل الكتلة الحرارية للطاقة الحرارية. ويؤدي المزيد من التسخين إلى تمدد العينات ، مما يزيد من حجمها ويقلل من الكثافة. وينتج التمدد عن زيادة معدل الاهتزاز الحراري الذي يزيد من الاتساع. وهكذا ينخفض معامل التوهين. وتنقص الزيادة في السماكة معامل التوهين الذي قد يكون مرتبطاً بعملية إعادة الانبعاث ، التي تصدر فيها النواة الذرية أشعة. وبالتالي يمكن وصف انخفاض معامل التوهين بقوانين إحصائية غير متزنة.

Contents

No.	Descriptions	Page No.
1	Ayah	i
2	Dedication	ii
3	Acknowledgement	iii
4	Abstract in English	iv
5	Abstract in Arabic	v
6	Contents	vi
7	List of figures	ix
8	List of tables	xi
Chapter One: Introduction		
9	1.1 Introduction	1
10	1.2 Research problem	2
11	1.3 Research Objective	2
12	1.4 Material and Methods	2
13	1.5 Thesis layout	3
Chapter Two: Theoretical Background		
14	2.1 Introduction	4
15	2.2 Concept of Heat and Temperature	4
16	2.2.1 Specific Heat	5
17	2.2.2 Heat Capacity	6
18	2.2.3 Thermodynamics	6
19	2.2.4 Systems and surroundings	7
20	2.2.5 Internal Energy	7
21	2.2.6 The Zeroth law	7
22	2.2.7 The first law of thermodynamics	7
23	2.3 Second law of thermodynamics	8
24	2.4 Entropy	9
25	2.5 Heat Transfer	12
26	2.5.1 Conduction	13
27	2.5.2 Convection	14
28	2.5.3 Radiation	15
29	2.6 Types of radiation	17
30	2.6.1 Non-ionizing radiation	17
31	2.6.2 Ionizing radiation	17
32	2.7 Gamma rays	17
33	2.7.1 Origin of gamma decay	18
34	2.7.2 Gamma photons energy	19
35	2.7.3 The absorption of gamma rays with matter	20
36	2.7.3.1 Linear attenuation coefficient	20
37	2.7.3.2 Half value layer (HVL)	22
38	2.7.3.3 Cross-section	22

39	2.7.4 Interaction of radiations with matter	22
40	2.7.4.1 Photoelectric effect	23
41	2.7.4.2 Compton scattering	24
42	2.7.4.3 Pair production	25
43	2.7.5 Gamma radiation shielding	27
44	2.7.6 Gamma rays shielding design	28
45	2.7.7 Gamma ray detection	29
46	2.7.7.1 Gas-filled Detectors	29
47	2.7.7.2 Scintillators Detectors	31
48	2.7.7.3 Solid state Detectors	32
49	2.8 Geiger-Muller Tube (GM Tube)	33
Chapter Three: Literature Review		
50	3.1 Introduction	35
51	3.2 Explanation of Intensity Spectral change of Bhutan, Carbon dioxide, Carbon Monoxide, Oxygen, Nitrogen Gases on the basic of Non Equilibrium	35
52	3.3 Interpretation of the Effect of Temperature on the Change of Spectra of Atmospheric Gases on the Basis of Modified Quantum Statistical Equations	43
53	3.4 Quantum Heat Flow Model for Heat Flow in Some Nanotubes	51
45	3.5 Thermal conductivity coefficients on the base of phonon model and Einstein energy relation for nanomaterial	51
55	3.6 The effect of annealing temperature, doping carbon nanotubes with TiO ₂ , CuO, ZnO and MgO on its conductivity and electrical primitively	51
56	3.7 The Effect of Annealing Temperature Change on Carbon Nano Tube Absorption and Refractive Index When Doped With TiOR ₂ R, CuO, ZnO and MgO	52
57	3.8 Effects of laser glazing on CMAS corrosion behavior of Y ₂ O ₃ stabilized ZrO ₂ thermal barrier coatings	52
58	3.9 The Concept of force for thermodynamic frictional system	53
59	3.10 The Concept of Energy for Thermodynamics Friction System	53
60	3.11 Internal heat generation effect on transient natural convection in a Nano fluid-saturated local thermal non-equilibrium porous inclined cavity	53
61	3.12 X-ray diffraction and thermodynamics kinetics of SiB 6 under gamma irradiation dose	54
62	3.13 Thermodynamics kinetics of boron carbide under gamma irradiation dose	55
63	3.14 Gamma ray shielding by a new combination of aluminum, iron, copper and lead using MCNP5	56

64	3.15 Thermodynamics of an austenitic stainless steel (AISI-348) under in situ TEM heavy ion irradiation	57
65	3.16 Development of Gamma-based Nondestructive Testing System for Thickness Measurement	57
66	3.17 DEVELOPMENT OF GAMMA-BASED NONDESTRUCTIVE TESTING SYSTEM FOR MATERIAL DISCRIMINATION:	58
	Chapter Four: Materials and Methods	58
67	4.1 Introduction	58
68	4.2 Apparatus	58
69	4.3 Samples preparing	58
70	4.4 Method	61
	Chapter Five: Results, Discussion and Conclusion	64
71	5.1 Introduction	64
72	5.2 Results	64
73	5.3 Discussion	79
74	5.3 Conclusion	84
75	References	85

LIST OF FIGURS

Figure	Descriptions	P.No.
Figure (2-1)	system, boundary, and surrounding	7
Figure (2-2)	Spectrum of electromagnetic radiation	16
Figure (2-3)	Gamma ray absorption in matter	21
Figure (2- 4)	Schematic diagram of the experimental setup for photoelectric effect	23
Figure (2-5)	Compton Scattering	24
Figure (2-6)	Pair production	26
Figure (2- 7)	The linear coefficient as a function of photon energy	27
Figure (2-8)	Schematic diagram of Gas-filled detector	30
Figure (2-9)	Scintillation Detector	31
Figure (2-10)	Geiger-Muller Tube	33
Fig (3-2-1-1)	Relation between Intensity and temperature	36
Fig(3-2-2-1)	relationship between intensity and temperature	37
Fig(3-2-3-1)	relationship between intensity and temperature	38
Fig (3-2-4-1)	relationship between intensity and temperature	39
Fig(3-2-5-1)	relationship between intensity and temperature	40
Fig (3-3-1)	Relation between Intensity and temperature	44
Fig (3-3-2)	Relation between line width and temperature	44
Fig (3-4-1)	Relation between Intensity and temperature	45
Fig (3-4-2)	Relation between line width and temperature	45
Fig (3-5-1)	Relation between Intensity and temperature	46
Fig (3-5-2)	Relation between line width and temperature	46
Fig (3-6-1)	Relation between Intensity and temperature	47
Fig (3-6-2)	Relation between line width and temperature	47
Figure (4-1-1)	Aluminum shavings	60
Figure (4-1-2)	Iron shavings	60
Figure (4-1-3)	Copper shavings	60
Figure (4-2)	Piston	61
Figure (4-3-1)	Aluminum + Gum-Arabic After compressing in the piston	61
Figure (4-3-2)	Iron + Gum-Arabic After compressing in the piston	61
Figure (4-3-3)	Copper + Gum-Arabic After compressing in the piston	62
Figure (4-4-1)	Experiment	63
Figure (4-4-2)	Experiment	63
Figure (5-1-1)	Relation between the count rate and temperature in different thicknesses of Aluminum	66
Figure (5-1-2)	Relation between the count rate and temperature in different thicknesses of Iron	66
Figure (5-1-3)	Relation between The count rate and temperature in different thicknesses of Copper	67
Figure (5-2-1)	Relation between the count rate and thickness in different temperatures of Aluminum	67

Figure (5-2-2)	Relation between The count rate and thickness in different temperatures of Iron	66
Figure (5-2-3)	Relation between the count rate and thickness in different temperatures of Copper	67
Figure (5-3-1)	Comparison Between The Count rate of Aluminum, Iron, and Copper at Room temperature (24⁰C)	67
Figure (5-3-2)	Comparison Between The Count rate of Aluminum, Iron, and Copper at temperature (70⁰C)	68
Figure (5-4-1)	Relation between the attenuation coefficient and thickness of Aluminum in different values of temperature.	70
Figure (5-4-2)	Relation between attenuation coefficient and thickness of Iron at different temperatures.	70
Figure (5-4-3)	Relation between attenuation coefficient and thickness of Copper at different temperatures.	71
Figure (5-5-1)	Relation between attenuation coefficient and temperature in different thicknesses of Aluminum	71
Figure (5-5-2)	Relation between the attenuation coefficient and temperature of Aluminum in different values of thicknesses.	72
Figure (5-5-3)	Relation between the attenuation coefficient and temperature of Aluminum in different values of thicknesses.	72
Figure (5-6-1)	Comparison between the attenuation coefficients of Aluminum, Iron, and Copper at temperature 24⁰C	73
Figure (5-6-2)	Comparison between the attenuation coefficients of Aluminum, Iron, and Copper at temperature 70⁰C	73
Figure (5-7-1)	relation between HVL and temperature at different thicknesses of Aluminum	74
Figure (5-7-2)	relation between HVL and temperature at different thicknesses of Aluminum	74
Figure (5-7-3)	relation between HVL and temperature at different thicknesses of Copper	75
Figure (5-8-1)	relation between HVL and thickness at different temperatures of Aluminum	75
Figure (5-8-2)	relation between HVL and thickness at different temperatures of Iron	76
Figure (5-8-3)	relation between HVL and thickness at different temperatures of Copper	76
Figure (5-9-1)	Comparison between the HVL and thickness of Aluminum, Iron, and Copper at temperature 24⁰C	77
Figure (5-9-2)	Comparison between the HVL and thickness of Aluminum, Iron, and Copper at temperature 70⁰C	77
Figure (5-10-1)	FTIR for Aluminum + Gum Before heating	79
Figure (5-10-2)	FTIR for Aluminum + Gum After heating	79
Figure (5-11-1)	FTIR for Iron + Gum Before heating	80
Figure (5-11-2)	FTIR for Iron + Gum After heating	81
Figure (5-12-1)	FTIR for Copper + Gum Before heating	82
Figure (5-12-2)	FTIR for Copper + Gum After heating	82

LIST OF TABLES

Table	Descriptions	P.No.
Table (3-2-1)	spectrum of Bhutan at different temperatures	35
Table (3-2-2)	spectrum of Carbon dioxide (CO ₂) at different temperatures	36
Table (3-2-3)	spectrum of Carbon Monoxide (CO) at different temperatures	37
Table (3-2-4)	spectrum of Oxygen (O ₂) at different temperatures	38
Table (3-2-5)	spectrum of Nitrogen (N ₂) at different temperatures	39
Table (3-2-1)	spectrum of Bhutan (C ₄ H ₁₀) at different temperatures	43
Table (3-2-2)	spectrum of Neon (Ne) at different temperatures	45
Table (3-2-3)	spectrum of Fluorine (F ₂) at different temperatures	45
Table (3-2-4)	spectrum of Chlorine (Cl ₂) at different temperatures	46
Table (5-1-1)	The count rate of Gamma –ray penetrating Aluminum samples at room temperature and after heating	63
Table (5-1-2)	The count rate of Gamma –ray penetrating Iron samples at room temperature and after heating	63
Table (5-1-3)	The count rate of Gamma –ray penetrating Copper samples at room temperature and after heating	64
Table (5-2-1)	Attenuation coefficient and HVL for Aluminum samples	68
Table (5-2-2)	Attenuation coefficient and HVL for Iron samples	69
Table (5-2-3)	Attenuation coefficient and HVL for Copper samples	69

Chapter One

Introduction

1.1 Introduction:

Thermodynamics is one of the most important sciences in our life, it also has applications and uses in wide fields [1,2]. Thermodynamics was discovered in the eighteenth century, but its applications are still renewed up-to-date [3]. This science is found to explain how heat converts to power [4].

Thermodynamics began with concept equilibrium and later the concept of non-equilibrium came up [2]. The equilibrium thermodynamics of the system comprises the thermal equilibrium and other forms of types of equilibrium rely on the type of thermodynamic system being studied, and it can be described by the zeroth law [5, 6]. Systems that are permanently stable are rare, thus almost all systems found in nature are not in thermodynamic equilibrium [7]. Non-equilibrium thermodynamics is a study of systems that are not in equilibrium thermodynamics. The field non-equilibrium thermodynamics give us a general idea for the macroscopic description of the irreversible process [8].

Non-equilibrium thermodynamics describes transport processes in systems that are not in global equilibrium [9]. Actually, almost all natural phenomena are in a non-equilibrium state [10].

In the recent century, the uses of gamma-rays have been increasing in different fields of science. Therefore, we need more information about electromagnetic rays and their interactions with matter to shield these radiations.

Many types of researches were made to understand the nature of heat energy, but few deals with its effect on the spectrum of absorption of radiation (e.g. gamma). In this work, Aluminum, Iron, and Copper samples were used to see how they absorb gamma rays when we raise the temperature. In the case of non-equilibrium thermodynamic, gamma rays interact with the matter with three processes: photoelectric effect, pair production, and Compton scattering [11]. When gamma rays pass through matter, their intensity will decrease, this decrease depends on the type of material and its thickness [12]. Using certain materials for reducing the intensity of gamma radiation is known as shielding [13].

In this study, Aluminum, Iron, and Copper were used to determine how to absorb gamma rays. When we raise its temperature, in the case of non-equilibrium thermodynamics. Gamma rays interact with the matter with three processes: photoelectric effect, pair production, and Compton scattering [11]. When gamma rays pass through matter, their intensity will decrease, this decrease depends on the type of material and its thickness [12].

Scientists are always looking for materials that can be used as shields from radiation. Copper and Iron are one of the oldest minerals discovered by humans [14].

1.2 Research problem:

Despite the remarkable success of thermodynamics in explaining the behavior of many physical systems, unfortunately it suffers from some setbacks for instance non equilibrium in irradiated materials cannot be explained by thermodynamics.

1.3. Research Objective:

This work is directed to verify some new statistical and thermodynamic models, specially the verification of irradiated materials (Al, Fe, and Cu).

1.4 Material and Methods:

1. Bring 3 different materials (al, Fe, and Cu) in shavings forms.
2. Then make six samples of each material by mixing the shavings with the Gum-Arabic and putting it in a piston to get a disc shape.
- 3 Let samples dry in the shade, and then scratch each sample to reach the required thickness (5, 10, 15, 20, 25, and 30mm for aluminum, 3, 6, 9,12, 15, and 18mm for iron 4, 8, 12, 16, 20 and 24mm for copper, and).
4. Put each disk in front of the gamma-ray source (at room temperature) and then put a GM tube in the other direction to measure the intensity of the radiation penetrating the disk.

5. Every time put on an extra disc with the first disk to increase the thickness and measure the radiation intensity that penetrates the samples (take six samples of each material).

6. Repeat this process, with heating the samples to (40, 50, 60, and 70)⁰C. During this experiment take care of radiation protection by using lead shielings, to get an experiment perfect as possible.

1.5 Thesis layout:

This work has come into five chapters. Chapter one is introduction, chapter two introduced for theoretical background, then in chapter three literature reviews, chapter four explains the experimental method, and chapter five the experimental results are discussion and conclusion remarks.

Chapter two

Theoretical Background

2.1 Introduction:

In physical science, heat is important to all aspects of life. Heat is a result of energy, which can be beneficial as well as dangerous. Understanding the properties and uses of heat can help increase efficiency of heat or energy use as well as increase understanding of things like weather changes and survival. Life on this earth depends on heat energy for survival. Therefore, this chapter is concerned with the concept of heat energy.

2.2 Concept of Heat and Temperature:

We all have an intuitive notion of what heat is: sitting next to a roaring fire in winter, we feel its heat warming us up, increasing our temperature; lying outside in the sunshine on a warm day, we feel the Sun's heat warming us up. In contrast, holding a snowball, we feel heat leaving our hand and transferring to the snowball, making our hand feel cold. Heat seems to be some sort of energy transferred from hot things to cold things when they come into contact. We therefore make the following definition: "heat is thermal energy in transit" [15].

We now stress a couple of important points about this definition.

(1) Experiments suggest that heat spontaneously transfers from a hotter body to a colder body when they are in contact, and not in the reverse direction. However, there are circumstances when it is possible for heat to go in the reverse direction. A good example of this is a kitchen freezer: you place food, initially at room temperature, into the freezer and shut the door; the freezer then sucks heat out of the food and cools the food down to below freezing point. Heat is being transferred from your warmer food to the colder freezer, apparently in the "wrong" direction. Of course, to achieve this, you have to be paying your electricity bill and therefore be putting energy in to your freezer. If there is a power cut, heat will slowly leak back into the freezer from the warmer kitchen and thaw out all your frozen food. This shows that it is possible to reverse the direction of heat flow, but only if you intervene by putting additional energy in. We will return to this point in Section 13.5 when we consider refrigerators, but for now let us note that we are defining heat as thermal energy in transit and not hard-wiring into the definition anything about which direction it goes.

(2) The “in transit” part of our definition is very important. Though you can add heat to an object, you cannot say that “an object contains a certain quantity of heat.” This is very different from the case of the fuel in your car: you can add fuel to your car, and you are quite entitled to say that your car “contains certain quantity of fuel”. You even have a gauge for measuring it! But heat is quite different. Objects do not and cannot have gauges which read out how much heat they contain, because heat only makes sense when it is “in transit”.¹ To see this, consider your cold hands on a chilly winter day. You can increase the temperature of your hands in two different ways: (i) by adding heat, for example by putting your hands close to something hot, like a roaring fire; (ii) by rubbing your hands together. In one case you have added heat from the outside, in the other case you have not added any heat but have done some work. In both cases, you end up with the same final situation: hands that have increased in temperature. There is no physical difference between hands that have been warmed by heat and hands that have been warmed by work.

Heat is measured in (SI) units in Joules (J).

Now we need to define temperature “Temperature is a physical water quality parameter since temperature can have a negative effect on aquatic life, especially the propagation of fish.

The concept of temperature has evolved from the common concepts of hot and cold. Human perception of what feels hot or cold is a relative one. For example, if you place one hand in hot water and the other in cold water, and then place both hands in tepid water, the tepid water will feel cool to the hand that was in hot water, and warm to the one that was in cold water. The scientific definition of temperature is less ambiguous than your sense of hot and cold [16]. Temperature is operationally defined to be what we measure with a thermometer.

2.2.1 Specific Heat:

Specific heat ‘c’ is defined “is the amount of heat required to raise the temperature of 1 kilogram of a substance by 1kelvin”. SI unit of specific heat capacity $\text{Jkg}^{-1}\text{K}^{-1}$. As 1K is commensurate with 1 °C, the specific heat capacity is often quoted using the letter unit. The word ‘specific’ in a definition indicates that the quantity is expressed in terms of units mass. The specific heat tell us how a certain amount of heat supplied to the system change its temperature. Specific heat capacity is often abbreviated to specific heat and must not be confused with term ‘heat capacity’ [17, 18].

We can calculate the specific heat from relation:

$$c = \frac{\Delta Q}{m\Delta T} \quad 2.1$$

Where ΔQ : The amount of heat in Joules (J), m: mass in kilograms (kg), and ΔT : temperature difference in Kelvin (K).

2.2.2 Heat Capacity:

Heat Capacity ‘C’ is defined as the amount of heat required to raise the temperature of a material by a unit of temperature [19], or in other words “The amount of heat needed to raise the temperature of an object by 1 degree kelvin measured in joules per kelvin (J/K) [20]:

$$C = \left[\frac{\Delta Q}{\Delta T} \right]_x \quad 2.2$$

Where x denotes any of the several constraints which can be imposed. The most common constraints are pressure (p), and volume (V). Contrarily to specific heat, heat capacity is an extensive quantity, which means that it depends on the size of the system.

2.2.3 Thermodynamics:

Thermodynamic behavior of matter is very important for human life. This is since human life requires proper temperature range. The growth of plants also needs proper temperature. To live inside your house needs temperature in the range. This needs preventing heat to enter in hot climates and prevent it also from escaping outside in cold climates. This requires controlling the temperature of the house by selecting the building materials.

Thermodynamics is the Science that deals with the relationship of heat and mechanical energy and conversion of one into the other. The Greek roots, therme, meaning heat, and dynamic, meaning, power or strength, suggest a more elegant definition: the power of heat (1).

Thermodynamic concepts are important in the development of many branches of sciences, such as fluids and solid mechanics, heat and mass transfer, material science, chemistry, biology, and life sciences. Thermodynamics points to the direction in which processes proceed and provides relationships for material and energy balances.

2.2.4 Systems and surroundings:

A system is part of the physical world in which one is interested and is defined as “any region of space or a finite quantity that occupies a volume and has a boundary” [21] as shown in figure (2.1). Everything external to the system is called surroundings [22]. We distinguish between several types of systems:

- 1) An isolated system is a system that is totally uninfluenced by the Surroundings. There is no possibility of exchange of energy or matter with surroundings.
- 2) A closed system is a system in which energy but not matter can exchange with the surroundings.
- 3) An open system is a system in which both energy and matter can exchange with the surroundings.

Isolated or closed systems are often referred to as bodies. Theorems will first be developed for isolated and closed systems and later generalized to open systems.

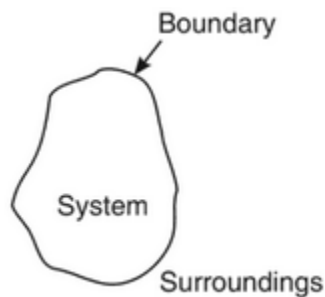


Figure 2.1 system, boundary, and surrounding

2.2.5 Internal Energy:

At microscopic level, the sum of the kinetic and potential energies, which cannot be seen, is referred to as the internal energy (U) in thermodynamics. Thermodynamics simply states that: (i) internal energy is an extensive property, and (ii) internal energy is a state function. The internal energy of a system is increased either by transferring heat to the system or by doing work on it [23].

2.2.6 The Zeroth law:

Zeroth Law states that if two bodies are in thermal equilibrium with a third, they are in thermal equilibrium with each other.

2.2.7 The first law of thermodynamics:

First law “Heat is a form of energy, and energy is conserved” [24].

A system has an internal energy U , which is the sum of the energy of all the internal degrees of freedom that the system possesses. U is a function of state because it has a well-defined value for each equilibrium state of the system. We can change the internal energy of the system by heating it or by doing work on it. The heat Q and work W are not functions of state since they concern the manner in which energy is delivered to (or extracted from) the system. After the event of delivering energy to the system, you have no way of telling which of Q or W was added to (or subtracted from) the system by examining the system's state. The following analogy may be helpful: your personal bank balance behaves something like the internal energy U in that it acts like a function of state of your finances; cheques and cash are like heat and work in that they both result in a change in your bank balance, but after they have been paid in, you can't tell by simply looking at the value of your bank balance by which method the money was paid in.

The change in internal energy U of a system can be written

$$\Delta U = \Delta Q + \Delta W \quad (2.3)$$

Where ΔQ is the heat supplied **to** the system and ΔW is the work done on the system.

Note the convention: ΔQ is positive for heat supplied to the system; if ΔQ is negative, heat is extracted from the system; ΔW is positive for work done on the system; if ΔW is negative, the system does work on its surroundings.

We define a thermally isolated system as a system that cannot exchange heat with its surroundings. In this case we find that $\Delta U = \Delta W$, because no heat can pass in or out of a thermally isolated system.

From microscopic point of view, the principle of conservation of energy was advanced by Helmholtz, assuming the atomic constitution of matter; Helmholtz extended the theorem of conservation of mechanical energy to the microscopic motion of atoms. That is, he assumed that the sum of the kinetic and potential energy of atoms is constant and therefore the internal energy of a body [6].

2.3 Second law of thermodynamics:

There are necessary to another law in thermodynamics, because while the 1st law allowed us to determine neither the quantity of energy transfer in a process it does not provide any information about the direction of energy transfer nor the quality of the energy transferred in the process. In addition, we cannot determine from the 1st law alone whether the process is possible or not. The second law will provide answers to these unanswered questions. A process will not occur unless it satisfies both the first and the second laws of thermodynamics.

There are two classical statements of the second law, known as Kelvin-Planck statement, and the Clausius statement.

The Kelvin-Planck statement: “It is impossible to construct a device that will operate in cycle and produce no effect other than the raising of a weight and the exchange of heat with single reservoir”.

In effect, it states that it is impossible to construct a heat engine that operates in a cycle, receives a given amount of heat from a high temperature body, and does an equal amount of work. The only alternative is some heat must be transferred from the working fluid at a lower temperature to low temperature body. Thus, work can be done by the transfer of heat only if there are temperature levels, and heat is transferred from the high temperature body to the heat engine and also from the heat engine to the low temperature body. This implies that it is impossible to build a heat engine that has a thermal efficiency of 100%.

The Clausius statement “It is impossible to construct a device that operates in a cycle and produces no effect other than transfer of heat from a cooler body to a warmer body”.

This statement related to the refrigerator or heat pump. In effect, it is states that it is impossible to construct a refrigerator that operates without an input of work. This also implies that the COP is always less than infinity [25].

There are many other important uses for the second law of thermodynamics, including means for: (i) predicting the direction of processes, (ii) establishing conditions for equilibrium, (iii) determine the best theoretical performance of cycles, engines, and other devices, (iv) evaluating quantitatively the factors that preclude the attainment of the best theoretical performance level, and (v) defining a temperature scale independent of the properties of any thermodynamic substance [26].

2.4 Entropy:

The measure of a system’s thermal energy per unit temperature that is unavailable for doing useful work. Because work is obtained from ordered molecular motion, the amount of entropy is also a measure of the molecular disorder, or randomness, of a system. The concept of entropy provides deep insight into the direction of spontaneous change for many everyday phenomena. Its introduction by the German physicist Rudolf Clausius in 1850 is a highlight of 19th-century physics

The idea of entropy provides a mathematical way to encode the intuitive notion of which processes are impossible, even though they would not violate the fundamental law of conservation of energy. For example, a block of ice placed on a hot stove surely melts, while the stove grows cooler. Such a process is called irreversible because no slight change will cause the melted water to turn back into ice while the stove grows hotter. In contrast, a block of ice placed in an ice-water

bath will either thaw a little more or freeze a little more, depending on whether a small amount of heat is added to or subtracted from the system. Such a process is reversible because only an infinitesimal amount of heat is needed to change its direction from progressive freezing to progressive thawing. Similarly, compressed gas confined in a cylinder could either expand freely into the atmosphere if a valve were opened (an irreversible process), or it could do useful work by pushing a moveable piston against the force needed to confine the gas. The latter process is reversible because only a slight increase in the restraining force could reverse the direction of the process from expansion to compression. For reversible processes the system is in equilibrium with its environment, while for irreversible processes it is not.

To provide a quantitative measure for the direction of spontaneous change, Clausius introduced the concept of entropy as a precise way of expressing the second law of thermodynamics. The Clausius form of the second law states that spontaneous change for an irreversible process in an isolated system (that is, one that does not exchange heat or work with its surroundings) always proceeds in the direction of increasing entropy. For example, the block of ice and the stove constitute two parts of an isolated system for which total entropy increases as the ice melts.

By the Clausius definition, if an amount of heat Q exchanges that occur in thermal processes via the relation $\Delta S = Q/T$ [27]. This equation effectively gives an alternate definition of temperature that agrees with the usual definition. Assume that there are two heat reservoirs R_1 and R_2 at temperatures T_1 and T_2 (such as the stove and the block of ice). If an amount of heat Q flows from R_1 to R_2 , then the net entropy change for the two reservoirs is:

$$\Delta S = Q \left(\frac{1}{T_2} - \frac{1}{T_1} \right) \quad (2.4)$$

which is positive provided that $T_1 > T_2$. Thus, the observation that heat never flows spontaneously from cold to hot is equivalent to requiring the net entropy change to be positive for a spontaneous flow of heat. If $T_1 = T_2$, then the reservoirs are in equilibrium, no heat flows, and $\Delta S = 0$.

The condition $\Delta S \geq 0$ determines the maximum possible efficiency of heat engines—that is, systems such as gasoline or steam engines that can do work in a cyclic fashion. Suppose a heat engine absorbs heat Q_1 from R_1 and exhausts heat

Q_2 to R_2 for each complete cycle. By conservation of energy, the work done per cycle is $W = Q_1 - Q_2$, and the net entropy change is:

$$\Delta S = \frac{Q_2}{T_2} - \frac{Q_1}{T_1} \quad (2.5)$$

To make W as large as possible, Q_2 should be as small as possible relative to Q_1 . However, Q_2 cannot be zero, because this would make ΔS negative and so violate the second law. The smallest possible value of Q_2 corresponds to the condition

$\Delta S = 0$, yielding:

$$\left(\frac{Q_2}{Q_1}\right)_{min} = \frac{T_2}{T_1} \quad (2.6)$$

As the fundamental equation limiting the efficiency of all heat engines. A process for which $\Delta S = 0$ is reversible because an infinitesimal change would be sufficient to make the heat engine run backward as a refrigerator.

The same reasoning can also determine the entropy change for the working substance in the heat engine, such as a gas in a cylinder with a movable piston. If the gas absorbs an incremental amount of heat dQ from a heat reservoir at temperature T and expands reversibly against the maximum possible restraining pressure P , then it does the maximum work $dW = P dV$, where dV is the change in volume. The internal energy of the gas might also change by an amount dU as it expands. Then by conservation of energy:

$$dQ = dU + PdV \quad (2.7)$$

Because the net entropy change for the system plus reservoir is zero when maximum work is done and the entropy of the reservoir decreases by an amount

$$dS_{reservoir} = -\frac{dQ}{dT} \quad (2.8)$$

This must be counterbalanced by an entropy increase of:

$$dS_{system} = \frac{dU + PdV}{T} = \frac{dQ}{T} \quad (2.9)$$

for the working gas so that $dS_{system} + dS_{reservoir} = 0$. For any real process, less than the maximum work would be done (because of friction, for example), and so the actual amount of heat dQ' absorbed from the heat reservoir would be less than the

maximum amount dQ . For example, the gas could be allowed to expand freely into a vacuum and do no work at all. Therefore, it can be stated that:

$$dS_{system} = \frac{dU + P dV}{T} \geq \frac{d\dot{Q}}{T} \quad (2.10)$$

With $dQ' = dQ$ in the case of maximum work corresponding to a reversible process.

This equation defines S_{system} as a thermodynamic state variable, meaning that its value is completely determined by the current state of the system and not by how the system reached that state. Entropy is an extensive property in that its magnitude depends on the amount of material in the system.

In one statistical interpretation of entropy, it is found that for a very large system in thermodynamic equilibrium, entropy S is proportional to the natural logarithm of a quantity Ω representing the maximum number of microscopic ways in which the macroscopic state corresponding to S can be realized; that is, $S = k \ln \Omega$, in which k is the Boltzmann constant that is related to molecular energy.

All spontaneous processes are irreversible; hence, it has been said that the entropy of the universe is increasing: that is, more and more energy becomes unavailable for conversion into work. Because of this, the universe is said to be “running down”.

2.5 Heat Transfer:

Whenever a temperature gradient exists within a system, or whenever two systems at different temperatures are brought into contact, energy is transferred. The process by which the energy transport takes place is known as heat transfer. The thing in transit, called heat, cannot be observed or measured directly. However, its effects are identified and quantified through measurements and analysis. The flow of heat like performance of work is process by which the initial energy of a system is changed [28].

Heat transfer is defined as the transmission of energy from one region to another as a result of temperature gradient takes place by the following three modes:

(i) Conduction, (ii) Convection, and (iii) Radiation.

Heat transmission, in majority of real situations, occurs as a result of combinations of these modes of heat transfer. Example: The water in a boiler shell receives its heat from the fire-bed by conducted, convicted and radiated heat from the fire to the shell, conducted heat through

The shell and conducted and convicted heat from the inner shell wall, to the water. Heat always flows in the direction of lower temperature. The above three modes are similar in that a temperature differential must exist and the heat exchange is in the direction of decreasing temperature; each method, however, has different controlling laws [29].

2.5.1 Conduction:

Thermal conduction is process by which heat is transmitted by the direct contact between particles of a body without any motion of the material as a whole. Conduction occurs in all media: solids, liquids, and gases when a temperature gradient exists [30].

Conduction is the transfer of heat from one part of a substance to another part of the same substance, or from one substance to another in physical contact, with it, without appreciable displacement of molecules forming the substance.

In solids, the heat is conducted by the following two mechanisms:

(i) By lattice vibration: the faster moving molecules or atoms in the hottest part of a body transfer heat by impacts some of their energy to adjacent molecules.

(ii) By transport of free electrons: free electrons provide an energy flux in the direction of decreasing temperature for metals, especially good electrical conductors, the mechanism is responsible for the major portion of the heat flux except at low temperature.

Fourier's law of heat conduction: Fourier's law of heat conduction is an empirical law based on observation and states as follows: "The rate of flow of heat through a simple homogenous solid is directly proportional to the area of the section at right angles to the direction of heat flow, and to change of temperature-with respect to the length of the path of the heat flow" [18].

Mathematically, it can be represented by the equation:

$$Q \propto A \cdot \frac{dT}{dx}$$

Where Q: heat flow through a body in (W), A: surface area of heat flow perpendicular to the direction of flow (m^2), dT: temperature difference of the faces of block in $^{\circ}C$ or K, dx: thickness of body indirection of flow in (m).

Thus:

$$Q = -K \cdot A \frac{dT}{dx} \quad (2.11)$$

The constant K is called the thermal conductivity. It obviously must have the dimensions (w/m^2).

In equation (2.10) there is negative sign because, the heat flux (Q) resulting from thermal conduction is proportional to the magnitude of the temperature gradient and opposite to it.

Equation (2.10), tells us that if temperature decreases with (x), (Q) will be positive; it will flow in the (x) direction. If (T) increases with (x) , (Q) will flow from higher temperatures to lower temperatures [31].

2.5.2 Convection:

Convection is the transfer of heat within a fluid by mixing of one portion of the fluid with another. Convection heat transfer is clearly a field at the interface between two older fields: heat transfer and fluid mechanics (32). Convection constitutes the macro form of the heat transfer since macroscopic particles of fluid moving in space because the heat exchange. The effectiveness of heat transfer by convection depends largely upon the mixing motion of the fluid.

This mode of heat transfer is met with in situations where energy is transferred as heat to a following fluid at any surface over which flow occurs. This mode is basically conduction in a very thin fluid layer at the surface and then mixing caused by the flow. The heat flow depends on the properties of fluid and is independent of the properties of the material of the surface. However, the shape of the surface will influence the flow and hence the heat transfer.

Free or natural convection occurs where the fluid circulates of hot and cold fluids, the denser portions the fluid move downward because of the greater force of gravity as compared with force on the less dense.

Forced convection when the work is done to blow or pump the fluid, it is said to be forced convection.

The rate equation for the convective heat transfer (regardless of particular nature)

Between a surface and an adjacent fluid is prescribed by Newton's law of cooling

$$Q = h A (T_s - T_f) \quad (2.12)$$

where, Q = Rate of conductive heat transfer, A = Area exposed to heat transfer, T_s = Surface temperature, T_f = Fluid temperature, and h = Co-efficient of conductive heat transfer.

The units of h are, $h = \frac{QA}{(ts\ tf)} W - m^2 C = ^\circ$ or $W/m^2^\circ C$ or $W/m^2 K$

The coefficient of convective heat transfer ' h ' (also known as film heat transfer coefficient)

May be defined as "the amount of heat transmitted for a unit temperature difference between the fluid and unit area of surface in unit time." The value of ' h ' depends on the following factors:

(i) Thermodynamic and transport properties (e.g., viscosity, density, specific heat etc.), (ii) Nature of fluid flow, (iii) Geometry of the surface, and (iv) Prevailing thermal conditions.

Since ' h ' depends upon several factors, it is difficult to frame a single equation to satisfy all [29].

2.5.3 Radiation:

“Radiation is transfer of heat through space or matter by means other than conduction or convection”. Radiation heat is thought of as electromagnetic waves or quanta (as convection) an emanation of the same nature as light and radio waves. All bodies radiate heat, so a transfer of heat by radiation occurs because hot body emits more heat than it receives and cold body receives more heat than it emits. Radiant energy (being electromagnetic radiation) requires no medium for propagation and will pass through a vacuum.

The rapidly oscillating molecules of the hot body produce electromagnetic waves in hypothetical medium called ether. These waves are identical with high waves, radio waves, and X-rays, differ from them only in wavelength and travel with an approximate velocity of light (3×10^8 m/s). These waves carry energy with them and transfer it to the relatively slow-moving molecules of the cold body on which they happen to fall. The molecular energy of the later increases and results in arise of its temperature. Heat travelling by radiation is known as radiant heat.

The properties of radiant heat in general, are similar to those of light. Some of the properties are:

- (i) It does not require the presence of a material medium for its transmission.
- (ii) Radiant heat can be reflected from the surfaces and obeys the ordinary laws of reflection.
- (iii) It travels with velocity of light.
- (iv) Like light, it shows interference, diffraction, and polarization.

The wavelength of heat radiation is longer than that of light waves; hence they are invisible to the eye.

The contribution of radiation to heat transfer is very significant at high absolute temperature levels such as those prevailing in furnaces, combustion chambers, nuclear explosions and in space applications. The solar energy incident upon the earth is also governed by the laws of radiation. The energy which a radiating surface releases is not continuous but is in the form of successive and separate (discrete) packet or quanta of energy called photons. The photons are propagated through space as rays; the movement of swarm of photons is described as electromagnetic waves. The photons travel (with speed equal to that of light) in straight paths with unchanged frequency ;when they approach the receiving surface, there occurs reconversion of wave motion into thermal energy which is partly absorbed, reflected or transmitted through the receiving surface (the magnitude of each fraction depends, upon the nature of the surface that receives the thermal radiation).

All types of electromagnetic waves are classified in terms of *wavelength* and are propagated at the speed of light (c) *i.e.*, 3×10^8 m/s. The electromagnetic spectrum

is shown in Fig. (2.2). The distinction between one form of radiation and another lies only in its frequency (f) and wavelength (λ) which are related by

$$c = \lambda \times f \quad (2.13)$$

The emission of thermal radiation (range lies between wavelength of 10^{-7} m and 10^{-4} m) depends upon the nature, temperature and state of the emitting surface. However, with gases the dependence is also upon the thickness of the emitting layer and the gas pressure.

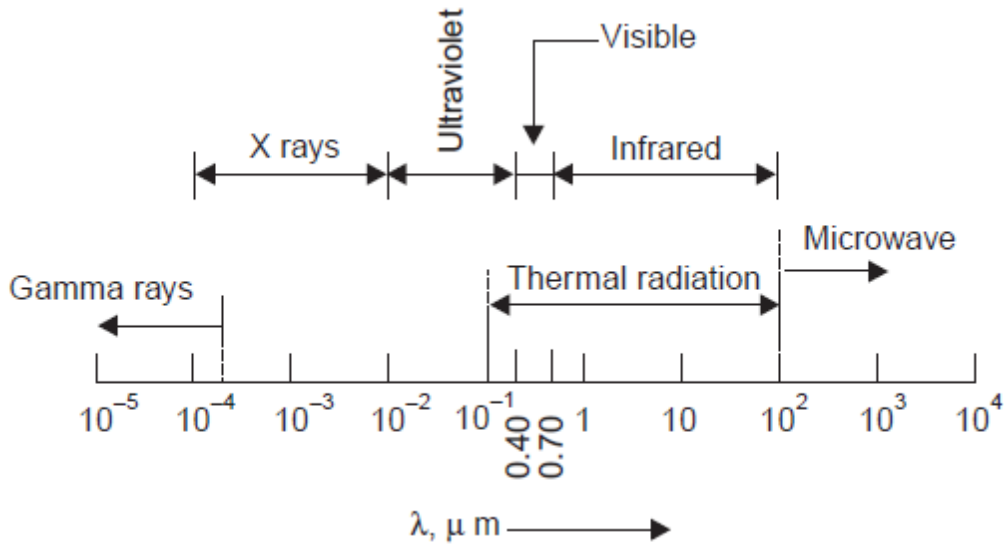


Figure 2.2 Spectrum of electromagnetic radiation.

Thermal radiations exhibit characteristics similar to those of visible light, and follow optical Laws. These can be reflected, refracted and are subject to scattering and absorption when they pass through a media. They get polarized and weakened in strength with Inverse Square of radial distance from the radiating surface.

The rate of emission of radiation by a body depends upon the following factors:

(i) The temperature of the surface, (ii) The nature of the surface, and (iii) The wavelength or frequency of radiation.

According to Stefan Boltzmann law, the amount of radiation emitted per unit time from an area A of a black body at absolute temperature T is directly proportional to the fourth power of the temperature:

$$\begin{aligned} \frac{Q}{T} &\propto T^4 \\ \frac{Q}{T} &= \sigma T^4 \\ Q &= \sigma A T^4 \end{aligned} \quad (2.14)$$

Where Q : Total energy released from the black body (w), A : Surface area of the black body in (m^2), T : temperature in (K), and σ : Stefan-Boltzmann constant ($\sigma = 5.67 \times 10^{-8} \text{ W/m}^2/\text{K}^4$ [29]).

The net amount of radiation heat transfer to or from a surface depends on the on the surface temperature of the surroundings (because the surroundings are radiating heat to the surface as well). Examples of situations where radiation heat transfer can be dominated heat transfer mechanisms are the sun heating the earth and heat lamp shining on a cold object. To have large amounts of radiation heat transfer, you need both a very hot surface (due the dependence of the radiation on the surface temperature to the fourth power) and a large temperature difference between the surface and the surroundings [33].

2.6 Types of radiation:

Radiation can be categorized into non-ionizing radiation and ionizing radiation.

2.6.1 Non-ionizing radiation: is the type of electromagnetic radiation with no enough energy to ionize atom. Although, considered less dangerous than ionizing radiation, over exposure to non-ionizing radiation can also be hazardous. Examples of this kind of radiation are radio waves, visible light and microwaves [34, 35].

2.6.2 Ionizing radiation: is radiation that carries enough energy to detach electrons from atoms causing the atom to become charged or ionized [35].

Ionizing radiation can affect the atoms in living things, so it poses a health risk by damaging tissue and DNA in genes. Ionizing radiation has many types like alpha particles, beta particles, gamma-rays, and X-rays. Radioactive elements emit ionizing radiation as their atoms undergo radioactive decay.

And we're going to focus this study on gamma rays, because they're basically used in this research.

2.7 Gamma rays:

Gamma rays are electromagnetic waves of very short wavelength of about 0.004\AA to 0.4\AA consisting of photons. It is more convenient to describe the radiation in terms of energy than in terms of wavelength since the energy absorbed from the radiation is basically of interest. Gamma rays have no charged particles; they are

not deflected by electric and magnetic fields. Since gamma-rays are electromagnetic waves, they travel with velocity of light [11].

The gamma rays are of nuclear origin. Experimentally it is observed that the gamma spectrum is always in the form of sharpness indicating the nuclei have discrete energy levels like atoms. Moreover, nuclear energy is characteristic of a particular nucleus. The gamma rays emitted from radioactive elements have very high energies of the order of few MeV which is greater than the energies of characteristic X-ray from k-level of those atoms. Cobalt-60, for example, gives equal number of gamma photons of energy 1.332 and 1.173 MeV. The high energy gamma radiation penetrates deeper into materials and induces processes not possible at low energies [36, 37].

2.7.1 Origin of gamma decay:

Radioactive decay is the process in which an unstable atomic nucleus spontaneously loses energy by emitting ionizing particles and radiation, this called the parent nuclide transforming to an atom of different type, named the daughter nuclide [38].

The very large values of energy of gamma rays of the order of few MeV show that they must be of the nuclear origin. In addition, the gamma rays spectrum consists of sharp lines which indicate the existence of a number of energy levels in the nucleus.

It has been proved that gamma rays arise from the transition of a nucleon from higher energy to lower energy level. When a nucleus emits an alpha or beta particles, the daughter nucleus is left in an excited state. The nucleus in excited state returns to the ground state by emitting gamma rays. The energies correspond to the states in the transitions involved [11].

For example, the nucleus ${}_Z X^{A*}$ in excited state comes down to lower energy state ${}_Z X^A$ emitting gamma ray. The gamma ray emission is represented by:



It is to be noted here that the daughter and parent nuclei have the same structure of nuclear particles. The only difference is that the parent nucleus is in an excited

state and the daughter is in lower energy state. If E^* is the energy associated with the parent nucleus in excited state and E is the energy of the daughter nucleus in lower energy state, the gamma rays emitted have the energy given by:

$$h\nu = E^* - E \quad (2.16)$$

Where ν is the frequency of the emitted gamma rays.

If E is ground state of nucleus, no further emission of gamma-ray photons will take place, otherwise the nucleus will emit one or more gamma-ray photons before reaching to ground state. During gamma decaying mass and charge of decaying nucleus does not change [39].

2.7.2 Gamma photons energy:

A particle of zero rest mass such as gamma photon will have a kinetic energy given by:

$$E = h\nu = h \frac{c}{\lambda} \quad (2.17)$$

Where: h is Planck's constant = 6.62×10^{-34} J.s, c is speed of light = 3×10^8 m/s,

ν is the frequency of gamma photon, and λ is wavelength of electromagnetic radiation(m).

In particular the complete annihilation of a particle of rest mass in (kg) releases an amount of energy (E) in units (J) given by formula:

$$E = mc^2 \quad (2.18)$$

Hence, we can write a universal energy-mass-radiation equivalence equation as:

$$E = mc^2 = h\nu = h \frac{c}{\lambda} \quad (2.19)$$

This relates mass and electromagnetic radiation through the interesting relationship:

$$m = \frac{h}{c^2} \nu = \frac{h}{c} \frac{1}{\lambda} \quad (2.20)$$

Therefore, electromagnetic radiation with high frequency and short wavelength, such as X- rays and gamma rays, are also the highest energy photon known while radio waves are of relatively low energy. This is why figure (EM Spectrum) is called electromagnetic spectrum. It is an arrangement of electromagnetic radiation according to energy (increase from right to left) of electromagnetic radiation is feared. Being more energetic has its consequences [40].

2.7.3 The absorption of gamma rays with matter:

When an x- and γ - ray beam passes through a medium, interaction between photons and matter can take place with the result that energy is transferred to the medium. The initial step in the energy transfer involves the ejection of electrons from the atoms of the absorbing medium. These high speed electrons transfer their energy by producing ionization and excitation of the atoms along their paths [41].

2.7.3.1 Linear attenuation coefficient:

Let us consider a mono-energetic and homogeneous beam of gamma ray of intensity I_0 be incident on a thin sheet of material. It has been experimentally observed that the gamma ray incident on the material is getting absorbed and I be the intensity of the emerging ray when passing through a thickness of (x). Hence, the decrease in intensity dI with respect to the thickness dx is proportional intensity I of emerging gamma ray.

$$\frac{dI}{dx} \propto -I$$

$$\frac{dI}{dx} = -\mu_L I \quad (2.21)$$

Where μ_L is proportionality constant and is called the linear attenuation coefficient. Negative sign indicates that as x increase, I decrease. Linear attenuation coefficient defined as “the fraction of how many photons are removed per path length either from scattering out from transferring their energy to electrons”, and measured in cm^{-1} [42, 43].

From eq.(2.21) we have:

$$\frac{dI}{I} = \mu dx$$

Integrating the above equation, we have:

$$\log I = -\mu x + C$$

At $t=0$, $I = I_0$, the initial intensity of gamma ray, then $C = \log_c I_0$

Therefore:

$$\log_c I = \mu x + \log_c I_0 \quad (2.22)$$

Or:

$$I = I_0 e^{-\mu x} \quad (2.23)$$

The equation (2.23) determines the intensity of radiation of gamma ray after traversing through a thickness (x) of the absorbing material. The gamma ray absorption in matter is pictorially represented in fig (2.3).

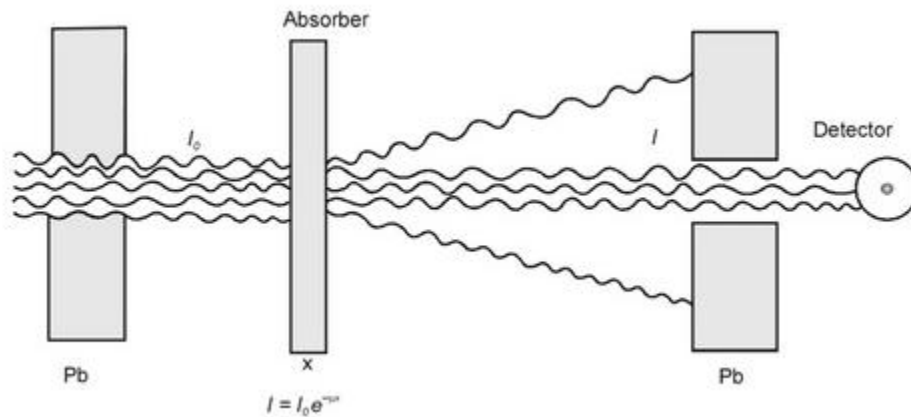


Figure 2.3 Gamma ray absorption in matter

Experiments have been performed using different energies. It has been found that:

- i. Attenuation coefficient μ depends upon the nature of absorber. μ is larger for heavier elements like Pb, Bi, etc, and is smaller for lighter elements like C, Al, etc.
- ii. Attenuation coefficient μ depends upon the energy of γ -rays. It is larger for low energy γ -rays and is smaller for high energy γ -rays.

2.7.3.2 Half value layer (HVL):

Half value layer is the thickness of an absorber of specified composition required to attenuate the intensity of the beam to half its original value [42, 44]. From equation (2.23):

$$I = \frac{I_0}{2}$$
$$\frac{I_0}{2} = I_0 e^{-\mu x}$$
$$e^{\mu x} = 2$$
$$\frac{\mu x_1}{2} = \ln 2$$

Where $x_{1/2}$ is half thickness, this can also written as:

$$HVL = \frac{\ln 2}{\mu} = \frac{0.693}{\mu} \quad (2.24)$$

2.7.3.3 Cross-section:

The probabilities for the occurrence of various processes initiated through collisions in atomic and nuclear physics are generally described in terms of cross-section for the process. The cross-section is a very useful concept for describing the partial probabilities for possible processes [45].

2.7.4 Interaction of radiations with matter:

In penetrating an absorbing medium, photons may experience various interactions with the atoms of the medium or these interactions involve either the nuclei of the absorbing medium or the orbital electrons of the absorbing medium: (i) the interactions with nuclei may be direct photon-nucleus interactions or interactions between the photon and the electrostatic field of the nucleus, and (ii) the photon-orbital electron interactions are characterized as interactions between the photon and either a loosely bound electron or a tightly bound electron [46].

Gamma ray interaction is important from the perspective of shielding against their effects on biological matter. They are considered as ionizing radiation whose

scattering by electrons and nuclei leads to the creation of radiation field containing negative electrons and positive ions.

We know that the gamma rays are highly penetrating, uncharged radiation which consists of small energy packets of photons. Hence, their interaction with matter is very much effective compared to the interaction of charged particles with matter. When a beam of gamma ray photons is incident on matter, there are three processes which are mainly responsible for the absorption of gamma rays. These processes are photoelectric effect, Compton scattering, and pair production.

2.7.4.1 Photoelectric effect:

In around 1880, Hertz and Lenard observed that when a clean metallic surface is irradiated by monochromatic light of proper frequency, electrons are emitted from it. This phenomenon of ejection of the electrons from the metal surface is called the photoelectric effect and electrons thus ejected called the photoelectrons as shown in figure (2.4).

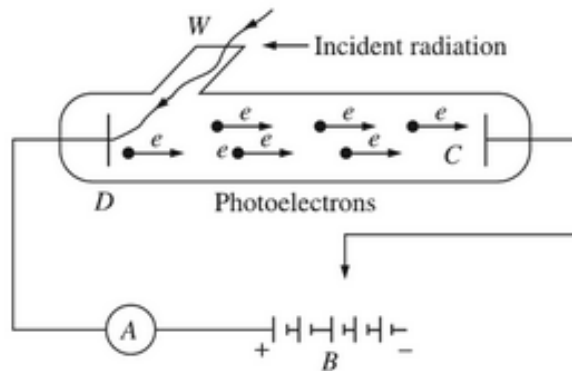


Figure 2. 4 Schematic diagram of the experimental setup for photoelectric effect.

Figure (2.4) In an evacuated glass tube, two metal plates C, acting as the collecting anode and D which acts as photosensitive are enclosed. These two plates are connected to a battery B and ammeter A. When the incident radiation falls in plate D through the window W, electrons are ejected out of the plate and current flows in the circuit. With the help of this apparatus, the following dependencies of the photoelectric effect were found.

(i) The number of electrons emitted by the metal is found to be directly proportional to the intensity of the light.

- (ii) The emitted electrons move faster if the light has a higher frequency.
- (iii) There is a cut-off frequency for the incident photons, below which no electrons are emitted [47, 48].

2.7.4.2 Compton scattering:

When a photon incident on an atom can be absorbed, the atom to eject an electron with a kinetic energy equal to the excess energy; that is, the kinetic energy is the difference between the photon energy and the binding energy of the electron. Alternatively, some or all of the excess energy can be given to a second electron [49].

The photon with diminished energy $h\nu'$ is scattered an angle θ with the direction of incident photon. The electron recoil at angle ϕ . The energy absorbed by the Compton electrons is only a small fraction of the total energy of the incident gamma rays unlike in the case of photoelectrons as shown in figure (2.5).

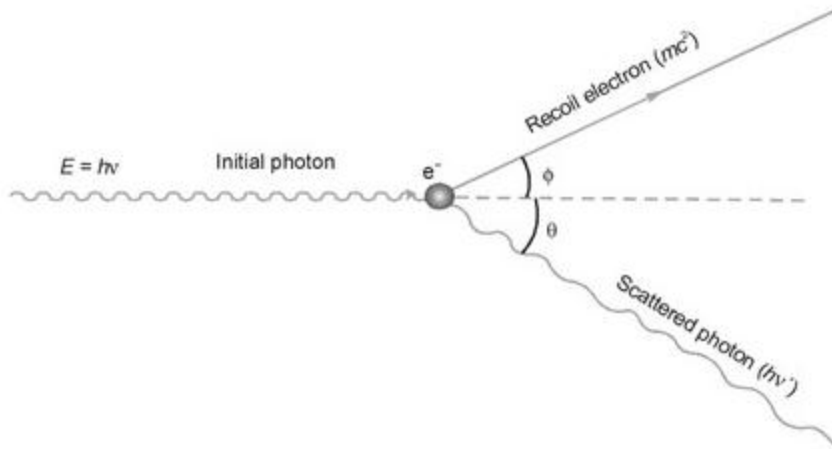


Figure 2.5 Compton Scattering

During this interaction, only a part of the total photon energy $h\nu$ is transferred to a free electron and scattered photon moves in a changed direction with lower energy $h\nu' < h\nu$. The photon energy decrease does not depend on energy but only on the scattering angle θ that ranges between 0 and π . The original wavelength λ changes to $\lambda' > \lambda$. The increase of the wavelength of scattered photon

$\Delta\lambda = \lambda' - \lambda$ is given by:

$$\Delta\lambda = \frac{h}{m_e c} (1 - \cos\theta) \quad (2.25)$$

Where m_e is the mass of electron, and c the velocity of electromagnetic wave in vacuum. The expression $h/m_e c$ is called the Compton wavelength of electron.

This type of interaction does not depend on the atomic number of absorber and the probability of its occurrence depends on incident photon energy [50, 51].

2.7.4.3 Pair production:

We have already seen that the photons give an electron all of its energy (photoelectric effect) or transfer only a part of its energy (Compton scattering). There is a third probability in which photon may suddenly disappear and create an electron and positron. This process called pair production. All the conservation laws are fulfilled during this process. For example, the sum of the charge of electron ($q = -e$) and of positron ($q = +e$) is zero and the charge on photon is also zero as shown in figure (2.6). The total energy which also includes the rest mass energy of electron and positron is equal to the gamma-ray photon energy.

The formation of electron-positron pair and remaining energy is shared by electron and positron as kinetic energy. This process is represented by the relation:

$$\gamma = e^- + e^+ \quad (2.26)$$

In this process, when the gamma ray is incident on matter, the photon disappears and is converted into an electron-positron pair figure (2.6). This process can take place only when the photon energy exceeds the total energy of electron and positron ($2m_0c^2$). The pair production process cannot occur in free space and usually takes place in the presence of nuclear field [39, 50].

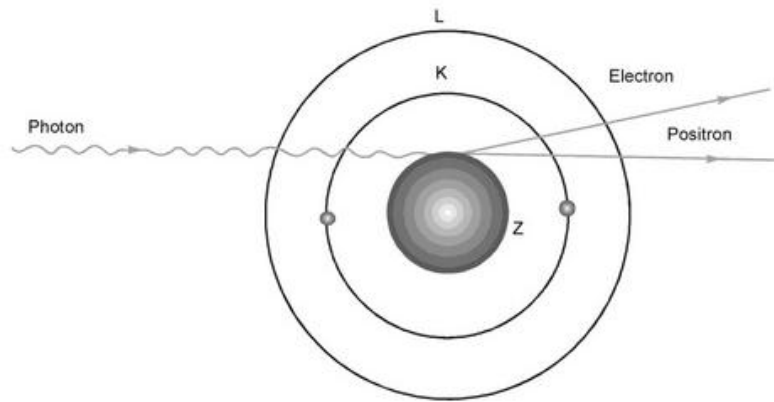


Figure 2.6 Pair production

The probability of each process is expressed as absorption coefficient. The total absorption coefficient is sum of absorption coefficients of the three processes. The various absorption coefficients depend upon the energy of the γ -rays as well as nature of absorbing material. Thus, the absorption of γ -rays cannot be expressed in single formula. Each partial absorption coefficient is expressed as function of energy for given material and tables have been prepared for different materials. The total absorption coefficient μ of a given material is expressed by the formula:

$$\mu(E) = \mu_{pe}(E) + \mu_{\sigma}(E) + \mu_{pp}(E) \quad (2.27)$$

Where indices pe, σ and pp stand for photoelectric effect, Compton scattering and pair product respectively.

A graph of the linear attenuation coefficient for photon in lead as function of photon energy. The contribution of linear absorption coefficient of photoelectric effect μ_{pe} , Compton scattering μ_{σ} , and pair production μ_{pp} is shown in figure (2.7).

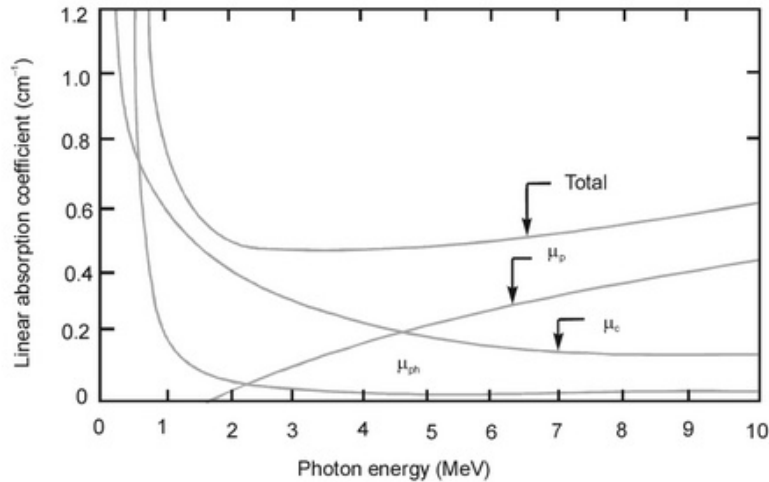


Figure 2. 7 The linear coefficient as a function of photon energy

2.7.5 Gamma radiation shielding:

When gamma radiation interacts with matter, its intensity will decrease as it travels through matter. The decrease in intensity of radiation is dependent mainly on the type of target material and its thickness in its path. The attenuation properties of radiation for particular target materials are required to determine the amount of shielding necessary and how much dosage one would receive if that particular target material is used for the shielding.

The type and amount of shielding required depend on: the type of radiation, the activity of radiation source, and the dose rate that is acceptable for outside the shielding material. However, there are other factors for choice of shielding material such as their cost and weight. An effective shield will result in a large energy more hazardous radiation.

Furthermore, the good shielding material should have high absorption cross-section for radiation and the same time irradiation effects on its mechanical and optical properties should be small. There are two main methods for radiation shielding materials: first, shielding materials are furnished on the wall surface or directly on it, and second, these materials are covered around the radiation source.

In general various materials have been used for the radiation shielding in different applications. The scattering and absorption of gamma radiations are related to density and effective atomic numbers of material. Knowing the mass attenuation

coefficient is prime importance. However, the linear (μ_L, cm^{-1}) has been described to investing the radiation shielding properties of any shielding material [52, 54].

2.7.6 Gamma rays shielding design:

For shielding design gamma ray is one of the main type of nuclear radiation, which have to be considered, since any shield that attenuates gamma rays will be more effective for attenuating other radiations. In principle, any material can be used for radiation shielding if it a sufficient thickness to absorb the incident radiations to a safe level.

The objective of gamma rays shield design is to find the thickness of material or a combination of materials that would attenuate the intensity of the radiation to a level that would not adversely affect individuals in the vicinity of the gamma rays radiation field.

The attenuation factor of a beam of initial intensity I_0 in a shield of thickness x is:

$$\frac{I(x)}{I_0} = B e^{-\mu x} \quad (2.28)$$

Where B is the buildup factor.

The buildup factor B is simply a multiplicative factor for extended sources [44, 55].

The value of B depends on the nature and thickness of the attenuating medium and on the gamma ray energy. The buildup factor is thus defined as:

$$B = \frac{\text{Actual gamma ray flux}}{\text{Flux obtained using exponential attenuation law}}$$

Taking the natural logarithm of both sides, we get:

$$\mu x = -\ln \left[\frac{1}{B} - \frac{I(x)}{I_0} \right] \quad (2.29)$$

If the desired attenuation factor and the attenuation factor in the medium used as shield are known, then we can estimate the needed thickness x from:

$$x = \frac{1}{\mu} \ln \left[\frac{1}{B} - \frac{I(x)}{I_0} \right] \quad (2.30)$$

2.7.7 Gamma ray detection:

All nuclear radiation detection is based on the interactions with matter. The detection methods are in general based on the process of excitation or ionization of atoms in the detector by the passage of charged particles. Electromagnetic radiation gives rise to energetic electrons by one of the three types of interactions with matter [56]. Radiation loses all or part of the energy by making interactions since enter into material. If photon sweeps away an electron from the atom of material, this atom becomes ionized. Excitation condition is the condition that exists for atomic nucleus [57].

Different factors are important in the choice of gamma detector:

- (i) The resolving power which determines the complexity of the spectrum that can conveniently be analyzed.
- (ii) The detection efficiency which dictates the source strength necessary for the measurement of spectrum.
- (iii) The simplicity of the arrangement and the ease of data accumulation.
- (iv) Secondary factors as the response linearity, the stability, the ratio of the photoelectric interactions to Compton interactions, the timing accuracy, etc.

Detectors may be employed in numerous ways as detectors recording all radiation passing through the sensitive detection volume, as rate meters recording the radiation flux, as spectrometers yielding information about the energies, and the intensities of the gamma radiation [56].

There are three types of detectors that are most commonly used depending on the specific needs of the device. These are Gas filled detectors, Scintillators and Solid state detectors. Each has various strengths and weakness that recommend them to their own specific roles.

2.7.7.1 Gas-filled Detectors:

The first type of radiation detector Gas filled detectors are amongst the most commonly used. There are several types of Gas filled detector, and while they have various differences in how they work, they all are based on similar principles.

Many radiation detectors are based on measuring the effects produced by the ionizing radiation as it passes through a gas filled chamber. As the radiation passes through the gaseous medium, the radiation excites and ionizes the gas molecules along its path. The gas-filled detectors include ionization chambers, proportional counters, Geiger tubes, etc. and in all these devices, the ionization produced by the incident radiation generates an electrical signal. They can be constructed with metal and ceramic components and are usually filled with inert gas. Therefore, these devices can be made relatively robust and tolerant to high radiation and temperature levels. They can be installed in the inaccessible areas in the nuclear facilities and their signals can be monitored remotely to obtain information about the radiation. The gas-filled detectors consist of a gas filled chamber with central electrode well insulated from the chamber walls as shown in figure (2.8). A voltage V is applied between the wall and the central electrode dissipates part or all of its energy by generating electron-ion pairs. Both electrons and ions are charge carriers that move under the influence of electrical field. Their motion includes a current on the electrode, which may be measured. Or, through appropriate electronics, the charge produced by the radiation may be transformed into a pulse, in which case particles are counted individually [48, 58, and 59].

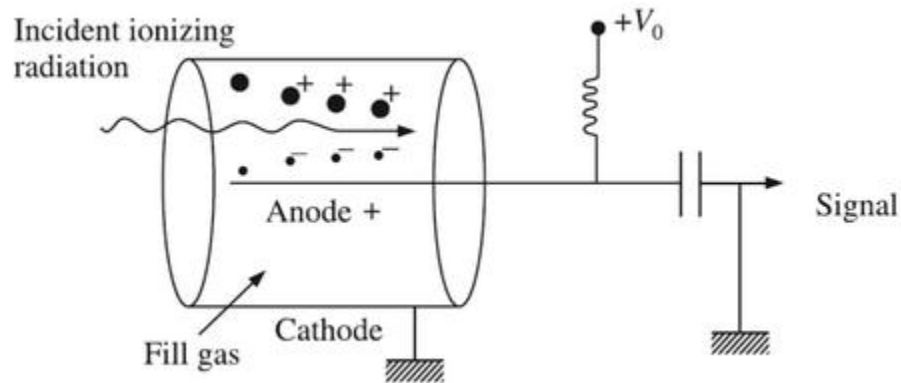


Figure 2.8 Schematic diagram of Gas-filled detector

The different types of Gas filled detector are: ionization chamber, proportional counters and Geiger-Muller (GM) tubes. The major differentiating factor between these different types is the applied voltage across the detector, which determines the types of response that detector, will register from an ionization event.

2.7.7.2 Scintillators Detectors:

The second major type of detectors utilized in radiation detection instruments are scintillation detectors. The name of these detectors comes from the fact that the interaction of a particle with some materials gives rise to a scintillation or flash of light [60]. The scintillation mechanism can be explained by means of the energy band theory. In this model, a band gap separates the valence band (filled band) of conduction band (usually empty). Thus, via the ionization process, an electron can be excited from the valence band to the conduction band or to the energy states located close to the mid-gap. An excitation is formed when the electron removed remains electrostatically bonded with the hole left in the valence band. The electron excited to these states decays to ground state emitting light in the visible range of electromagnetic spectrum. This visible light interacts with photo cathode and electrons are emitted by photoelectric effect or Compton scattering, producing a current in the circuit. However, scintillation detectors produce currents of low intensity and only after the advent of photomultiplier tubes has its use become feasible [61] as shown in figure (2.9).

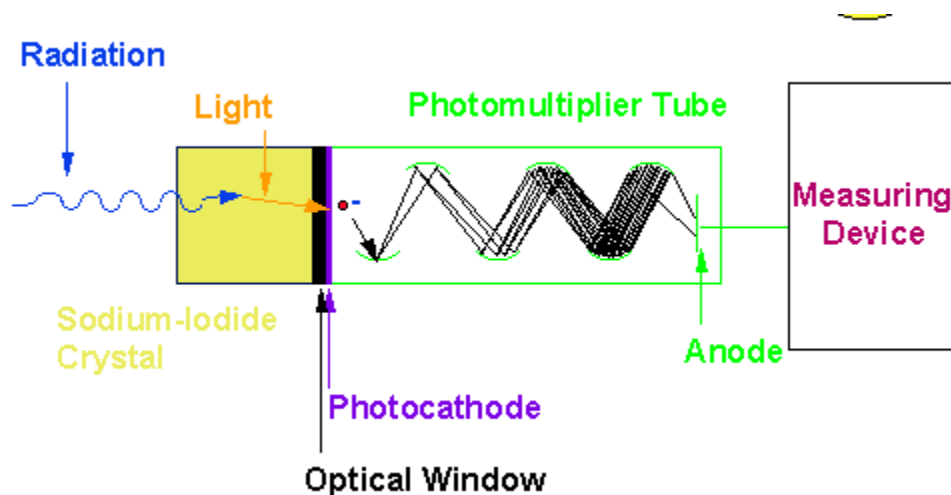


Figure 2.9 Scintillation Detector

Due their high sensitivity and their potential ability to “identity” radioactive sources, scintillation detectors are particularly useful for radiation security applications. These can take many forms, from handheld devices used to screen containers for hidden or shielded radioactive material, to monitors set up to screen large areas or populations, able to differentiate between natural or medical sources

of radiation and sources of more immediate concern, such as special nuclear material (SNM).

2.7.7.3 Solid state Detectors:

The last major detector technology used in radiation detection instruments are solid state detectors. Solid state detectors referred to as semiconductor detectors, are made from semiconductor materials. These detectors benefit from a small energy gap between the semiconductor valence- and conduction- bands. Therefore, a small energy deposition can move electrons from the valence-band to the conduction band, leaving holes behind when an electric field is applied, the two charge carriers (electron and hole) drift toward their respective electrodes and produce a signal. Therefore, the passage of ionizing particle in the sensitive part of a solid state detector can be detected by collecting the charge carriers liberated by energy deposition in the semiconductor [62].

Silicon solid state detectors are composed of two layers of silicon semiconductor material, one “n-type”, which means it contains a greater number of electrons compared to holes, and one “p-type”, meaning it has a greater number of holes than electrons. Electrons from the n-type migrate across the junction between the two layers to fill the holes in the p-type, creating what’s called depletion zone.

This depletion zone acts like the detection area of an ion chamber. Radiation interacting with the atoms inside the depletion zone causes them to re-ionize, and create an electronic pulse which can be measured. The small scale of the detector and of the depletion zone itself, means that the ions pairs can be collected quickly, meaning that the instruments utilizing this type of detector can have a particularly quick response time. This, when coupled with their small size, makes this type of solid state detector very useful for electronic dosimetry.

Semiconductor detectors, in particular silicon and germanium detectors were used for quite some time, but not too frequently, in Nuclear Physics for the purpose of measuring particle and X-ray photon energies, not however for position measurement [63].

2.8 Geiger-Muller Tube (GM Tube):

The Geiger-Mueller counter (commonly referred to as the G-M counter, or simply Geiger tube) is one of the oldest radiation detector types in existence, having been introduced by Geiger and Mueller in 1928. However, the simplicity, low cost, and ease of operation of these detectors have led to their continued use to the present time [64]. A Geiger counter (Geiger-Muller tube) is a device that can detect and measure all types of radiation: alpha, beta and gamma radiation. It consists of a tube filled with low pressure (0.1 atm) inert gas (The gas used is usually Helium or Argon) and an organic vapor. Inside the chamber, there are two electrodes, between which a potential difference of several hundred volts created without any flow of current [65]. The ions (and electrons) are attracted to the electrodes and an electric current is produced. A scale counts the current pulses, and one obtains a "count" whenever radiation ionizes the gas [66].

2-8-1 Principle: It works on the principle that nuclear radiations while passing through the gas contained in GM counter ionized it.

2-8-2 Construction: The GM tube is cylindrical in shape as shown in figure (2.10). This cylinder is either made up of conducting metal like copper, which acts as a cathode or it is made up of glass, in which a metallic cylinder is supported which acts as a cathode. However, in some cases when the tube is of glass, inner sides of the tube are coated with a conducting metal like copper or silver. This coating acts as cathode. Anode is generally made up of tungsten wire which stretched from the cylindrical tube. The thickness of this wire is generally (0.02 to 0.05) mm.

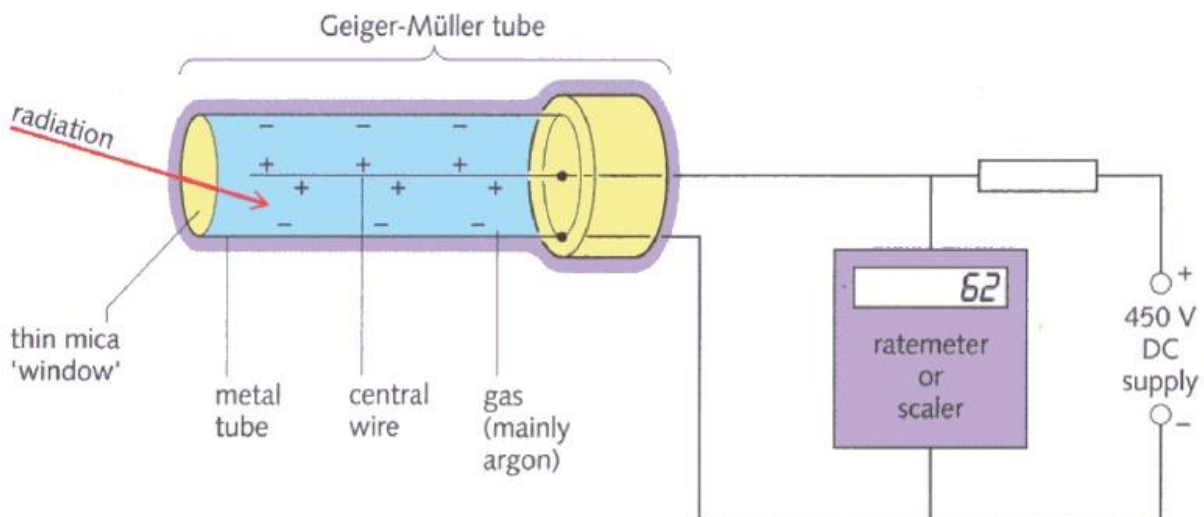


Figure 2.10 Geiger-Muller Tube

Depending upon the requirement, the GM tubes are available in a variety of sizes. The diameters of the tubes vary from 0.3 cm to about 15 cm while their lengths vary from 1 cm to 100 cm. Commercially available GM tubes are filled with 90%

argon (as the filling gas) and 10% ethyl alcohol (as the quenching gas) or 0.1% either chlorine or bromine (as quenching gas) and the rest is neon or argon gas. A thin glass, mica or polymer window ($\sim 10\mu\text{m}$) isolates the gases present in GM counter from the atmosphere.

3-8-3 Working: The charged particles entering the GM tube ionize the gas present in the tube. This event is been known as primary ionization. The electrons liberated in the primary ionization are accelerated towards the central anode wire. Because of high potential present on the wire, the electrons may gain sufficient energy to cause further ionization of the natural gas molecules (known as secondary ionization). This leads to chain of ionizing events which is known Townsend avalanche.

Beside these processes, there is a possibility of excitation of molecules and atoms. Such excited molecules and atoms, while de-exciting, may emit ultra violet (UV) or visible photons. These photons again lead to the production of electrons due to ionization of gas atoms or molecules or due to photoelectric interaction with walls of counter. Each such liberated electron would again cause a Townsend avalanche. Such a series of avalanches would lead to discharged in the tube called Geiger discharge. In such a state, there is a formation of dense envelop of electron-ion pairs distributed around the anode. The voltage applied to anode collects all the electrons pertaining to single event leading to Geiger discharge.

3-8-4 Characteristics of GM tubes: The important parameters which decide the quality of functioning of GM tubes are (i) Dead time, (ii) Recovery time, and (ii) Geiger plateau length and plateau slope.

Chapter Three

Literature Review

3.1 Introduction:

Different attempt were made to relate thermodynamics properties of matter to the physical properties of bulk matter. Theoretical models were also constructed to explain some of these properties which are slight bit complex since matter is in non-equilibrium state. Some of these attempts were presented here.

3.2 Explanation of Intensity Spectral change of Bhutan, Carbon dioxide, Carbon Monoxide, Oxygen, Nitrogen Gases on the basic of Non Equilibrium:

In this work an attempt was made to relate temperature change to the change of spectra of some gases, which are Bhutan (C_4H_{10}), Carbon dioxide (CO_2), Carbon Monoxide (CO), Oxygen (O_2), Nitrogen (N_2). The spectra of this gas were displayed by USB2000 spectrometer, when their temperature changes from (300 to 337) K considerable change in the spectral intensity was observed. These changes can be explained theoretically by using non-equilibrium statistical distribution by using plasma equation, beside the laws of quantum mechanics.

She gets these results of her study:

Table (3-2-1): spectrum of Bhutan () at different temperatures

T = temperature λ = wavelength I = Intensity A = area W=width

T(K)	λ (nm)	A(m2)	W (nm)	I(a.u)
300	630.73	4390.43	6.92	126.8
301	630.78	2536.69	6.96	125.89
303	630.83	2282.57	7.07	125.74
305	630.79	1645.95	7.03	125.79
307	630.78	1645.9	7.02	125.79
309	630.84	1855.9	7.16	125.13
311	630.78	1888.66	7.1	124.64
313	630	1698.66	7.03	124.79
315	630.83	1482.01	7.003	124.53
317	630.86	1560.78	7.03	123.96
318	630.84	1717.5	7.04	123.5
319	630.89	2037.01	7.08	123.46
320	630.95	1310.88	6.95	117.62
323	631.01	1265.28	7.02	116.95
324	631.01	1276.02	7.05	116.65

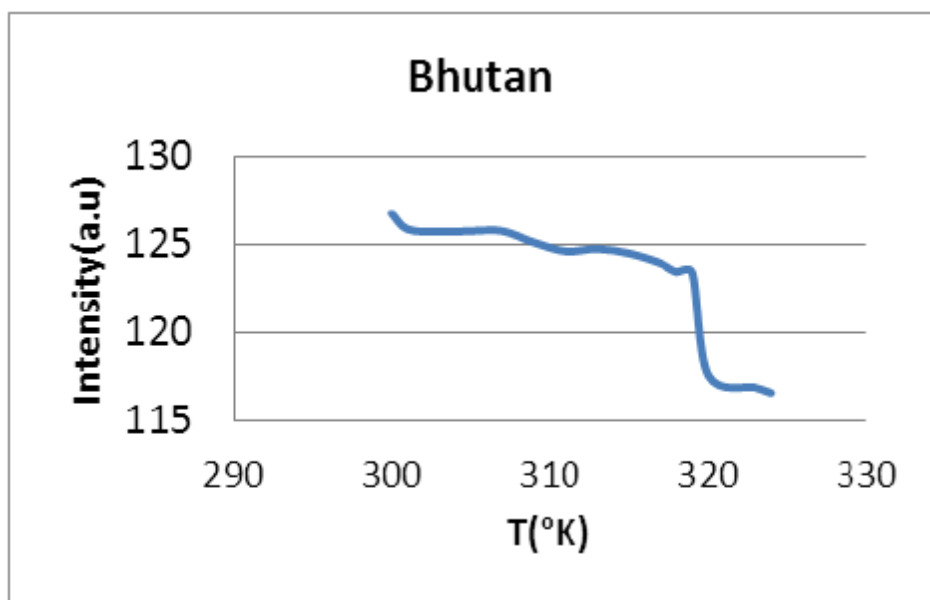
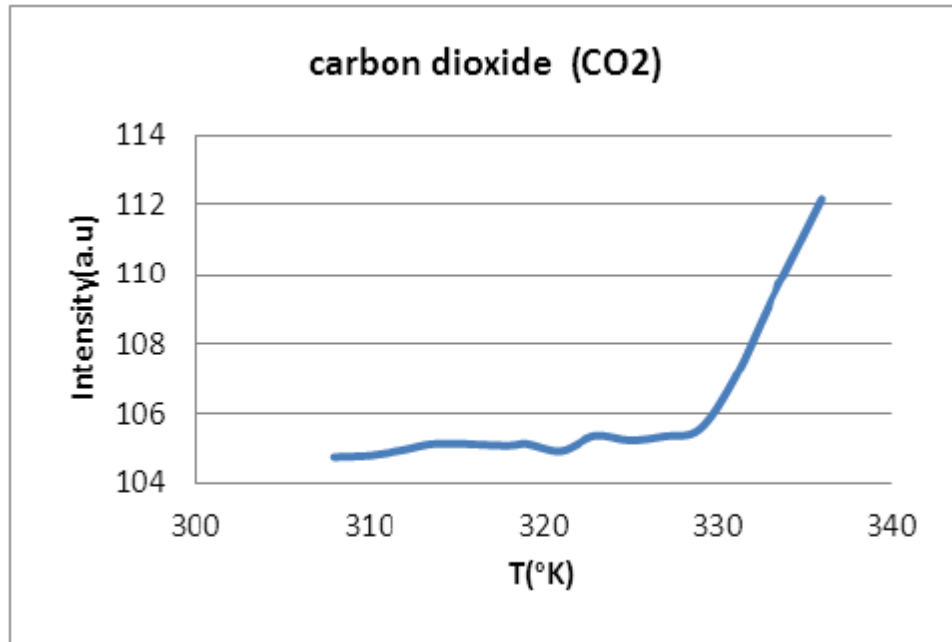


Fig (3-2-1-1) Relation between Intensity and temperature

Table (3-2-2): spectrum of Carbon dioxide (CO₂) at different temperatures

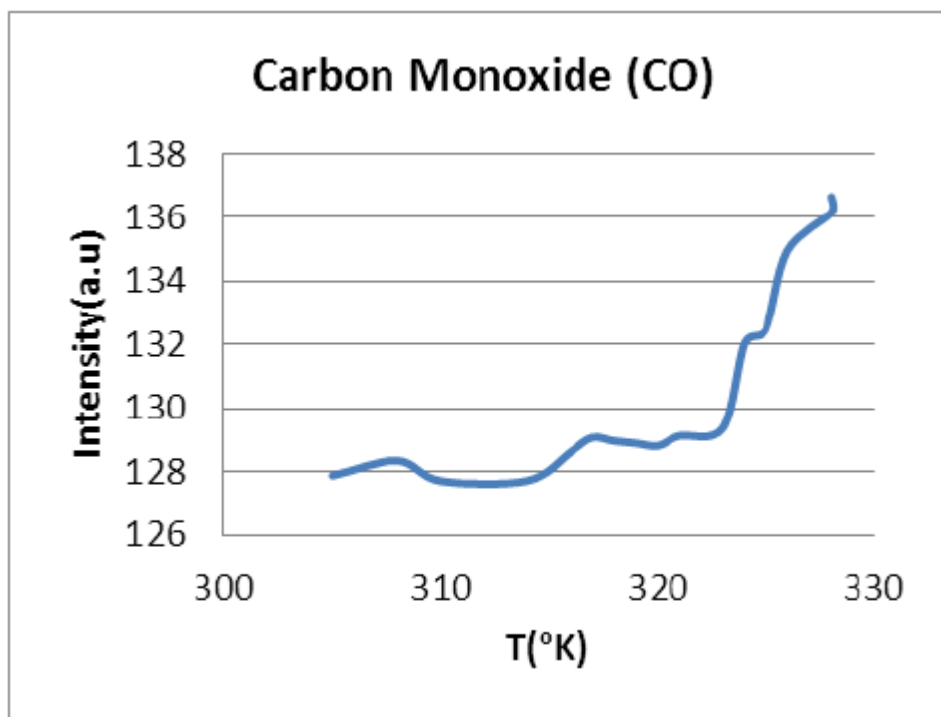
T(K)	λ(nm)	A(m2)	W(nm)	I(a.u)
308	631.09	6721.97	7.09	104.78
310	630.69	3971.93	6.56	104.82
312	630.71	2990.83	6.61	104.98
314	630.68	2313.09	6.67	105.16
318	630.67	2672	6.59	105.105
319	630.73	2562.34	6.62	105.16
321	630.77	2788.17	6.63	104.95
323	630.75	2604.82	6.71	105.38
325	630.81	2746.3	6.76	105.25
327	630.75	2630.97	6.68	105.37
329	630.77	2896.99	6.58	105.56
331	630.66	3235.75	6.72	107.02
333	630.7	2852.53	6.67	109.16
336	630.64	2867.93	6.73	112.15



Fig(3-2-2-1) relationship between intensity and temperature

Table (3-2-3): spectrum of Carbon Monoxide (CO) at different temperatures

T(K)	λ (nm)	A(m2)	W(nm)	I(a.u)
305	630.81	7727.23	7.19	127.88
308	630.83	17902.95	7.52	128.35
310	631.15	23879.64	7.95	127.71
314	631.24	28752	8.02	127.72
316	630.95	35431.03	7.82	128.63
317	630.87	33455.02	7.63	129.07
318	630.97	35343.99	7.67	128.96
319	630.75	36682	7.59	128.89
320	630.5	31212.8	6.31	128.81
321	630.54	30925.51	6.29	129.12
323	630.53	35011.42	6.37	129.37
324	630.62	29236.35	6.28	132.05
325	630.62	30482.95	6.83	132.47
326	630.61	32561.45	6.4	134.94
328	630.6	28986.9	6.43	136.16



Fig(3-2-3-1) relationship between intensity and temperature

Table (3-2-4): spectrum of Oxygen (O₂) at different temperatures

T(K)	λ (nm)	A(m²)	W (nm)	I(a.u)
307	630.38	6.33	8357.87	121.82
309	630.39	6.45	8237.15	124.16
310	630.36	6.29	10776.64	105.39
312	630.39	6.34	9984.4	107.28
313	630.33	6.26	10333.1	108.35
317	630.36	6.36	10055.14	111.84
319	630.25	6.29	8871.58	114.79
320	630.1	6.37	10285.94	126.56
322	630.17	6.31	6953.2	126.2
323	630.14	6.37	7661.5	126.12

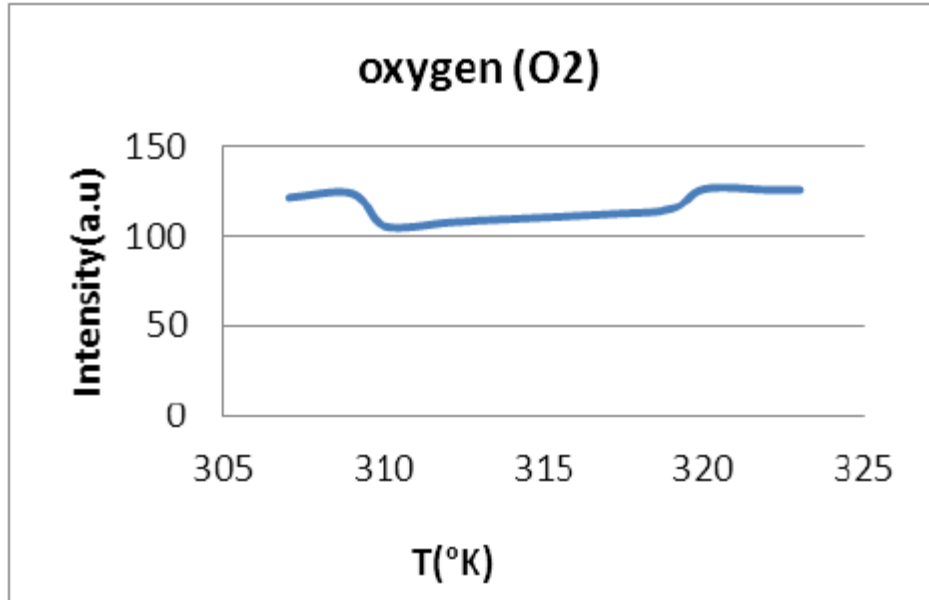
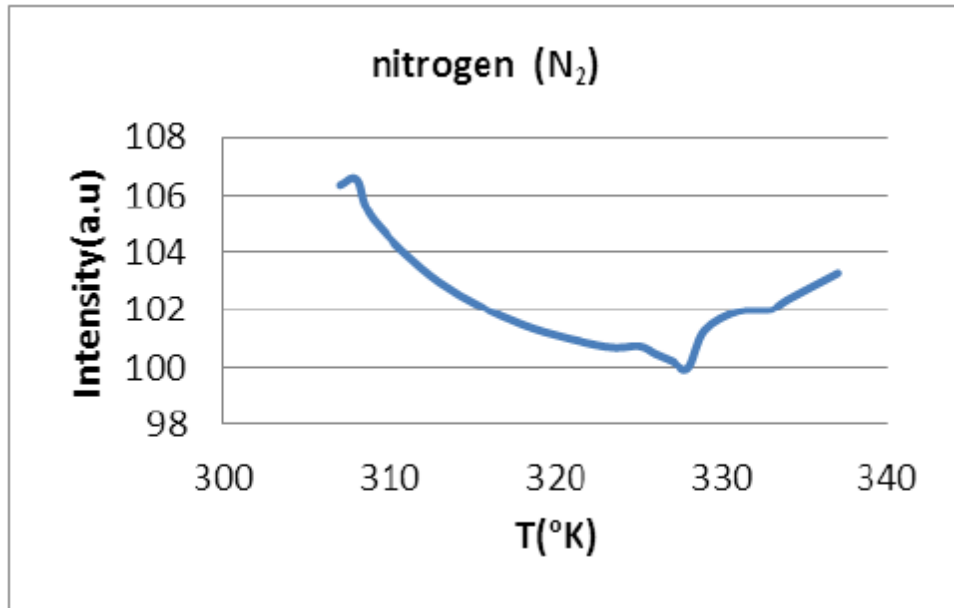


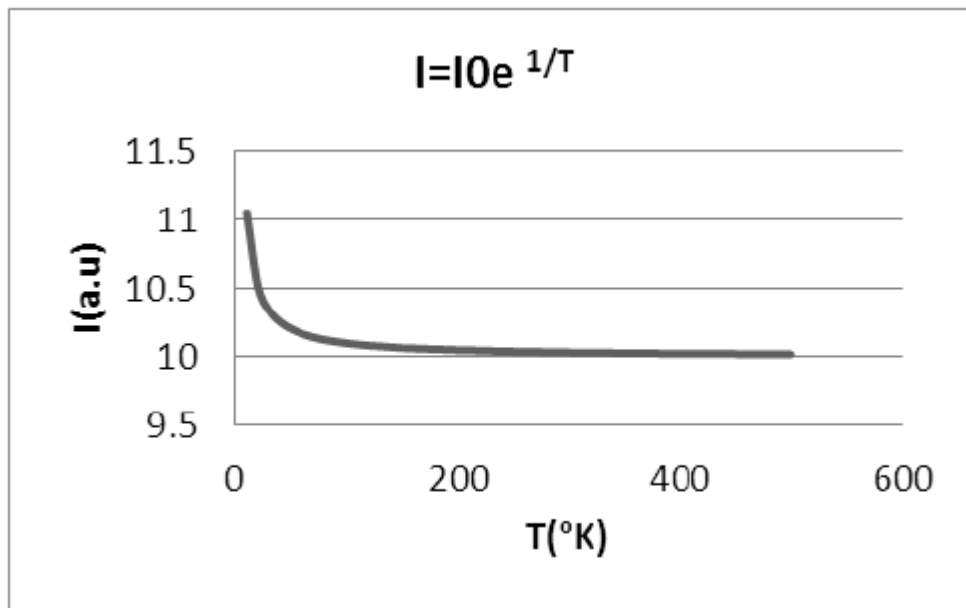
Fig (3-2-4-1) relationship between intensity and temperature

Table (3-2-5): spectrum of Nitrogen (N₂) at different temperatures

T(K)	λ (nm)	A(m2)	W(nm)	I(a.u)
307	630.57	13210.75	6.46	106.37
308	631.05	22845	7	106.55
309	631.17	19689.5	7.03	105.14
313	631.14	26622.9	7.06	102.97
318	631.03	37660.7	7.02	101.47
323	631.04	22161.25	7.04	100.71
325	631.02	17831.8	6.99	100.73
326	631.15	20802.4	6.99	100.46
327	631.07	20115.56	7.05	100.21
328	631.05	23555.87	7.12	99.97
329	631.07	13968.94	6.99	101.27
331	631.1	13849.26	7.07	101.94
333	631.13	13601.3	7.07	102
334	631.15	14948.05	7.06	102.37
337	631.01	13328.25	7.02	103.29



Fig(3-2-5-1) relationship between intensity and temperature



Fig(3-2—5-2)

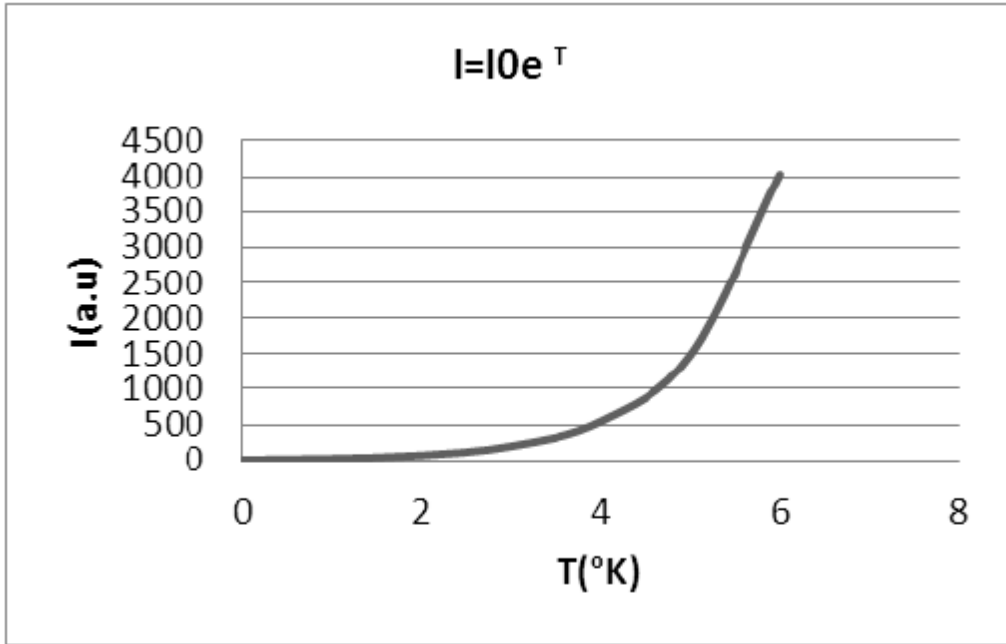


Fig (3-2-2)

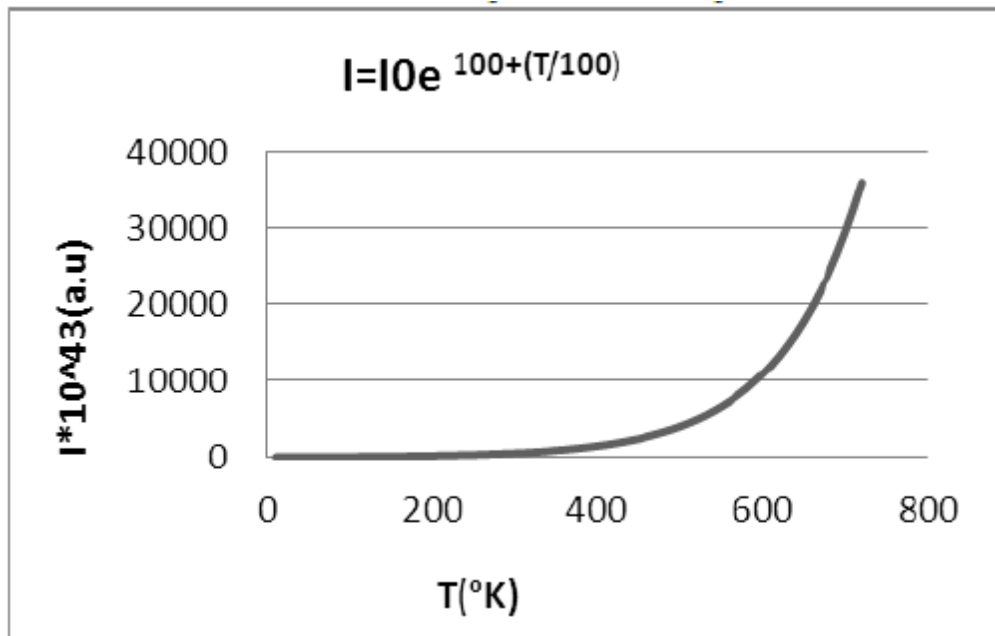


Fig (3-2-3)

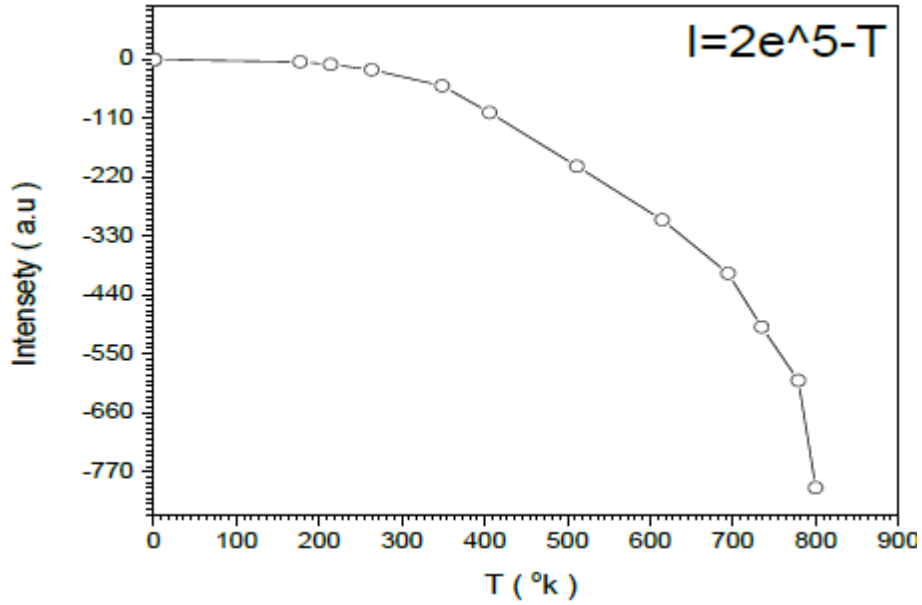


Fig (3-2-4)

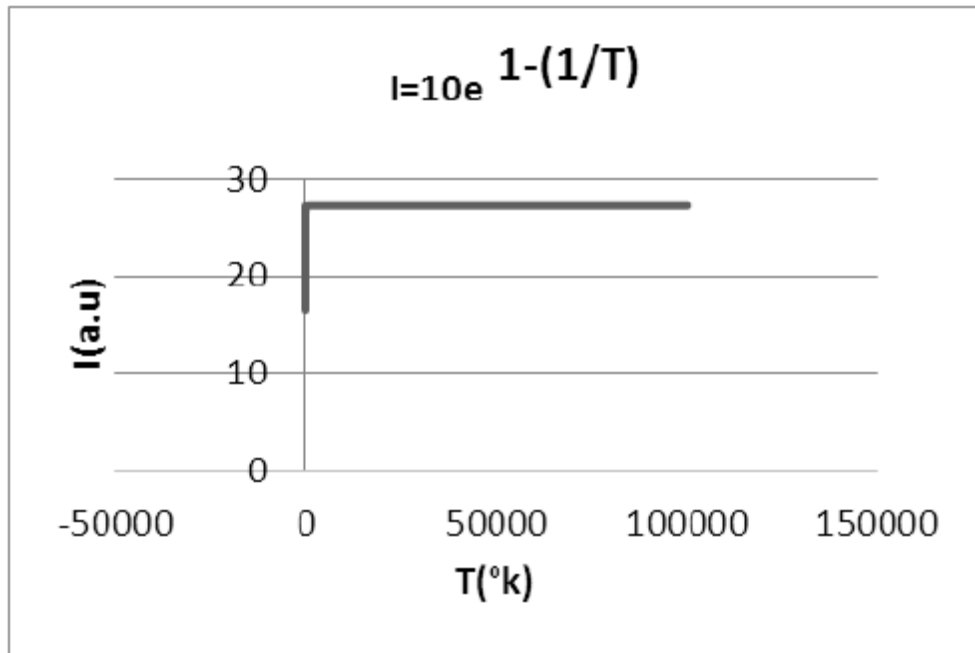


Fig (3-2-5)

Fig (3-1-1) shows the Relation between Intensity and temperature for Bhutan (),the curve of this relation resembles that of fig(3-2-4).This means the Bhutan gas the homogenous repulsive electron gas potential is almost constant compared to attractive ion potential and temperature. Fig (3-1-2) shows the Relation between Intensity and temperature for Carbon dioxide (CO2) which has a curve that resembles the curve in figs (3-2-2)and (3-2-3) .This indicates that the attractive positive ions looks homogeneous and stable compared to temperature. This is not

surprising since the gas was heated at the bottom by a heater. This means that the bottom is hotter than the top part of the gas. Thus the temperature is not uniformities. In Fig (3-1-3) the Relation between Intensity and temperature for Carbon Monoxide (CO) which is displayed in this fig, resembles the curve of figs (3-2-2) and (3-2-3). This is not surprising, since for both figures the statistical distribution is based on the homogeneity of the ionic field and non-homogeneity of temperature. The non-homogeneity of temperature results again from the fact that the bottom of the gas exposed to a heater is very hot compared to the top of the gas. However Fig (3-1-4) shows that the Relation between Intensity and temperature for Oxygen (O₂) can be easily explained by fig (3-2-5) where the repulsive homogeneous electron field dominates compared the attractive ionic field. Fig (3-1-5) shows for Nitrogen (N₂) its spectrum is displayed by the Relation between Intensity and temperature. The curve of this relation resembles fig (3-2-1) which shows homogeneity of temperature compared to less homogenous attractive crystal field (67).

3.3 Interpretation of the Effect of Temperature on the Change of Spectra of Atmospheric Gases on the Basis of Modified Quantum Statistical Equations:

The determination of atmospheric temperature requires a new approach for temperatures determination by using simple and cheap technology. To perform this task an attempt was made in this research to relate temperature change to the change of spectra of some gases which are Butane (C₄H₁₀), Neon (Ne), Fluorine (F₂) and chlorine (Cl₂). These gases were heated at temperature in the range (300 - 337)K. The spectra of these gases were displayed by USB2000 spectrometer. The result shows appreciable change in the spectral intensity and line width. These changes were shown to be explained theoretically on the basis of non-equilibrium statistical physics by using plasma equation and quantum mechanical laws that relates the photon intensity to atomic and electronic wave functions.

Table (3-2-1): spectrum of Bhutan (C_4H_{10}) at different temperatures

T = temperature λ = wavelength

I = Intensity **A** = area **W**=width

T(K)	λ (nm)	A(m2)	W (nm)	I(a.u)
300	630.73	4390.43	6.92	126.8
301	630.78	2536.69	6.96	125.89
303	630.83	2282.57	7.07	125.74
305	630.79	1645.95	7.03	125.79
307	630.78	1645.9	7.02	125.79
309	630.84	1855.9	7.16	125.13
311	630.78	1888.66	7.1	124.64
313	630	1698.66	7.03	124.79
315	630.83	1482.01	7.003	124.53
317	630.86	1560.78	7.03	123.96
318	630.84	1717.5	7.04	123.5
319	630.89	2037.01	7.08	123.46
320	630.95	1310.88	6.95	117.62
323	631.01	1265.28	7.02	116.95
324	631.01	1276.02	7.05	116.65

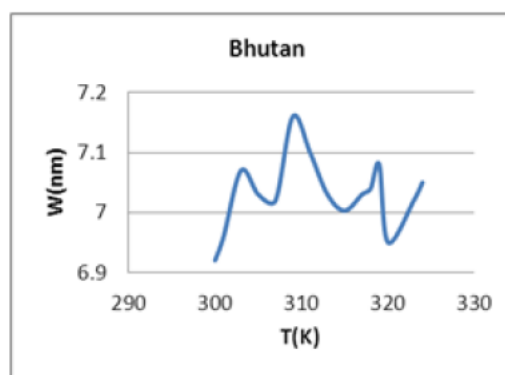
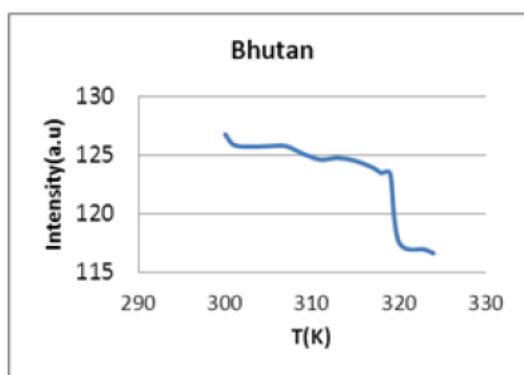


Fig (3-3-1): Relation between Intensity and temperature

Fig (3-3-2): Relation between line width and temperature

Table (3-2-2): spectrum of Neon (Ne)at different temperatures

T(K)	λ (nm)	A(m2)	W(nm)	I(a.u)
307	630.66	6071.9	6.41	102.94
312	630.7	2287.59	6.48	103.25
313	630.76	1941.9	6.51	103.04
315	630.74	2111.14	6.46	103.45
317	630.73	3099.17	6.51	103.21
319	630.77	2276.22	6.53	103.26
320	630.78	3762.85	6.46	103.34
321	630.8	3515.7	6.51	103.39
322	630.77	2276.22	6.53	103.25
323	630.77	3179.53	6.48	103.4

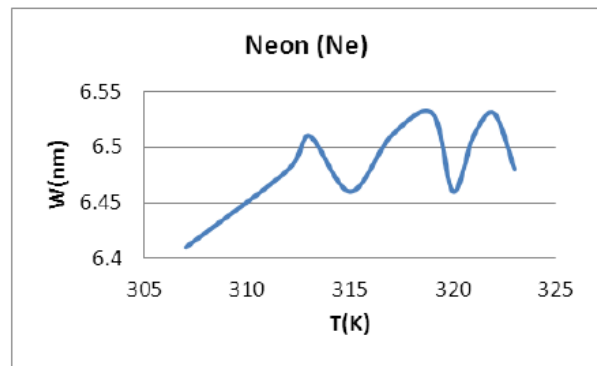
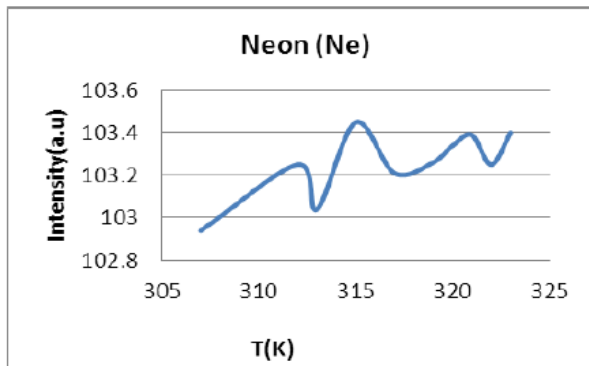


Fig (3-4-1): Relation between Intensity and temperature

Fig (3-4-2): Relation between line width and temperature

Table (3-2-3): spectrum of Fluorine (F2)at different temperatures

T(K)	λ (nm)	A(m2)	W(nm)	I(a.u)
304	631.02	6337.97	7.04	100.25
305	630.81	5964.04	6.44	98.63
307	630.9	5565.97	7.11	102.13
309	630.01	4442.99	7.16	102
311	631.01	5302.56	7.23	101.88
312	630.98	5332.11	7.25	101.52
314	631.06	4669.27	7.23	101.95
316	631.05	5193.09	7.16	101.82
317	631.08	5193.92	7.19	101.37
319	631.04	4549.7	7.2	101.66
321	631.11	3541.63	7.21	102.04
323	631.07	3351.55	7.13	102.3
325	631.08	4702.13	7.18	102.5

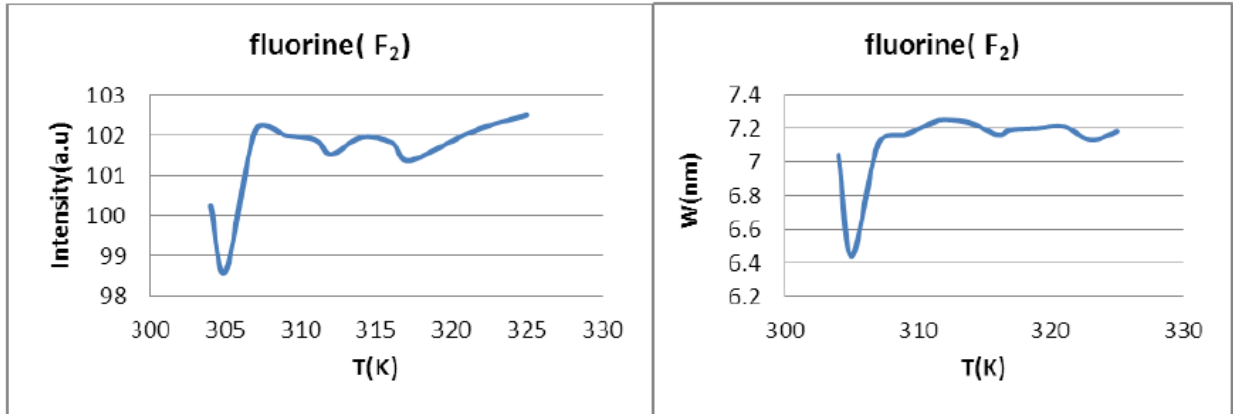


Fig (3-5-1): Relation between Intensity and temperature Fig (3-5-2): Relation between line width and temperature

Table (3-2-4): spectrum of Chlorine (CL₂) at different temperatures

T(K)	λ (nm)	A(m2)	W(nm)	I(a.u)
301	630.86	15934.5	6.92	122.23
303	630.83	7706.45	7.03	130.73
306	630.96	7478.8	7	124.24
308	630.95	8890.52	7.01	124.92
311	630.88	5738.32	7.08	126.31
313	630.94	5137.66	7.11	127.67
315	630.87	4995.6	7.01	127.81
317	630.88	4764.68	7.11	128.59
319	630.85	6501.06	7.006	129.27
321	630.93	4897.88	7.09	130.43
323	630.72	7777.74	6.88	131.22
325	630.77	6840.38	7.012	132.51
327	630.75	4907.18	6.92	134.15
329	630.75	5803.33	7.001	135.56
330	630.77	2866.74	7.05	137.006
331	630.83	2045.54	7.09	137.77

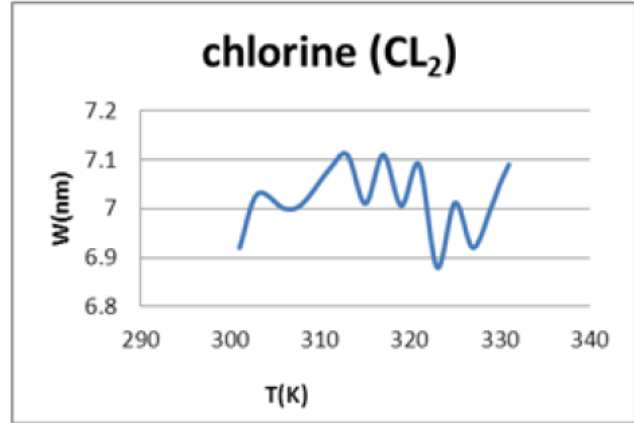
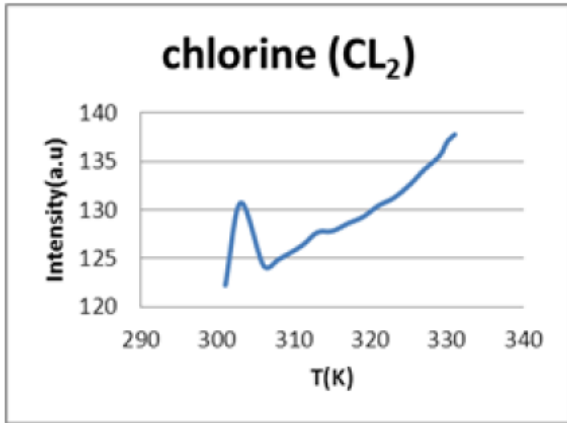


Fig (3-6-1): Relation between Intensity and temperature

Fig (3-6-2): Relation between line width and temperature

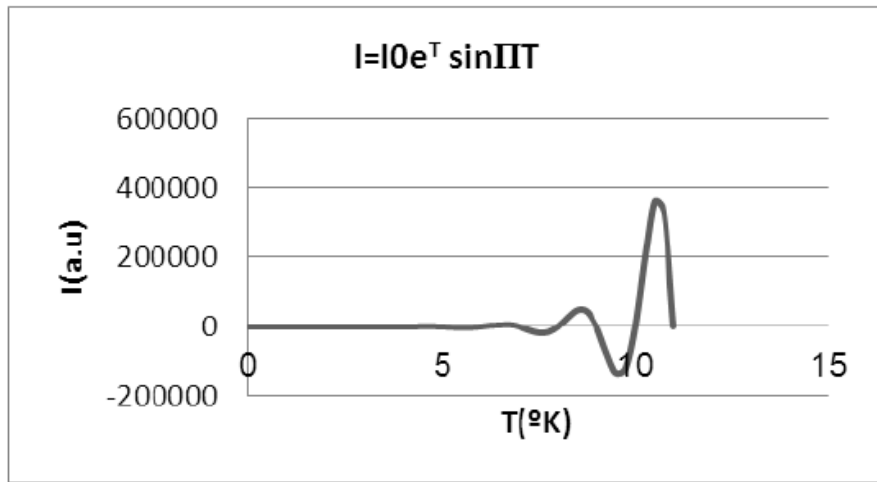


Fig (3-7-1)

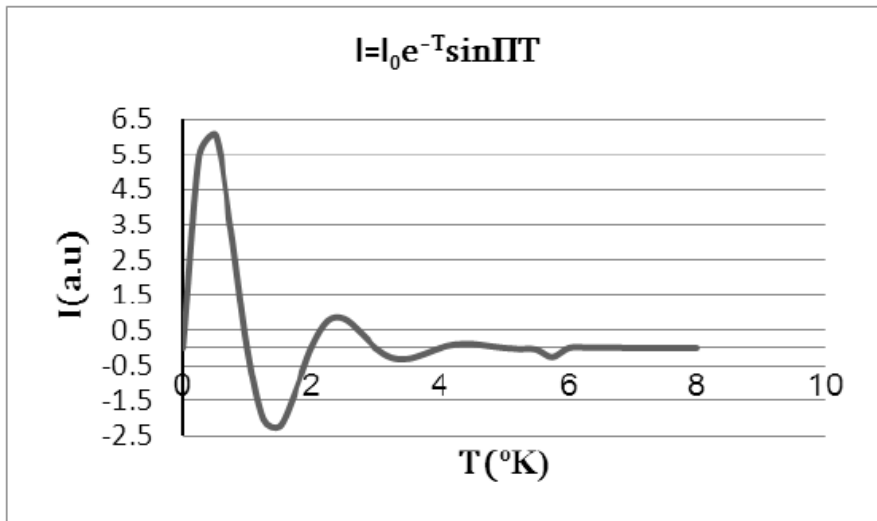


Fig (3-7-2)

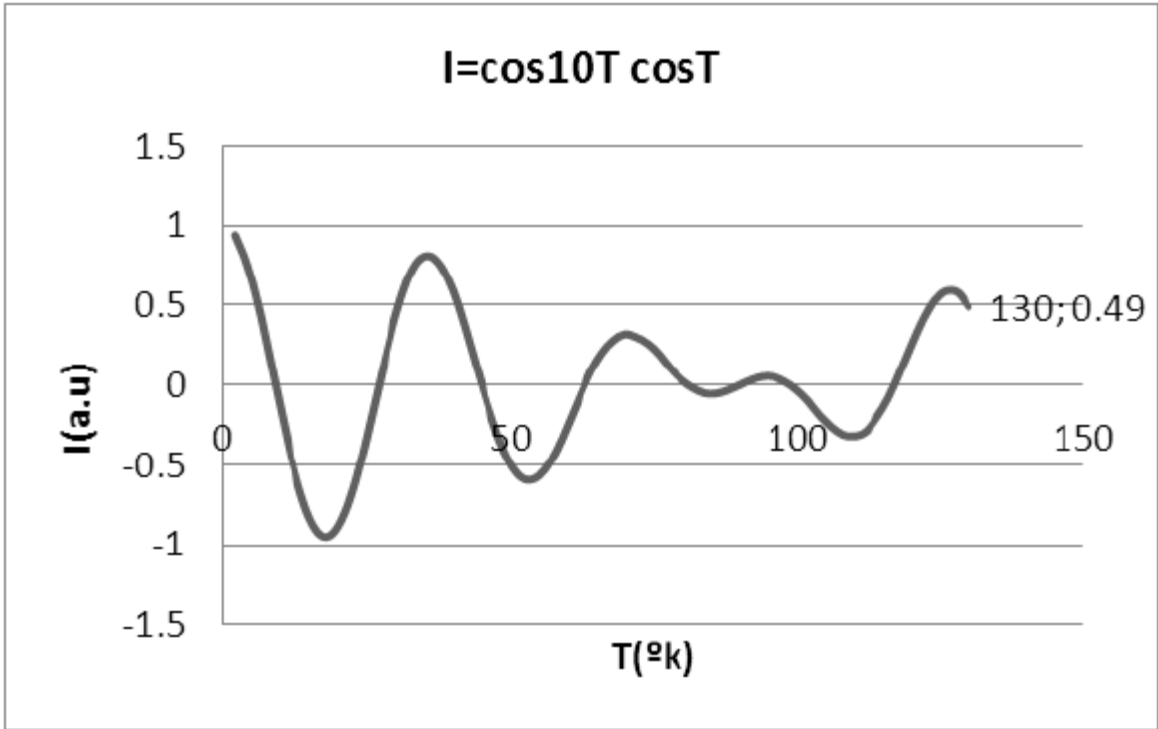


Fig (3-7-3)

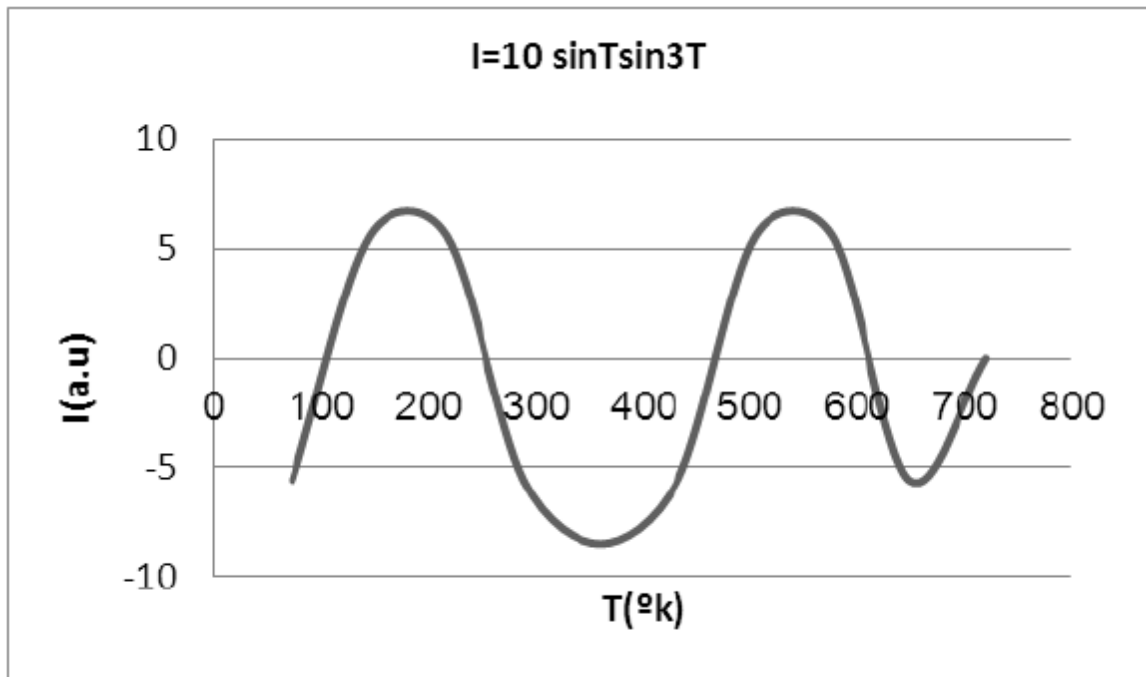


Fig (3-8-1)

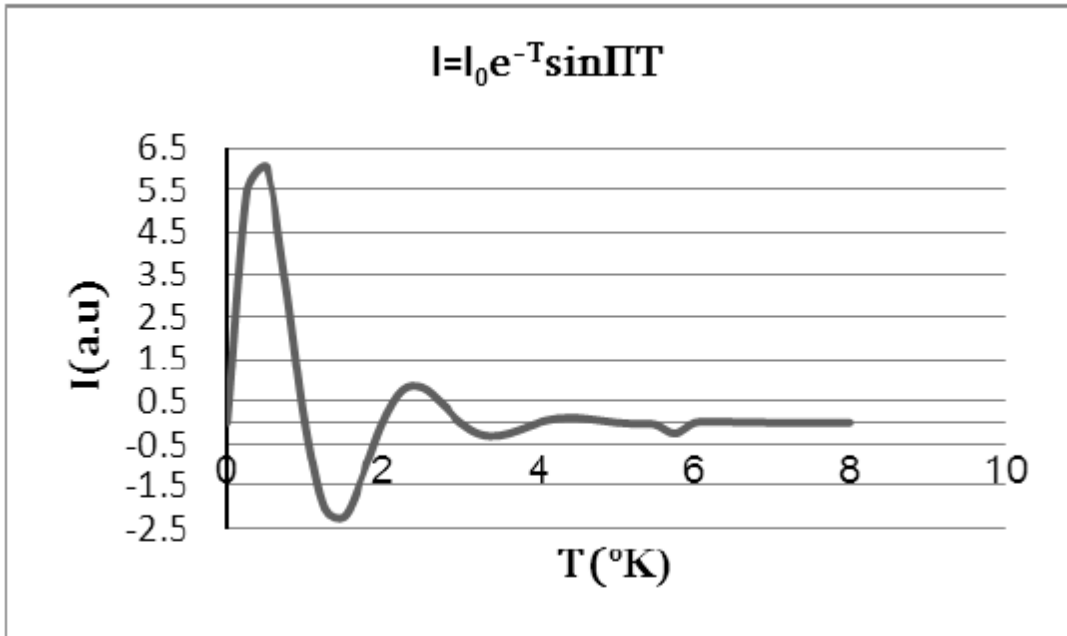


Fig (3-9-1)

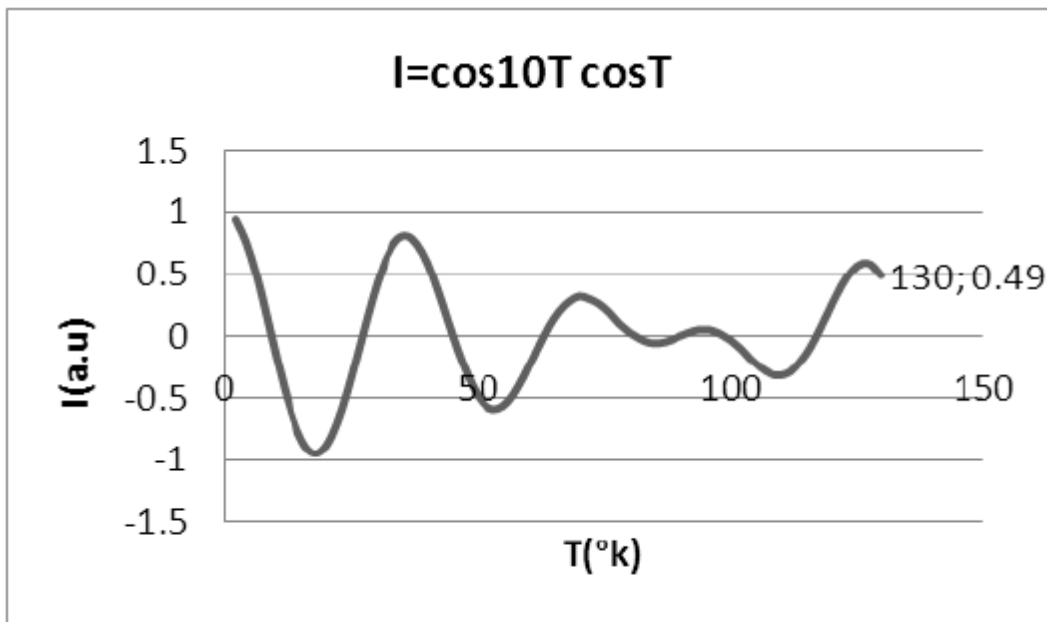


Fig (3-9-2)

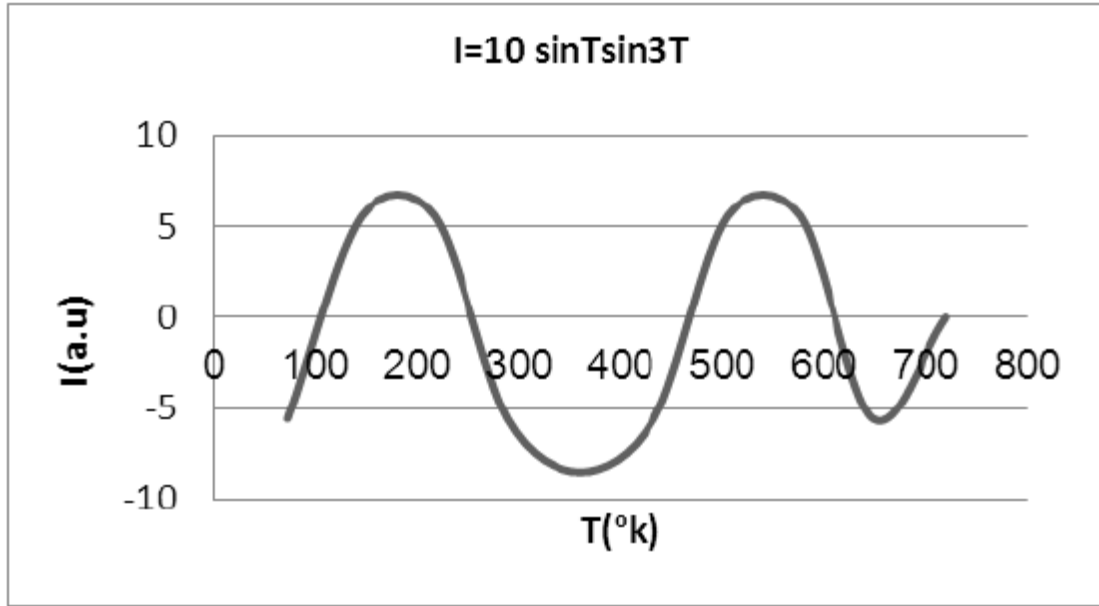


Fig (3-9-3)

The relation between Intensity and temperature for Neon (Ne) see fig. (3-4-1) resembles that obtained theoretically in equations:

$$I = I_0 e^{\left(\frac{E_1}{V_m}\right)} \left[\sin \frac{E_2}{V_m} \right] \dots \dots \dots (3 - 1 - 1)$$

And

$$I = I_0 e^T \sin C_0 T \dots \dots \dots (3 - 1 - 2)$$

$C_0 = \pi$

Where:

E_1 : Kinetic thermal energy, E_2 : the lost thermal energy, T : temperature, and V_m : Ion potential.

(3-1-5) and (3-1-8) ,for the case when the temperature Is non-uniform[see fig (3-7-1)]. Thus And the electric static potential is assumed to be uniform. This agrees with the fact that the gas is heated at the bottom, where it is very hot, while its temperature at the top is less. The same empirical relation for Ne can be explained by using quantum mechanics model in Fig (3-8-1).

The model based on semi classical harmonic oscillator and quantum mechanics explains the effect of temperatures on the line width of the spectrum for the gases Bhutan (C_4H_{10}), Neon (Ne), Fluorine (F_2) and chlorine (CL_2). The comparison of Figs (3-3-2) with Fig (3-9-2), (3-4-2) with Fig (3-9-3) , (3-6-2) with Fig (3-9-2) and(3-5-2) with Fig (3-7-2) shows that the theoretical relations of line width with temperatures resembles the corresponding empirical relation (68).

3.4 Quantum Heat Flow Model for Heat Flow in Some Nanotubes:

Using Schrodinger equation for resistive medium a useful expression for heat flow through Nano tubes has been found. Fortunately, this equation resembles that obtained by Moran Wang et al, and Hai- Dong Wang teal. The ordinary thermal conductivity is constant. The effective thermal conductivity temperature dependent resembles that obtained for carbon Nano tubes and Boron Nitride Nano tubes. It is also finite at low temperature which also conforms with experimental data for carbon and Boron. Since Nano materials are described by quantum lows, this new model is thus more suitable for Nano tubes, as for as it is derived using quantum laws (69).

3.5 Thermal conductivity coefficients on the base of phonon model and Einstein energy relation for nanomaterial:

In this work the dependence of phonon speed on temperature is shown to be affected by the physical constraints on the system. for low speed phonon it is directly proportional to the square root of temperature ,while for high speed it is directly proportional to the temperature .however for thermally agitated medium it is inversely proportional to the temperature .The latter dependence has been used to construct a model to find the thermal conductivity coefficient .Where the heat flow rate by massive phonons together with Einstein energy-momentum relations have been used to find the thermal conductivity coefficient .This expressions agrees with the models of Moran-Zeng and Hai-Bing, explain the thermal behavior of carbon Nano tubes to the conventional more over it one at high temperature (70).

3.6 The effect of annealing temperature, doping carbon nanotubes with TiO₂, CuO, ZnO and MgO on its conductivity and electrical primitively:

In this work TiO₂, CuO, ZnO, and MgO, were used to dope carbon nano tube at different annealing temperatures 450, 500, 550, and 600 °C. The spectrum of the conductivity and dielectric constants were displayed at different annealing temperatures. It was found that the conductivity and dielectrics constants decrease when the temperature is increased for all samples except for MgO where they increase. These relations are explained theoretically (71).

3.7 The Effect of Annealing Temperature Change on Carbon Nano Tube Absorption and Refractive Index When Doped With TiO₂, CuO, ZnO and MgO :

Carbon nano tubes were doped with TiO₂, CuO, ZnO and MgO at different annealing temperatures 450, 500, 550 and 600 °C respectively. The absorption coefficients and refractive index for all samples as function of temperature were displayed graphically at different wave lengths. It was found that the absorption coefficient for TiO₂ and CuO decreases upon increasing temperature, while that of ZnO and MgO increases with temperature. The refractive index decreases when temperature increases for all doping component except for MgO, where it increase. These relations are explained theoretically (72).

3.8 Effects of laser glazing on CMAS corrosion behavior of Y₂O₃ stabilized ZrO₂ thermal barrier coatings:

Calcium-magnesium-alumina-silicate (CMAS) is a serious threat to thermal barrier coatings (TBCs). The goal of this study is to tailor YSZ coating microstructures by laser for alleviating CMAS attack. A smooth laser glazed layer with a columnar microstructure and some open channels is produced on the coating surface. Under molten CMAS conditions, the glazed layer remains phase stability and has little evidence of dissolution. Exposed to thermal shock tests with CMAS deposits, the glazed layer keeps structural integrity. However, the open channels also act as the paths for CMAS penetration, which brings destructive damages to the coating beneath the glazed layer.

This study confirms that laser glazing is an effective method to alleviate CMAS attack to APS YSZ TBCs. Compared with the as-sprayed coating, the laser modified coating has three main microstructural changes, i.e., columnar grains, smooth surface, and open channels consisting of vertical cracks and inter-columnar gaps. Exposed to CMAS at 1250 °C for 10 h, the laser glazed layer still keeps phase stability and has little microstructure degradation. The open channels benefit the thermal shock performance of the coating due to the enhanced strain tolerance, but it also acts as the CMAS penetration path. As a result, the glazed layer becomes dense due to the sintering additive function of CMAS components, and the coating beneath the glazed layer is severely destroyed based on a dissolution/re-precipitation mechanism. This causes the glazed layer deformation or even spallation. To explore the possible applications of the laser modified coatings, future work should be conducted on the laser parameters optimization and the microstructure design of the laser glazed layer (73).

3.9 The Concept of force for thermodynamic frictional system:

A new thermodynamic first Law is proposed to account for the effect of friction and gravity force. This Law proposes existence of thermal impulsive force which produces pressure force and overcomes the frictional and gravity forces. This new Law is verified experimentally by allowing a cylindrical piston made from AL, Cu, and fiber glass to move under the action of water vapor thermal force. Strikingly the empirical relations between the different parameter and physical quantities concerning thermal, pressure, friction and gravity force agrees completely with the proposed theoretical ones. This law also in complete agreement with the fluid energy equation (74).

3.10 The Concept of Energy for Thermodynamics Friction System:

Using the fluid energy equation, the first Law of thermodynamics for frictional system in the presence of gravity is formulated. According to this new model thermal energy is equal to pressure work beside kinetic energy in addition to work against gravity and frictional energy. This formula is verified experimentally by deriving a piston, moving inside a cylindrical tube, by water vapor. Three pistons made from AL, Cu, and fiberglass were used. The piston and cylinder system is inclined subtend the angles 0, 10, 20... 90, in steps of 10 degree for each reading. The vapor thermal force tries to push the piston up word against frictional and gravity force. The relations between kinetic energy with net work done, frictional and gravity energy is in complete agreement with this new thermodynamic model. This Law was verified and confirmed experimentally (75).

3.11 Internal heat generation effect on transient natural convection in a Nano fluid-saturated local thermal non-equilibrium porous inclined cavity:

The aim of the study is to analyze the convective flow and heat transfer of Nano fluid in an inclined cavity filled with heat generating porous medium using the local thermal non-equilibrium model. The horizontal bottom wall of the cavity is maintained at a constant higher temperature while the left and right vertical walls are maintained at a constant lower temperature. The top wall is to be kept as adiabatic. The Darcy model is adopted for flow through the porous medium and the Boussinesq approximation is taken into account. The pores are saturated by a water-based Nano fluid consisting of Cu nanoparticles. The governing equations are solved iteratively by finite difference based Alternating Direction Implicit (ADI) method. The average heat transfer rate decreases when increasing the values of nanoparticle volume fraction for the case of high Rayleigh numbers. The heat

transfer rate is enhanced by increasing values of the modified conductivity ratio and the porosity of the media.

The transient and internal heat generation effects on convective flow and heat transfer of Nano fluid in an inclined porous cavity using the LTNE model are numerically examined. The governing equations are solved iteratively by the Alternating Direction Implicit method. According to this study the flow speed increases by increasing the internal heat generation parameter and these results in the enhancement on heat transfer. The flow pattern is changed drastically when changing the inclination of the cavity. The weighted-average Nusselt number increases as solid-volume fraction increases for low values of Rayleigh number and it decreases as solid-volume fraction increases for high values of Rayleigh number.

(d) The weighted-average Nusselt number decreases when increasing the values of the dimensionless heat generation (Q). The weighted-average Nusselt number enhances with increased the values of modified conductivity ratio, porosity of the medium and solid volume fraction (76).

3.12 X-ray diffraction and thermodynamics kinetics of SiB 6 under gamma irradiation dose:

In the work of M.N. Mirzayev silicide hexaboride (B_6Si) was irradiated with ^{60}Co at room temperature to study the structural changes and weight kinetics.

The B_6Si samples were irradiated using a gamma source with a dose rate (D) of 0.27 Gy/s. At adsorption dose range of 9.7, 48.5, 97, 145.5 and 194 kGy. The samples were analysed using X-ray diffraction (XRD) and Energy dispersive spectroscopy (EDS) to study the microstructural and composition changes. The XRD results showed the crystalline structure for the sample before and after irradiation (with gamma irradiation dose 9.7, 48.5 and 97 kGy). Amorphization of the sample began at the gamma irradiation dose of 145.5 kGy. Increase in gamma irradiation dose had an inverse effect on the activation energy and had a directly proportional effect on the lattice volume.

The effect of irradiation of B_6Si and determining the energy state of the system before and after gamma irradiation was investigated. XRD and EDS were used to analyse the microstructural changes. A change in the lattice parameters was observed due to irradiation. The lattice volume of the B_6Si sample was observed to increase with increase in gamma. irradiation dose. The increase in volume was attributed to the stress/stain experienced by the samples due to increase in gamma irradiation dose. A structural change from crystalline to amorphous state after irradiation was observed. Low irradiation dose (9.7 kGy, 48.5 kGy and 97 kGy) retained the crystalline structure while 145.7 kGy partial amorphization of the material was observed. Irradiating at 194 kGy led to an increase in amorphization

on the B6Si. At 145.5 kGy a processes of oxygen chemisorption was observed to increase by 1.5%. After gamma irradiated of the samples, two energy barrier states were created. The first energy barrier changed from 0.14 eV (0 kGy) to 0.26 eV (197 kGy) and second energy barrier changes from 0.22 eV (0 kGy) to 0.46 eV (197 kGy) at room temperature (77).

3.13 Thermodynamics kinetics of boron carbide under gamma irradiation dose:

In this paper, high purity boron carbide samples were irradiated by ^{60}Co gamma radioisotope source (0.27 Gy/s dose rate) with 50, 100, 150 and 200 irradiation hours at room-temperature. The unirradiated and irradiated boron carbide samples were heated from 30 $^{\circ}\text{C}$ to 1000 $^{\circ}\text{C}$ at a heating rate of 5 $^{\circ}\text{C}/\text{min}$ under the argon gas atmosphere of flow rate 20 ml/min. Thermo gravimetric (TG) and Differential Scanning Calorimetry (DSC) were carried out in order to understand the thermodynamic kinetics of boron carbide samples. The weight kinetics, activation energy and specific heat capacity of the unirradiated and irradiated boron carbide samples were examined in two parts, $T \leq 650$ $^{\circ}\text{C}$ and $T \geq 650$ $^{\circ}\text{C}$, according to the temperature. The dynamic of quantitative changes in both ranges is deferent depending on the irradiation time. While the phase transition of unirradiated boron carbide samples occurs at 902 $^{\circ}\text{C}$, this value shifts up to 940 $^{\circ}\text{C}$ in irradiated samples depending on the irradiation time. The activation energy of the unirradiated boron carbide samples decreased from 214 to 46 J/mol in the result of 200 h gamma irradiation. The reduction of the activation energy after the irradiation compared to the initial state shows that the dielectric properties of the irradiated boron carbide samples have been improved. After the gamma irradiation, two energy barrier states depending on the absorption dose of samples were formed in the irradiated samples. The first and second energy barriers occurred in 0.56{0.80 and 0.23{0.36 eV energy intervals, respectively. The existence of two energy levels in the irradiated boron carbide indicates that the point defects are at deep levels, close to the valence band.

TG and DSC were carried out in order to understand the behaviors of the thermodynamic kinetics of boron carbide samples. All thermophysical parameters were determined based on the heat flow rate. The weight kinetics of unirradiated boron carbide samples were investigated in the two temperature intervals as $T \leq 623$ $^{\circ}\text{C}$ and $674 \leq T \leq 950$ $^{\circ}\text{C}$. The inverse relationship is obtained between the weight kinetics and heat flow rate for unirradiated boron carbide samples in the range of $T \leq 623$ $^{\circ}\text{C}$. The weight loss was observed in this temperature interval due to chemisorption reactions. The weight loss was obtained around 11.3% for unirradiated samples. In addition, the weight loss of irradiated boron carbide samples increased upto 9.1% with increasing irradiation time. On the other hand,

the weight of the unirradiated boron carbide samples showed an increase of 10% in the temperature range of $674 \leq T \leq 950$ °C. This value reached 12% of the maximum with 200 h gamma-irradiated boron carbide samples. It is considered that this increase is dependent on the occurrence of the oxidizing of boron carbide due to the chemical reaction between B₄C and oxygen at the interface of B₄C/B₂O₃. The experimental results showed that the activation energy of the irradiated boron carbide samples decreased 4.65 times compared to the initial state in the result of 200 h gamma irradiation. It can be concluded that the dielectric properties of the irradiated boron carbide samples have been improved after gamma irradiation. The specific heat capacity and energy of area in irradiated boron carbide samples increased with increasing irradiation time and temperature. The phase transition of unirradiated boron carbide sample was determined to be 902 °C. Depending on the irradiation time of irradiated boron carbide samples, the phase transition temperature of irradiated boron carbide samples ranges from 933 °C to 940 °C. After the gamma irradiation, two energy barriers are formed in the irradiated samples depending on the absorption dose of the samples. The first and second energy barriers emerged at 0.56-0.80 and 0.23-0.36 eV energy ranges, respectively. The presence of two energy levels in the irradiated boron carbide indicates that the point defects are close to the valence band at deep levels (78).

3.14 Gamma ray shielding by a new combination of aluminum, iron, copper and lead using MCNP5:

Different materials are used for the radiation shielding in different areas and for different situations. In this study, a shielding material contains aluminum, iron, copper and lead was simulated as shielding for gamma radiation. This work is concerned with four alloys with different concentrations of the four given materials to get shielding material with high efficiency, and at the same time light to be easily portable and stored. The samples were irradiated by simulated photons emitted from ¹³⁷Cs radioactive point source with 662 keV. The photon linear attenuation coefficients were calculated using MCNP5 computer code for the simulated shielding materials. Calculated values of attenuation coefficients and Half Value Layer of the all studied samples were compared with each other and with lead as a standard material used in shielding. Consequently, a new shielding material could be preferred as shielding materials against gamma radiation especially sample 4. A cylinder of about 5 cm thickness which is suitable to shield gamma rays emitted by Cs-137 source. The mass of a simulated container from sample 4 is not exceeding 22.5 kg comparing with 32.53 kg of pure lead. It is easy to be handled and stored in laboratories.

A new combination of shielding materials were developed using different compositions from aluminum, iron, copper and lead. The linear attenuation

coefficients, mass attenuation coefficients and the HVL of the selected material showed that the alloys used in this study may be preferred as shielding materials against gamma radiation. This work shows that sample No. 4 was the best composition alloy for shielding purpose of ^{137}Cs gamma rays source.

Finally, it is vital to follow the good geometry conditions in measuring the attenuation characteristics of a shielding material which is successfully achieved with computer-based model such as MCNP (53).

3.15 Thermodynamics of an austenitic stainless steel (AISI-348) under in situ TEM heavy ion irradiation:

The stability of the face-centred cubic austenite ($\gamma\text{-Fe}$) phase in a commercial stainless steel (AISI-348) was investigated through in situ transmission electron microscopy (TEM) with heavy ion irradiation at 1073 K up to a fluence of 1.3×10^{17} ions. cm^{-2} (corresponding to a dose of 46 dpa). The $\gamma\text{-Fe}$ phase was observed to decompose at a fluence of around 7.8×10^{15} ions. cm^{-2} (3 dpa) when a new phase nucleated and grew upon increasing irradiation dose. Scanning transmission electron microscopy (STEM) with energy dispersive X-ray (EDX) spectroscopy and multivariate statistical analysis (MVSA) were used to characterize the irradiated specimens. The combination of such experimental techniques with calculated equilibrium phase diagrams using the CALPHAD method led to the conclusion that the new phase formed upon irradiation is the body-centred cubic Cr-rich α' phase. At the nano scale, precipitation of M_{23}C_6 (τ -carbide) was also observed. The results indicate that ion irradiation can assist the austenitic stainless steel to reach a non-equilibrium state similar to a calculated equilibrium state observed at lower temperatures (79).

3.16 Development of Gamma-based Nondestructive Testing System for Thickness Measurement:

In this work, a simple gamma transmission-based nondestructive system has been developed for scanning thickness defects in flat rolled products and discriminated samples with respect to their density. Based on radiation attenuation, the study involved the measurement of the thickness in centimeters scales for a flat sheets of Alumina ceramic, borated glass, aluminum and iron. The practicality of using the system to detect thickness flaws in millimeter range was calculated considering a scenario that a thickness change by 1mm is present along the sheet of each sample. This is done through the assessment of the degree of transmitted attenuation experienced by a beam of high energy ionizing radiation, such as ^{241}Am directed perpendicular to the planar surface of the material. The results confirmed the sensitivity of the system for detection of flaws in both thickness scales. The sensitive of the system is about 1mm .

These results demonstrate clearly the possibility of using the proposed gamma-transmission- based sensor for thickness detection in millimeters ranges. A change by 1mm for all four samples produced detectable transmitted flux(80).

3.17 DEVELOPMENT OF GAMMA-BASED NONDESTRUCTIVE TESTING SYSTEM FOR MATERIAL DISCRIMINATION:

In this work, a simple gamma nondestructive system has been developed for discriminating samples with respect to their spectrum . Based on radiation spectra of Alumina ceramic, borated glass, aluminum and iron. The variation of the transmitted intensity with energy was considered to explore the possibility of discrimination between materials under test. The spectra haracteristic peaks of Alumina ceramic, borated glass, aluminum and iron was found to be 13kev, 40eV, 20eV ,and 17eV respectively

The gamma non destructive system can be utilized to determine the sample elemental content. Thus it can act as a simple economical spectrometer (81).

Chapter Four

Materials and Methods

4.1 Introduction:

The materials used in this work and the experimental procedures and methodology are all exhibited in this chapter.

4.2 Apparatus:

The following apparatus were used in the experiments

- Iron
- Aluminum
- Copper
- Gum Arabic
- Micrometer
- Sand paper
- Geiger-Muller Counter
- Geiger –Muller Tube
- Oven
- Gamma source (Cobalt-60)
- Lead Shielding's
- Digital thermometer

4.3 Samples preparing:

We processed three samples of materials, aluminum, iron and copper, in the form of shavings as shown in figure (4-1). Then we made six samples of each material by mixing the shavings with the Gum-Arabic and putting it in a piston (figure 4-2) to get us a disc shape after figure (4-3). Copper and Iron samples analyzed by X-Ray Fluorescence (XRF) and we found that the sample of Iron contains (99% of Fe and 1% Ti) , and the sample of Copper contains (61% Cu, 31% Zn, 5%Pb, and 3% Fe)



Figure (4-1-1): Aluminum shavings



Figure (4-1-2): Iron shavings



Figure (4-1-3): Copper shavings



Figure (4-2): Piston



Figure (4-3-1): Aluminum + Gum-Arabic After compressing in the piston



Figure (4-3-2): Iron + Gum-Arabic After compressing in the piston



Figure (4-3-3): Copper + Gum-Arabic After compressing in the piston

The samples were left to dry in the shade, and then we scratch each sample to reach the required thickness (5mm for aluminum, 4mm for copper, and 3mm for iron).

4.4 Method:

We put each disk in front of the gamma-ray source (at room temperature) and we put a GM tube in the other direction so we could measure the intensity of the radiation penetrating the disk figure (4-4). Every time we put on an extra disc with the first disk to increase the thickness and measure the radiation intensity that penetrates the samples (we take six samples of each material).

We repeated this process, with heating the samples to (40, 50, 60, and 70)⁰C. During this experiment, we took care of radiation protection by using lead shielings, so that the experiment can be as perfect as possible.



Figure (4-4-1): Experiment



Figure (4-4-2): Experiment

Chapter Five

Results, Discussion and Conclusion

5.1 Introduction:

In this chapter one exhibit the results made for the measurements of gamma radiation intensity emerged from samples of Al, Fe, and Cu having different thicknesses at different temperatures. Discussion and conclusion are presented also in this chapter.

5.2 Results:

After the experiment was completed, we got the results in the following tables.

Table (5-1-1): The count rate of Gamma –ray penetrating Aluminum samples at room temperature and after heating

Thickness (mm)	Counter rate (cps) $T_c=24^{\circ}\text{C}$	Counter rate (cps) 40°C	Counter rate (cps) 50°C	Counter rate (cps) 60°C	Counter rate (cps) 70°C
5mm	3.3	1.1	1.2	1.31	1.45
10mm	2.85	1.05	1.1	1.21	1.38
15mm	2.6	1	1.08	1.13	1.18
20mm	2.31	1.2	1.2	1.24	1.16
25mm	1.9	0.61	0.76	0.83	1.11
30mm	1.85	0.88	0.7	1.03	0.98

Table (5-1-2): The count rate of Gamma –ray penetrating Iron samples
at room temperature and after heating

Thickness (mm)	Counter rate (cps) $T_C=24^{\circ}\text{C}$	Counter rate (cps) 40°C	Counter rate (cps) 50°C	Counter rate (cps) 60°C	Counter rate (cps) 70°C
4mm	2.18	2.08	2.11	2.2	2.43
8mm	1.9	2.05	2.08	2.15	2.16
12mm	1.8	1.93	1.63	1.7	1.81
16mm	1.75	1.35	1.33	1.18	1.33
20mm	1.58	1.73	1.3	1.5	1.35
24mm	1.43	1.08	1.28	1.6	1.66

Table (5-1-3): The count rate of Gamma –ray penetrating Copper samples
at room temperature and after heating

Thickness (mm)	Counter rate (cps) $T_C=24^{\circ}\text{C}$	Counter rate (cps) 40°C	Counter rate (cps) 50°C	Counter rate (cps) 60°C	Counter rate (cps) 70°C
3mm	4.26	7.33	7.7	7.78	7.63
6mm	4.01	5.06	5.26	5.31	5.53
9mm	3.58	2.75	3.21	3.6	3.65
12mm	3.45	2.35	2.45	2.68	3.16
15mm	2.7	2.36	2.56	2.81	2.95
18mm	0.98	1.45	1.58	1.78	1.9

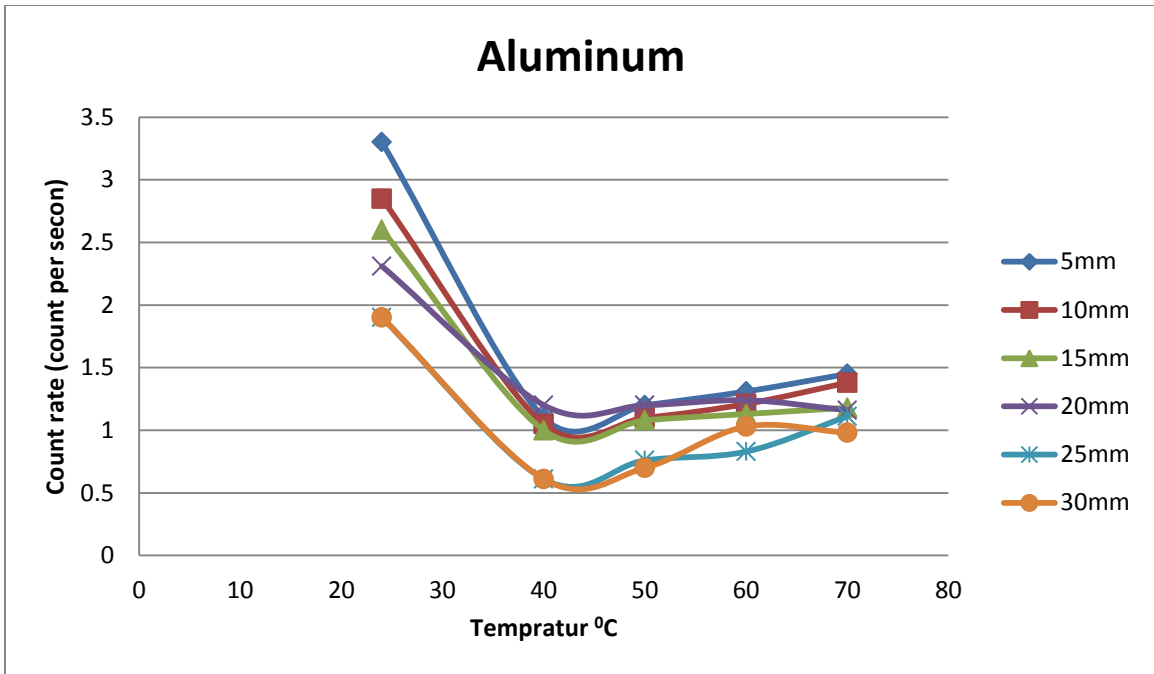


Figure (5-1-1): Relation between the count rate and temperature in different thicknesses of Aluminum

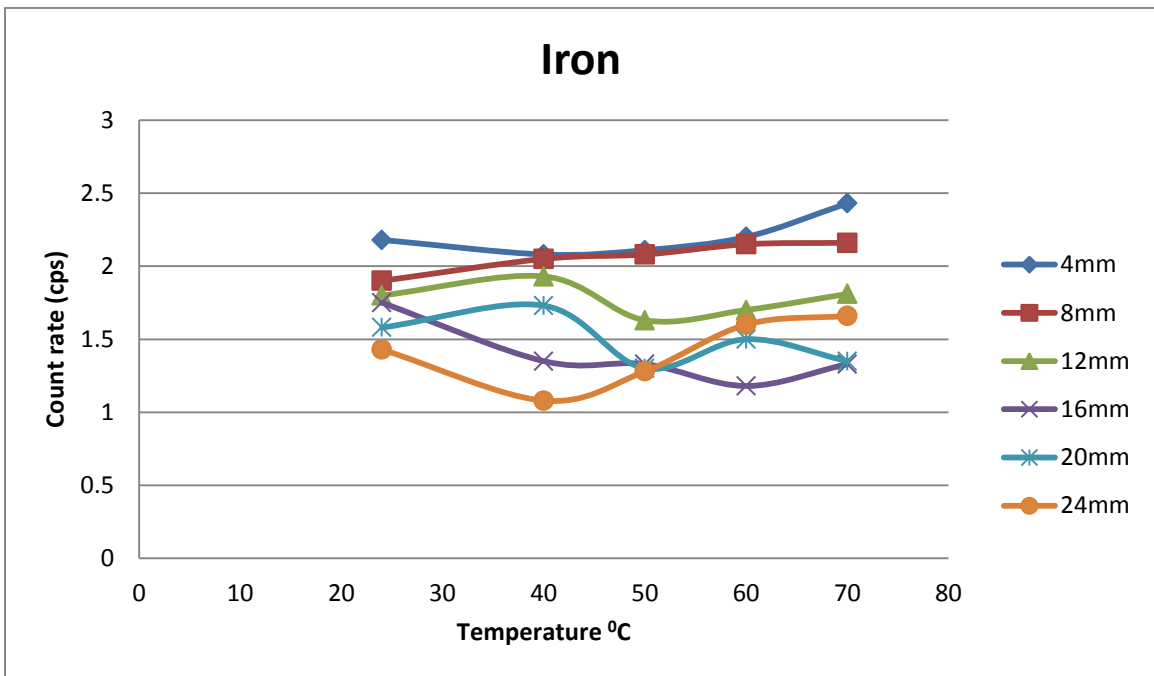


Figure (5-1-2): Relation between the count rate and temperature in different thicknesses of Iron

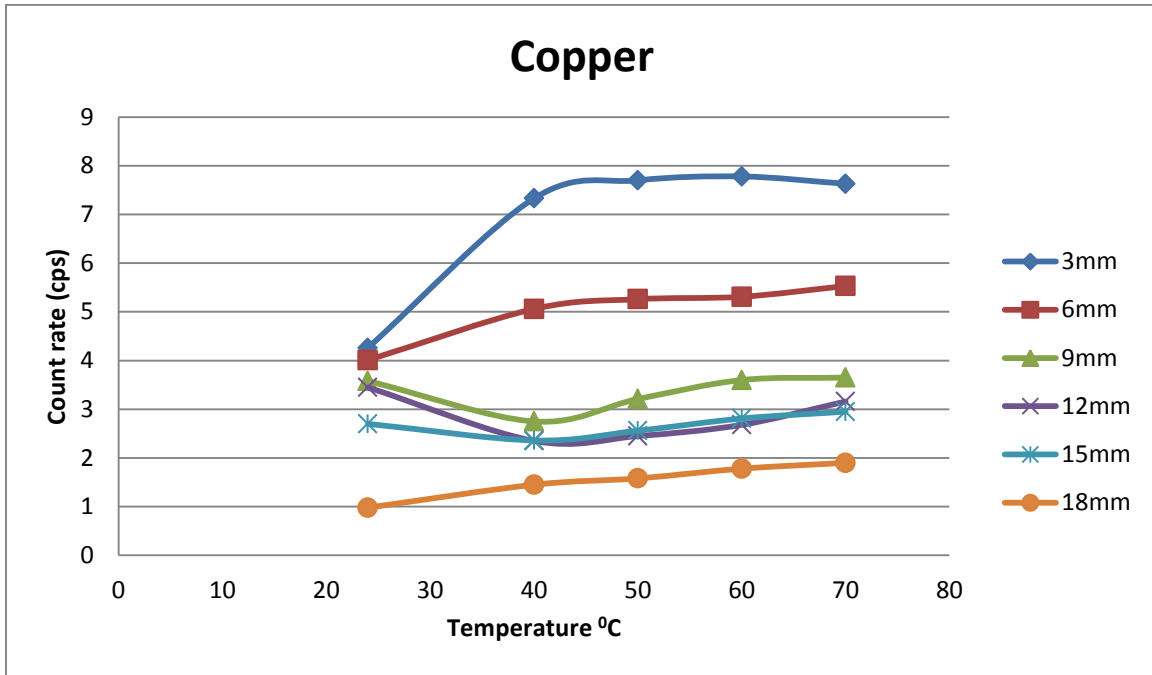


Figure (5-1-3): Relation between The count rate and temperature in different thicknesses of Copper

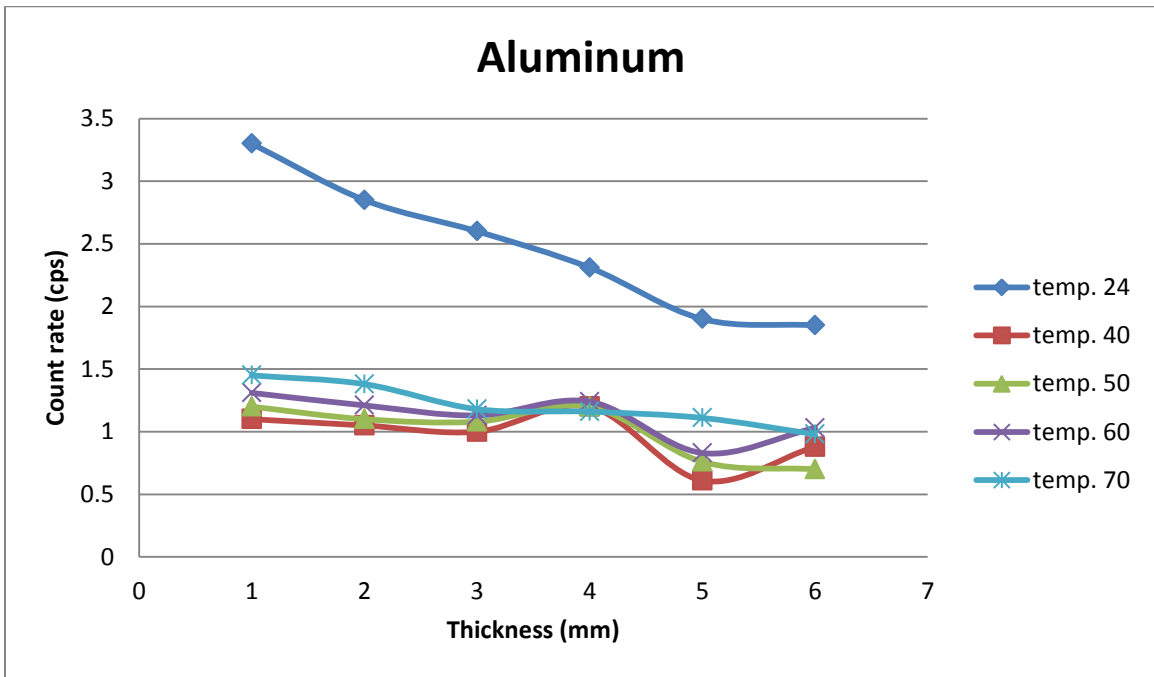


Figure (5-2-1): Relation between the count rate and thickness in different temperatures of Aluminum

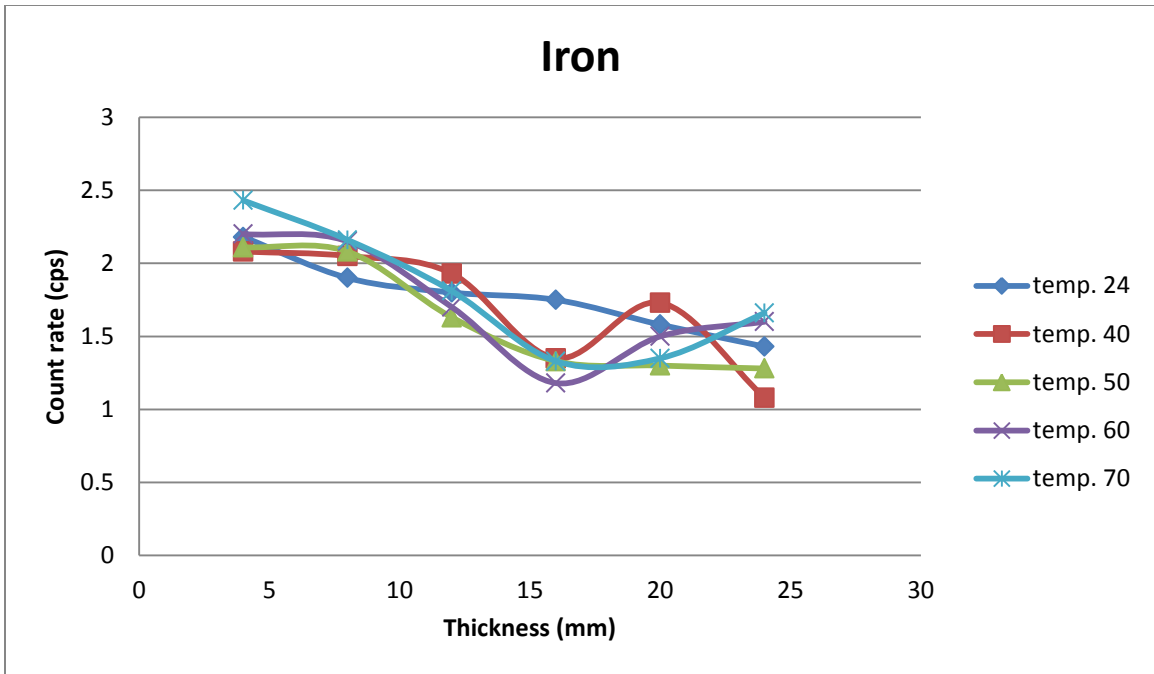


Figure (5-2-2): Relation between The count rate and thickness in different temperatures of Iron

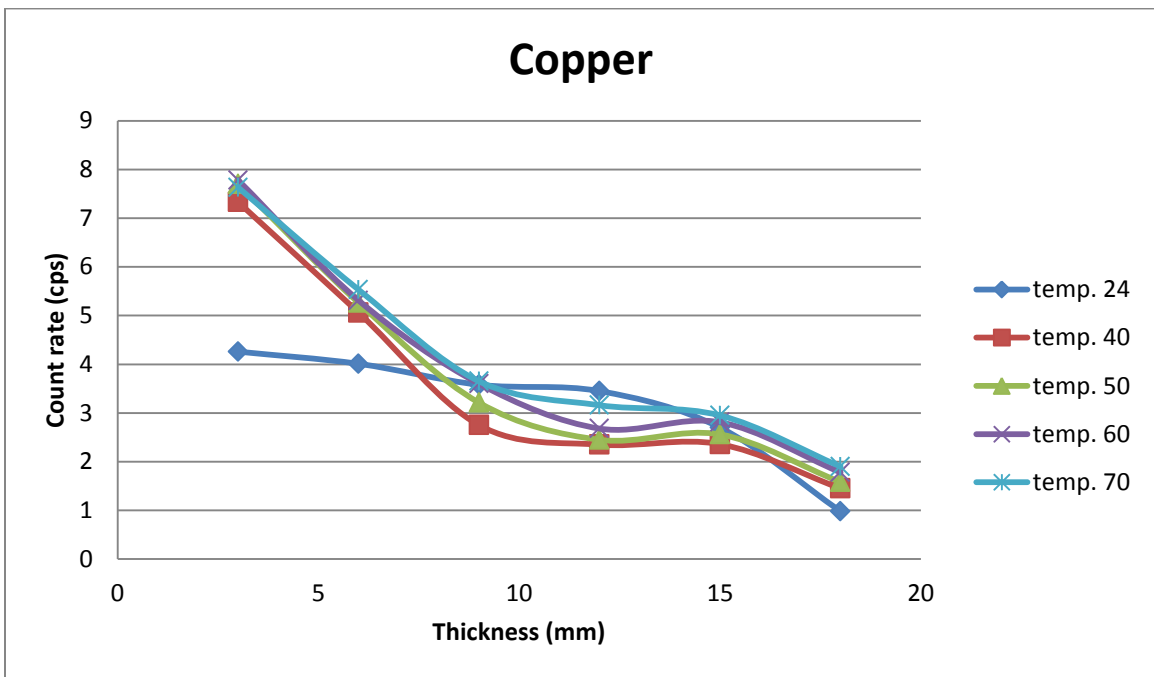


Figure (5-2-3): Relation between the count rate and thickness in different temperatures of Copper

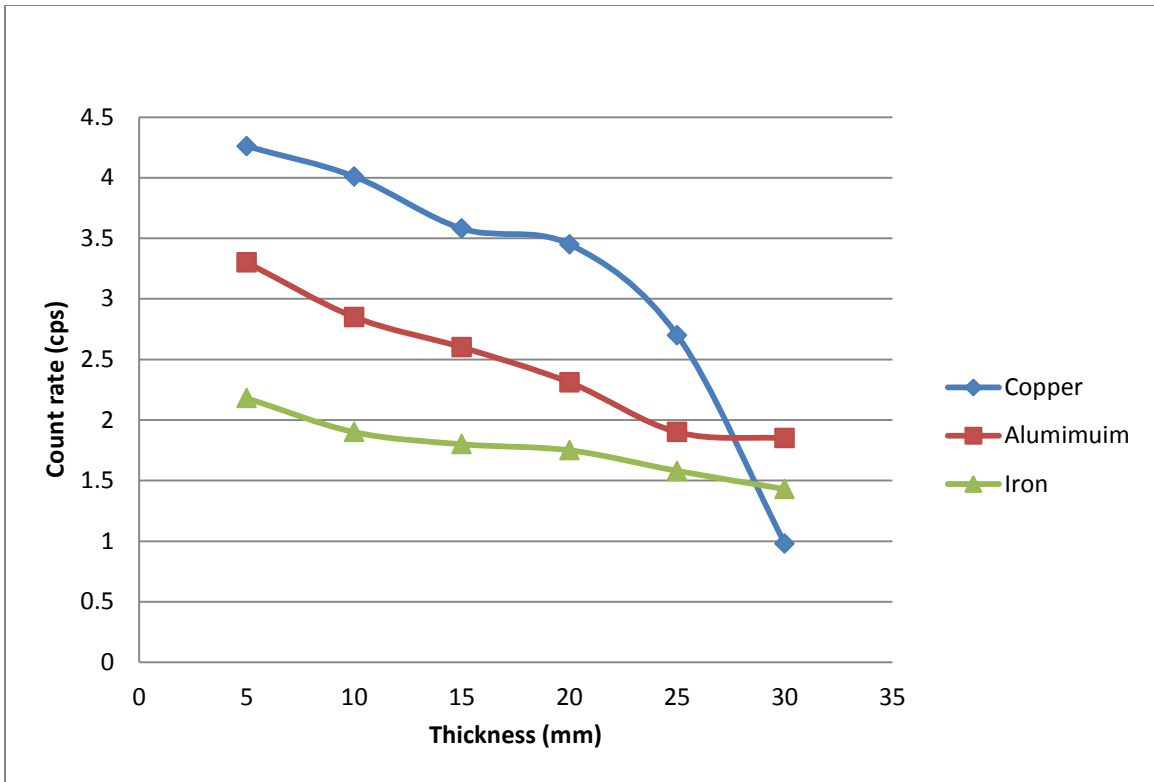


Figure (5-3-1): Comparison Between The Count rate of Aluminum, Iron, and Copper at Room temperature (24⁰C)

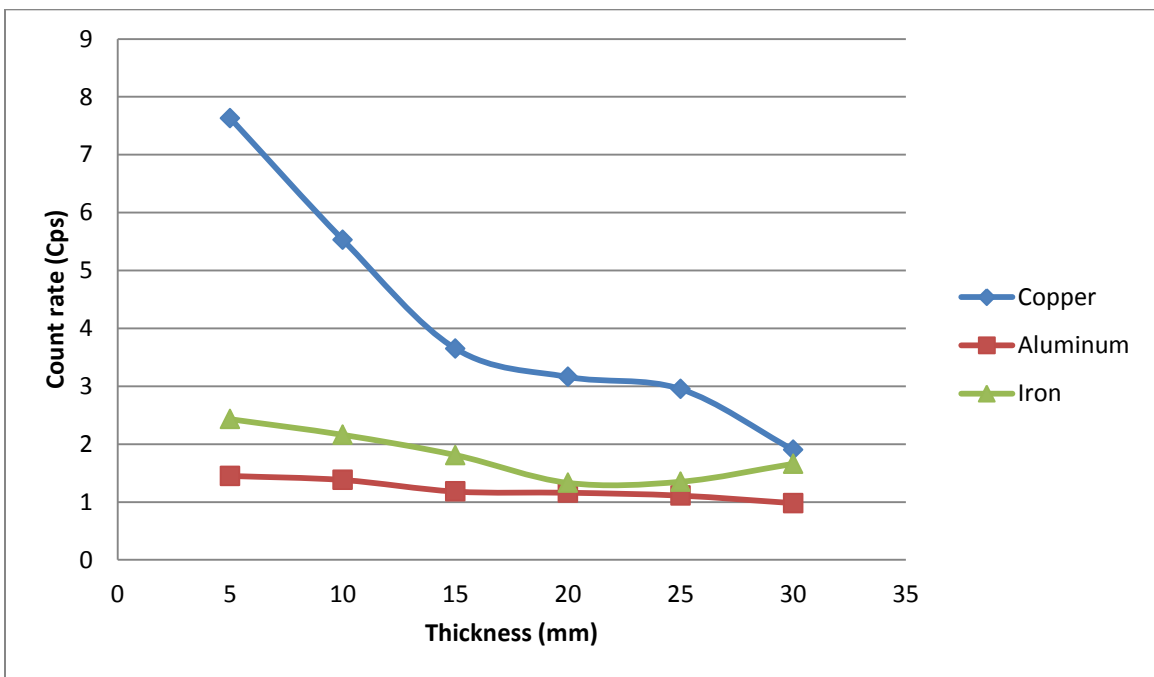


Figure (5-3-2): Comparison between the Count rate of Aluminum, Iron, and Copper at temperature (70⁰C)

Table (5-2-1): Attenuation coefficient and HVL for Aluminum samples

Thickness (mm)	T _C =24 ⁰ C		40 ⁰ C		50 ⁰ C		60 ⁰ C		70 ⁰ C	
	μ _{L1}	HVL ₁	μ _{L2}	HVL ₂	μ _{L3}	HVL ₃	μ _{L4}	HVL ₄	μ _{L5}	HVL ₅
5mm	0.146	4.747	0.366	1.893	0.349	1.986	0.331	2.094	0.311	2.228
10mm	0.088	7.875	0.188	3.686	0.183	3.787	0.174	3.983	0.160	4.331
15mm	0.065	10.662	0.128	4.414	0.123	5.634	0.120	5.775	0.117	5.923
20mm	0.054	12.833	0.087	7.966	0.087	7.966	0.086	8.058	0.089	7.787
25mm	0.051	13.588	0.097	7.144	0.088	7.875	0.084	8.250	0.073	9.493
30mm	0.044	15.750	0.068	10.191	0.076	9.118	0.063	11.000	0.065	10.662

Table (5-2-2): Attenuation coefficient and HVL for Iron samples

Thickness (mm)	T _C =24 ⁰ C		40 ⁰ C		50 ⁰ C		60 ⁰ C		70 ⁰ C	
	μ _{L1}	HVL ₁	μ _{L2}	HVL ₂	μ _{L3}	HVL ₃	μ _{L4}	HVL ₄	μ _{L5}	HVL ₅
4mm	0.287	2.415	0.298	2.326	0.295	2.349	0.284	2.440	0.259	2.676
8mm	0.160	4.332	0.151	4.589	0.149	4.651	0.145	4.779	0.144	4.813
12mm	0.111	6.243	0.106	6.538	0.120	5.775	0.116	5.974	0.111	6.243
16mm	0.085	8.153	0.102	6.794	0.103	6.728	0.110	6.300	0.103	6.728
20mm	0.073	9.493	0.069	10.043	0.083	8.349	0.076	9.118	0.081	8.556
24mm	0.065	10.662	0.077	9.000	0.070	9.900	0.060	11.550	0.059	11.746

Table (5-2-3): Attenuation coefficient and HVL for Copper samples

Thickness (mm)	T _C =24 ⁰ C		40 ⁰ C		50 ⁰ C		60 ⁰ C		70 ⁰ C	
	μ _{L1}	HVL ₁	μ _{L2}	HVL ₂	μ _{L3}	HVL ₃	μ _{L4}	HVL ₄	μ _{L5}	HVL ₅
3mm	0.433	1.6000	0.252	2.750	0.236	2.936	0.232	2.987	0.239	2.900
6mm	0.227	3.052	0.188	3.686	0.181	3.829	0.180	3.850	0.173	4.006
9mm	0.164	4.226	0.193	3.591	0.176	3.938	0.163	4.252	0.161	4.304
12mm	0.126	5.500	0.158	4.386	0.154	4.500	0.147	4.714	0.133	5.211
15mm	0.117	5.923	0.126	5.500	0.121	5.727	0.114	6.079	0.111	6.243
18mm	0.154	4.500	0.132	5.250	0.127	5.457	0.121	5.727	0.117	5.923

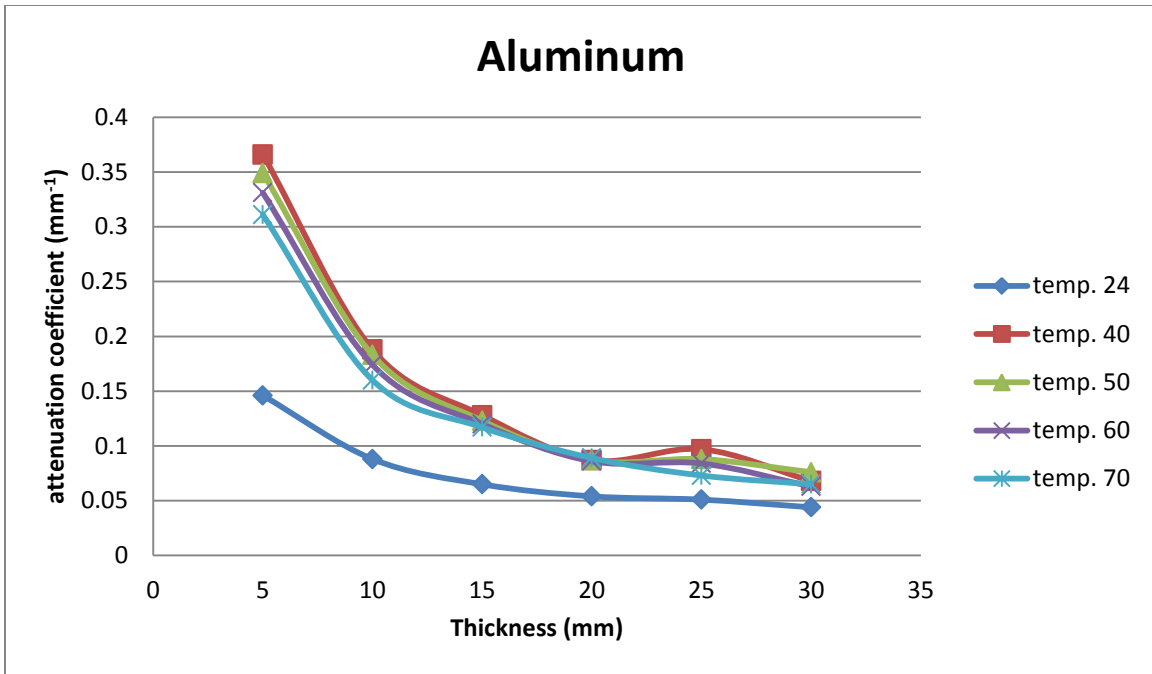


Figure (5-4-1): Relation between the attenuation coefficient and thickness of Aluminum in different values of temperature.

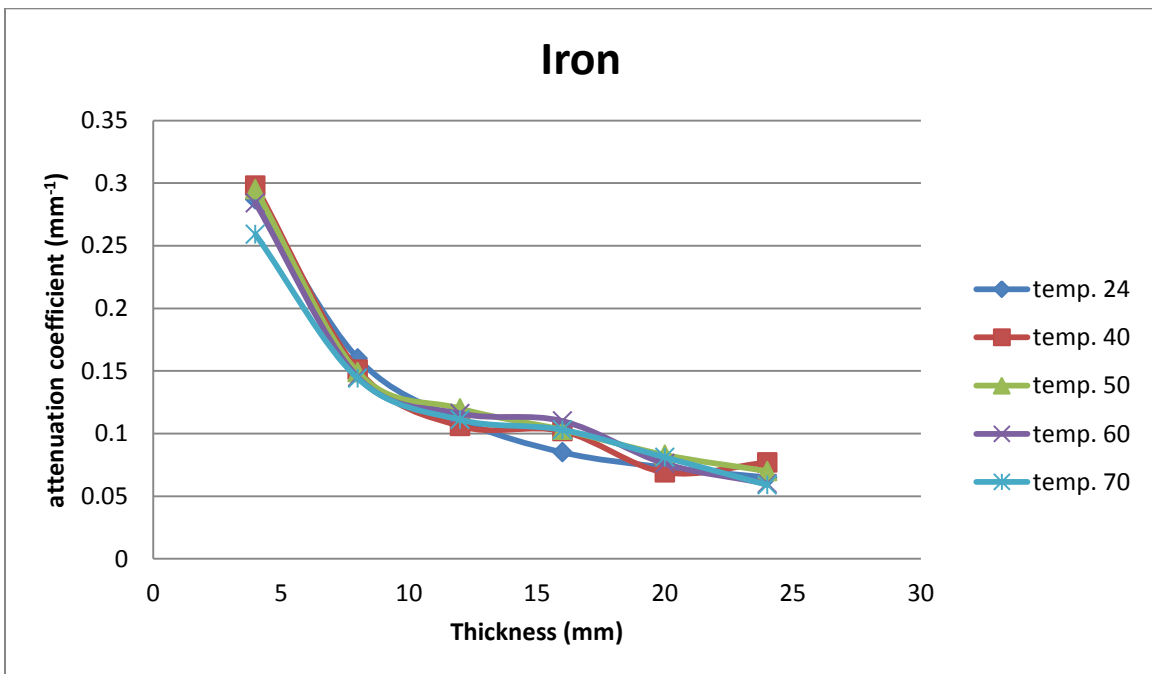


Figure (5-4-2): Relation between attenuation coefficient and thickness of Iron at different temperatures.

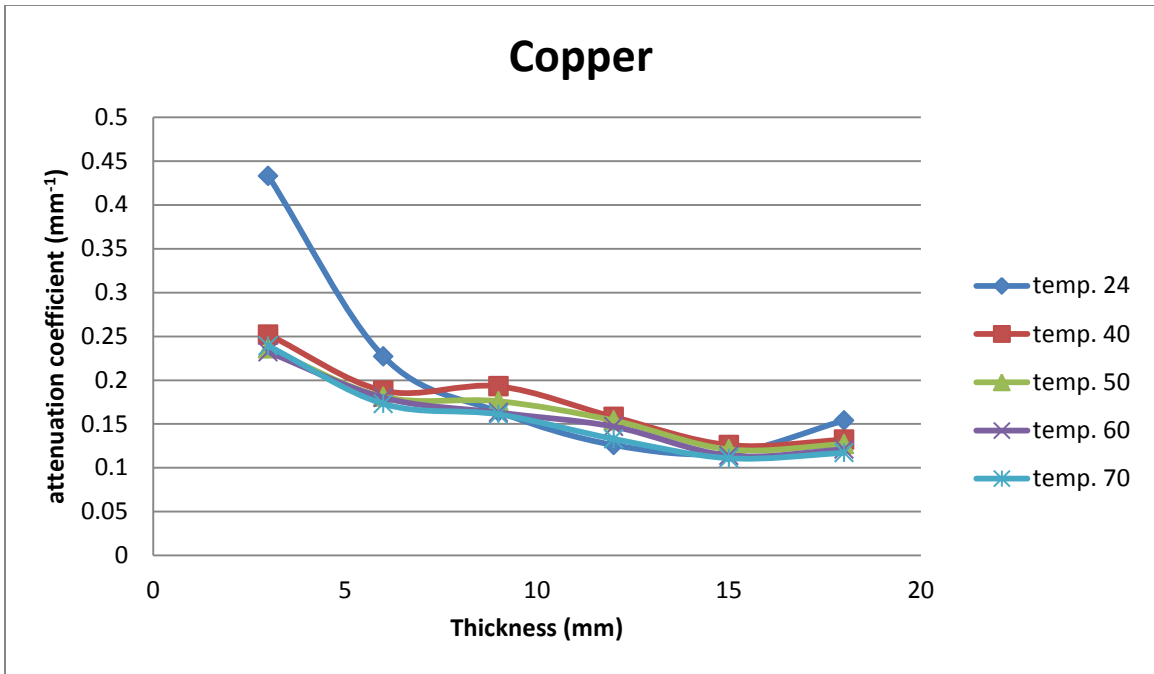


Figure (5-4-3): Relation between attenuation coefficient and thickness of Copper at different temperatures.

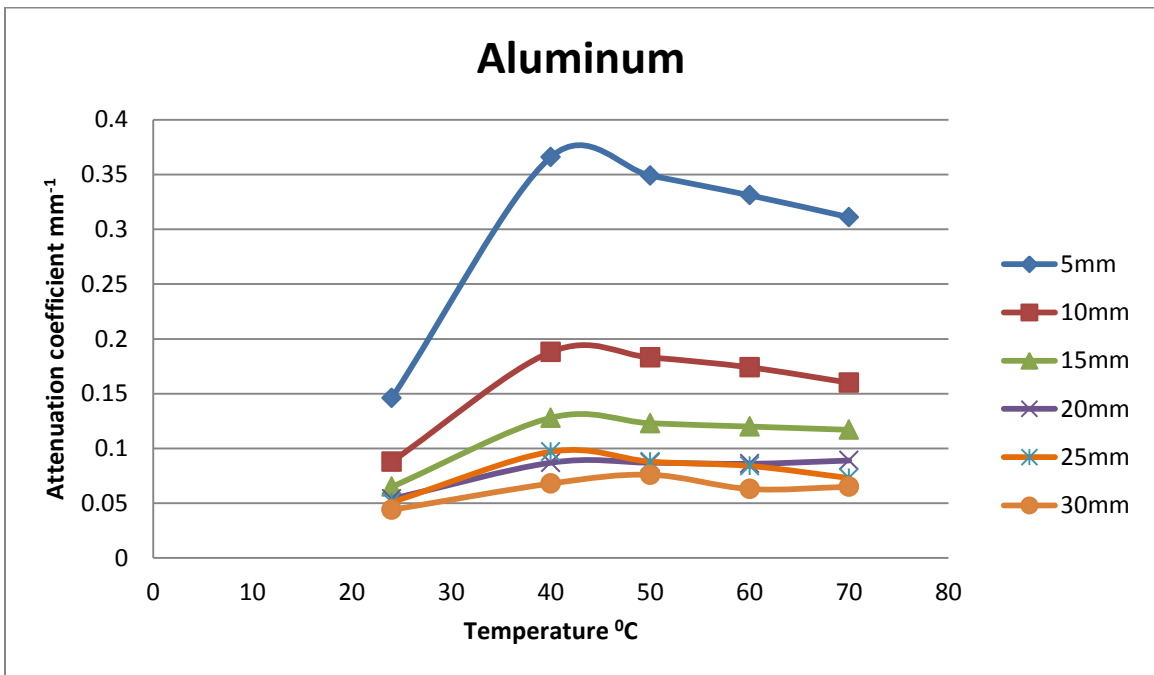


Figure (5-5-1): Relation between attenuation coefficient and temperature in different thicknesses of Aluminum

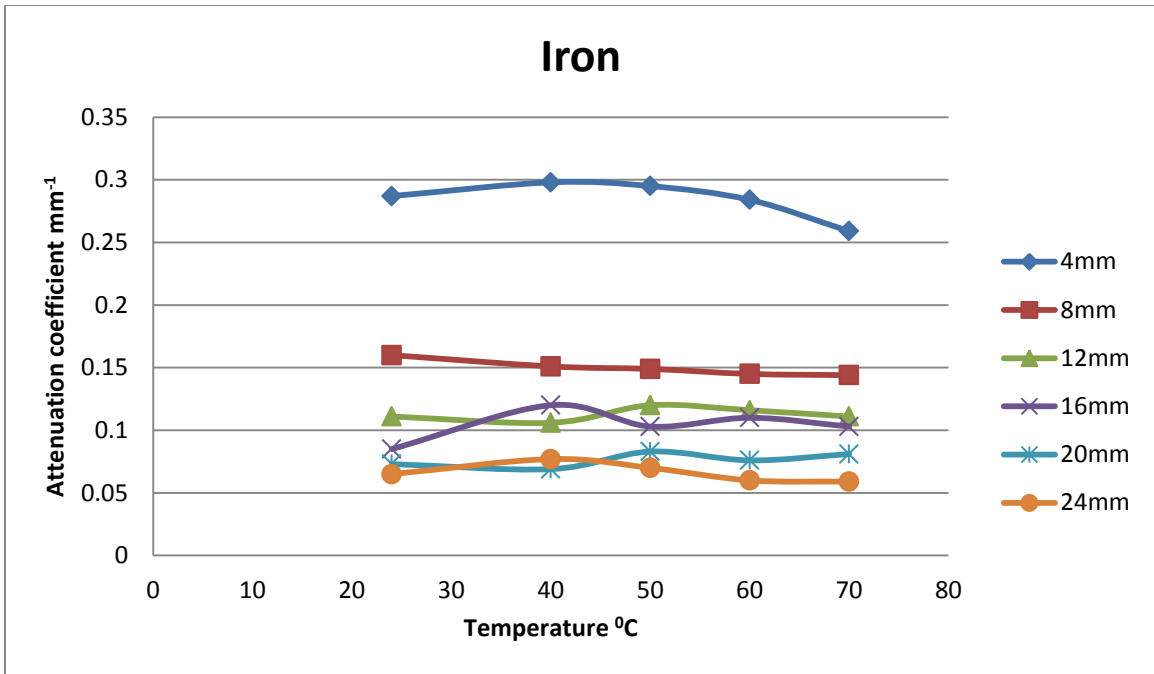


Figure (5-5-2): Relation between the attenuation coefficient and temperature of Aluminum in different values of thicknesses.

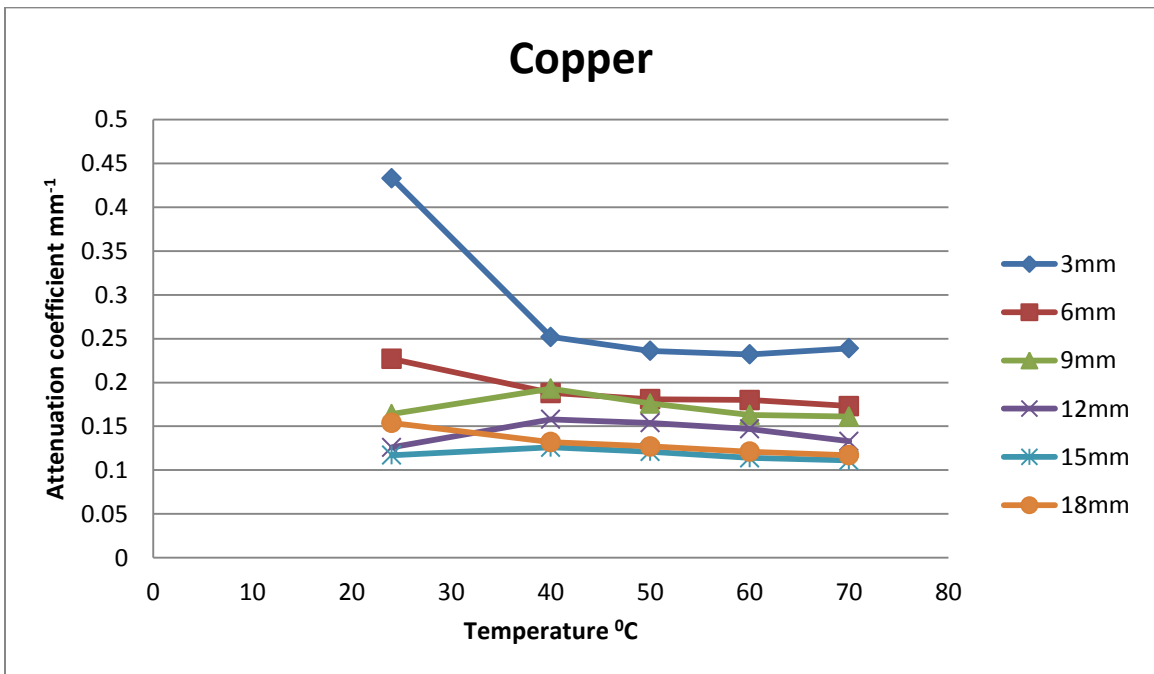


Figure (5-5-3): Relation between the attenuation coefficient and temperature of Aluminum in different values of thicknesses.

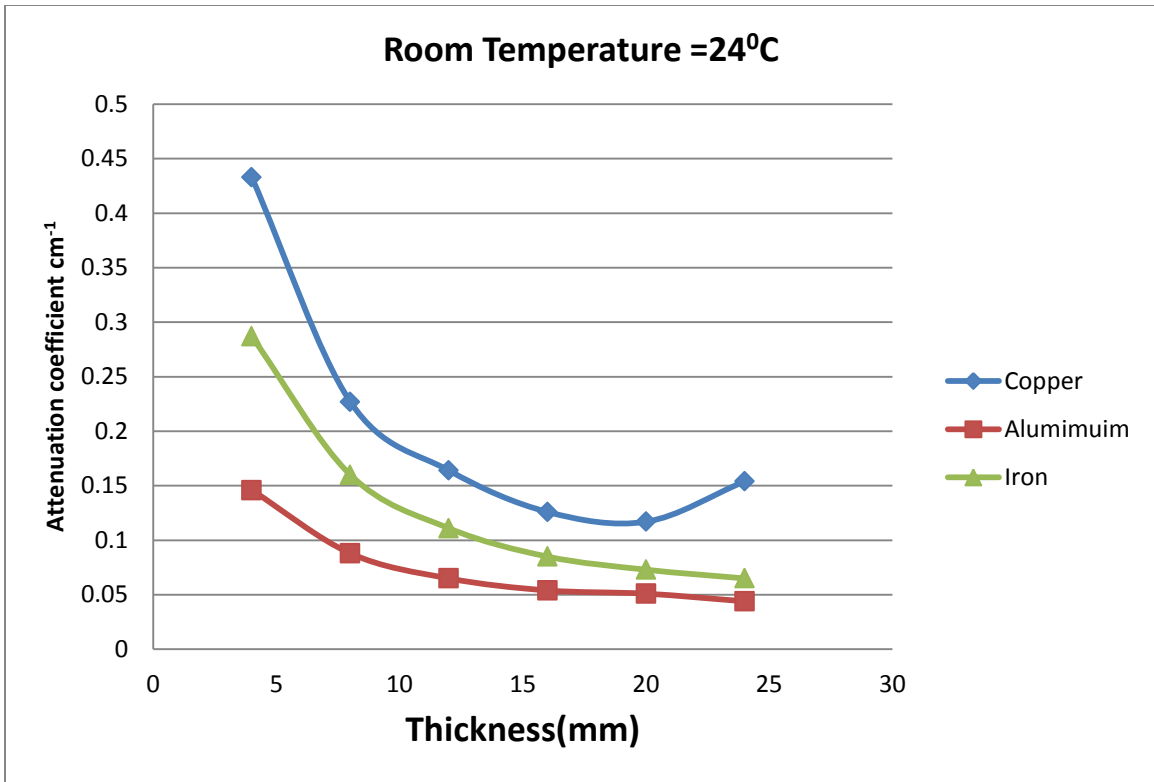


Figure (5-6-1): Comparison between the attenuation coefficients of Aluminum, Iron, and Copper at temperature 24°

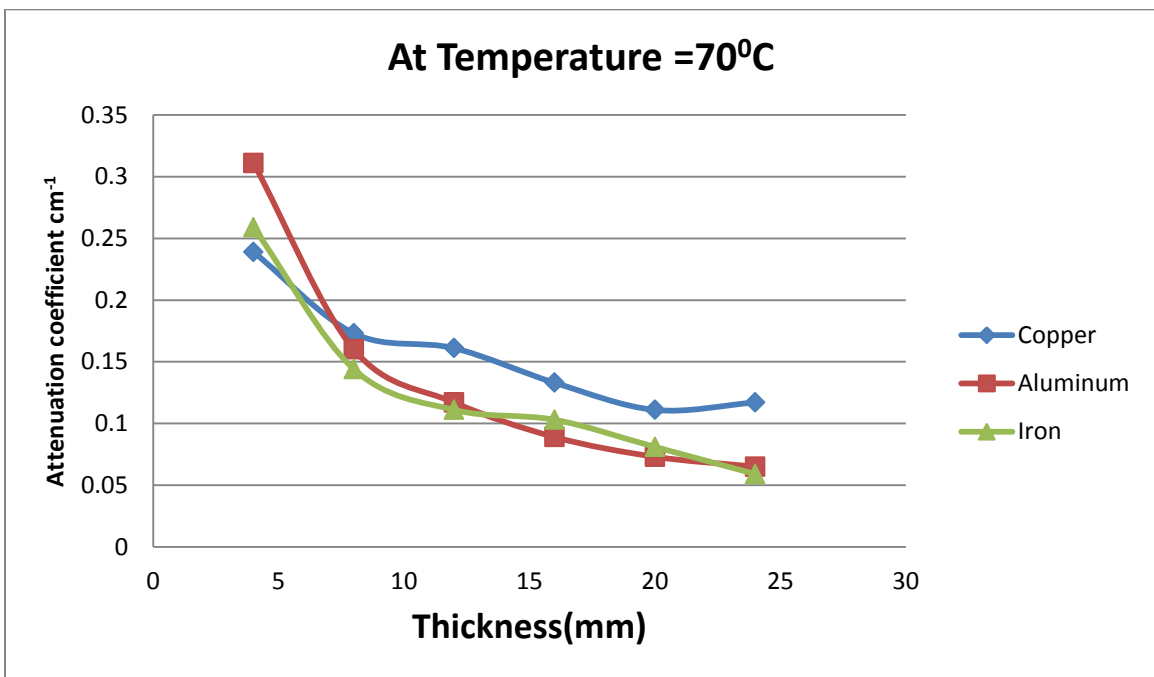


Figure (5-6-2): Comparison between the attenuation coefficients of Aluminum, Iron, and Copper at temperature 70°

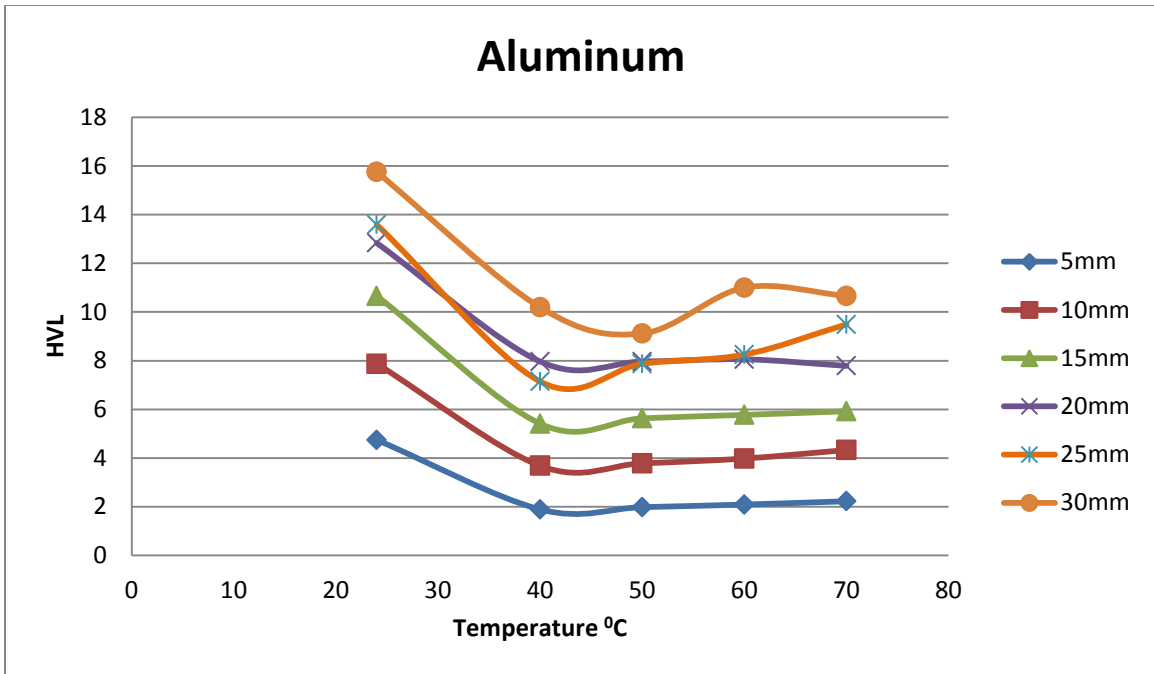


Figure (5-7-1): relation between HVL and temperature at different thicknesses of Aluminum

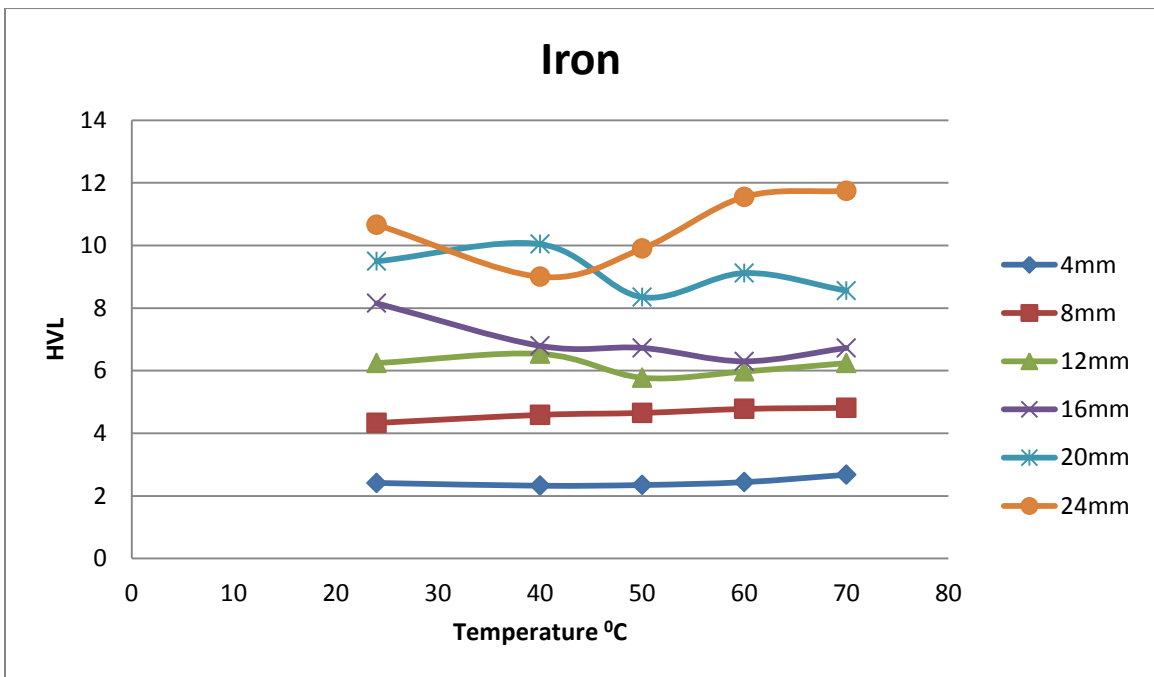


Figure (5-7-2): relation between HVL and temperature at different thicknesses of Aluminum

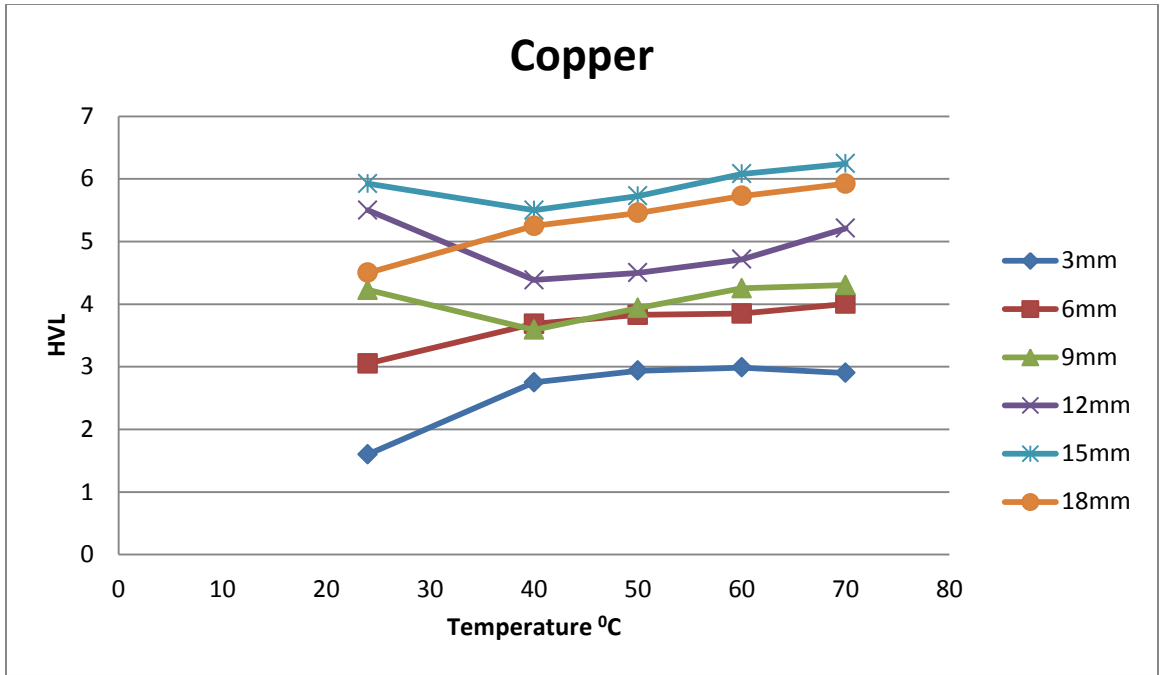


Figure (5-7-3): relation between HVL and temperature at different thicknesses of Copper

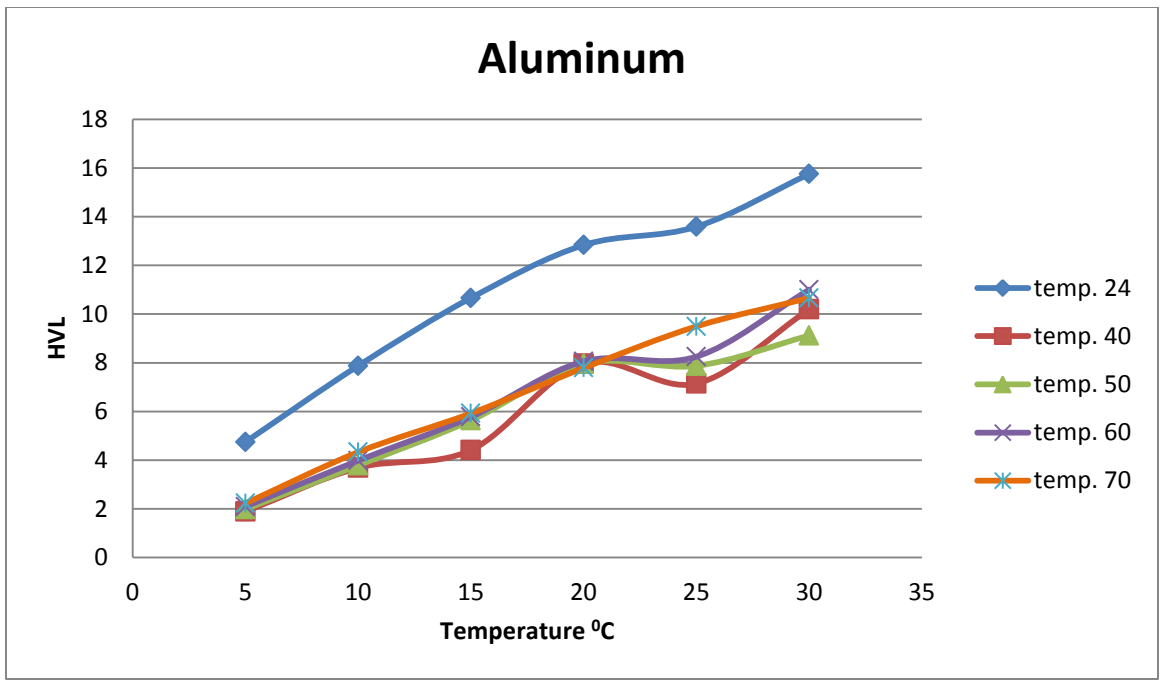


Figure (5-8-1): relation between HVL and thickness at different temperatures of Aluminum

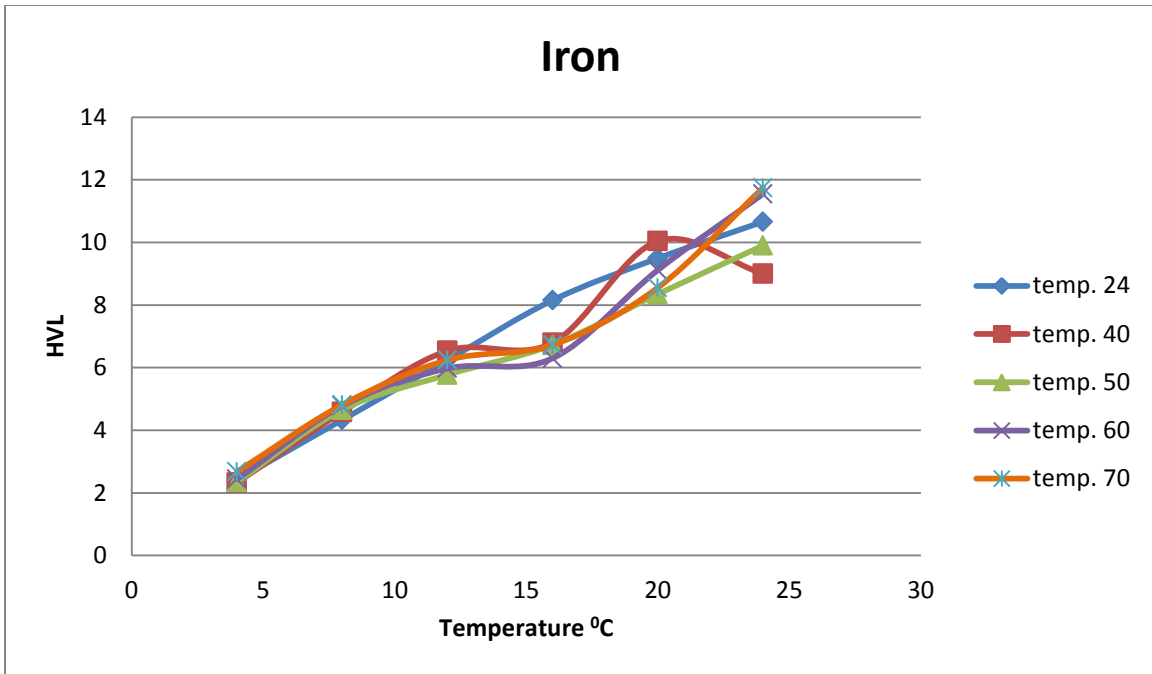


Figure (5-8-2): relation between HVL and thickness at different temperatures of Iron

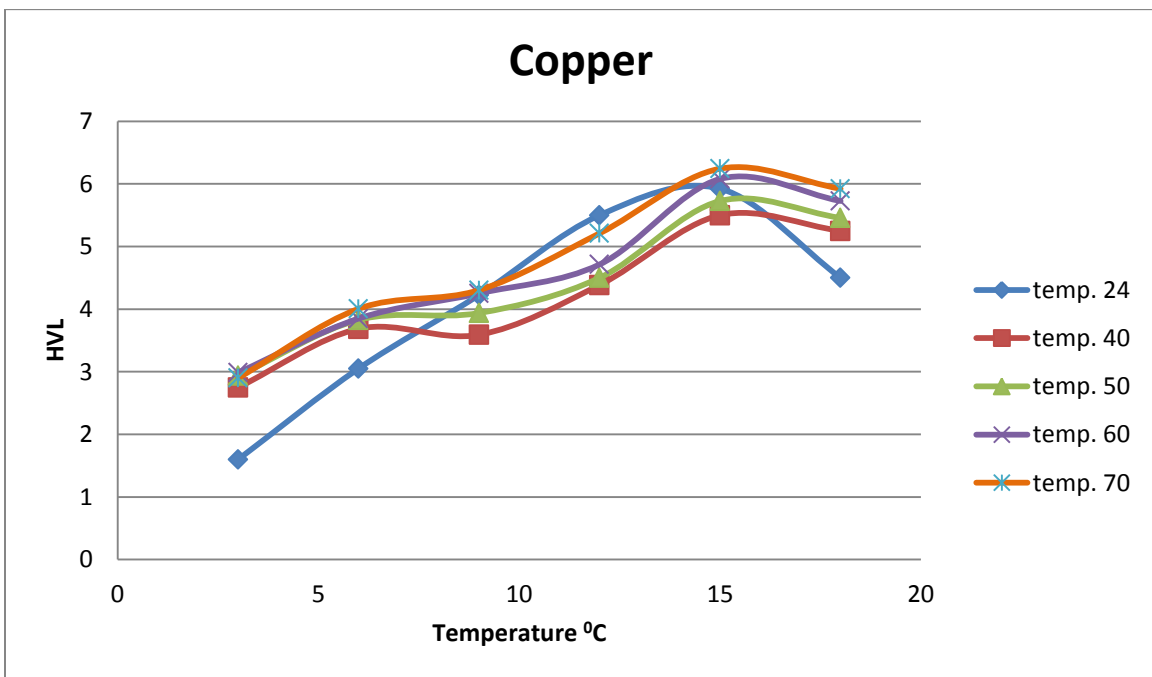


Figure (5-8-3): relation between HVL and thickness at different temperatures of Copper

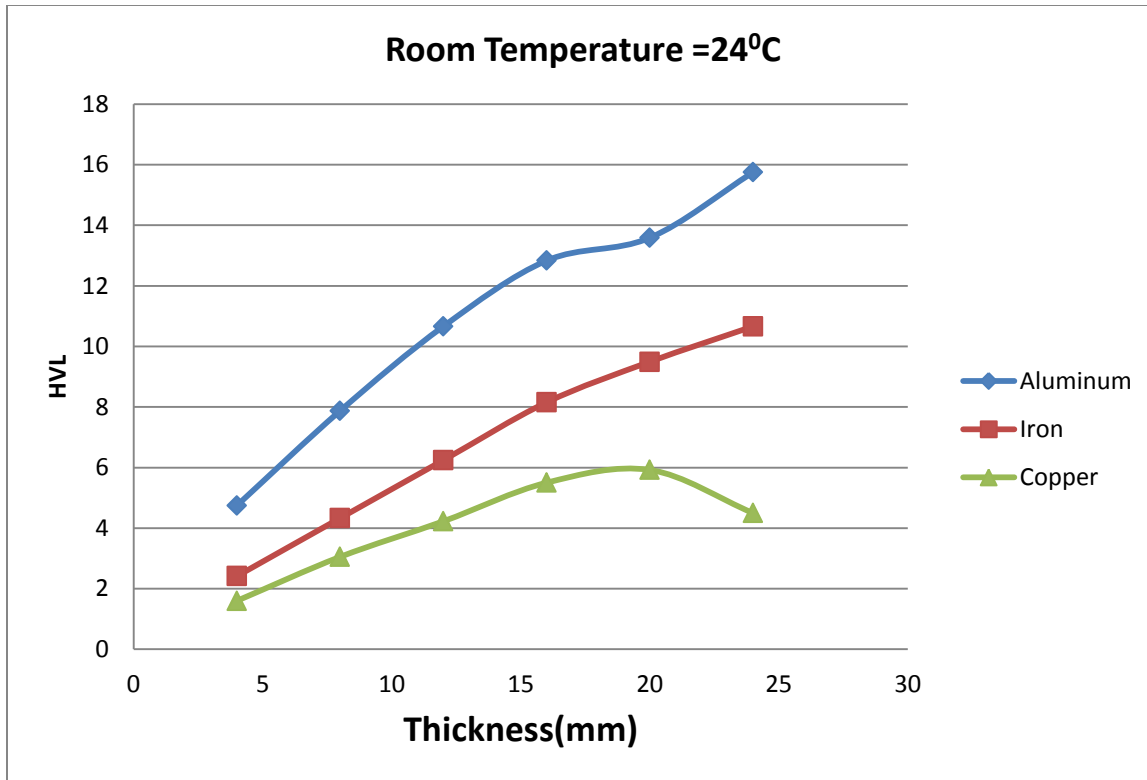


Figure (5-9-1): Comparison between the HVL and thickness of Aluminum, Iron, and Copper at temperature 24°C

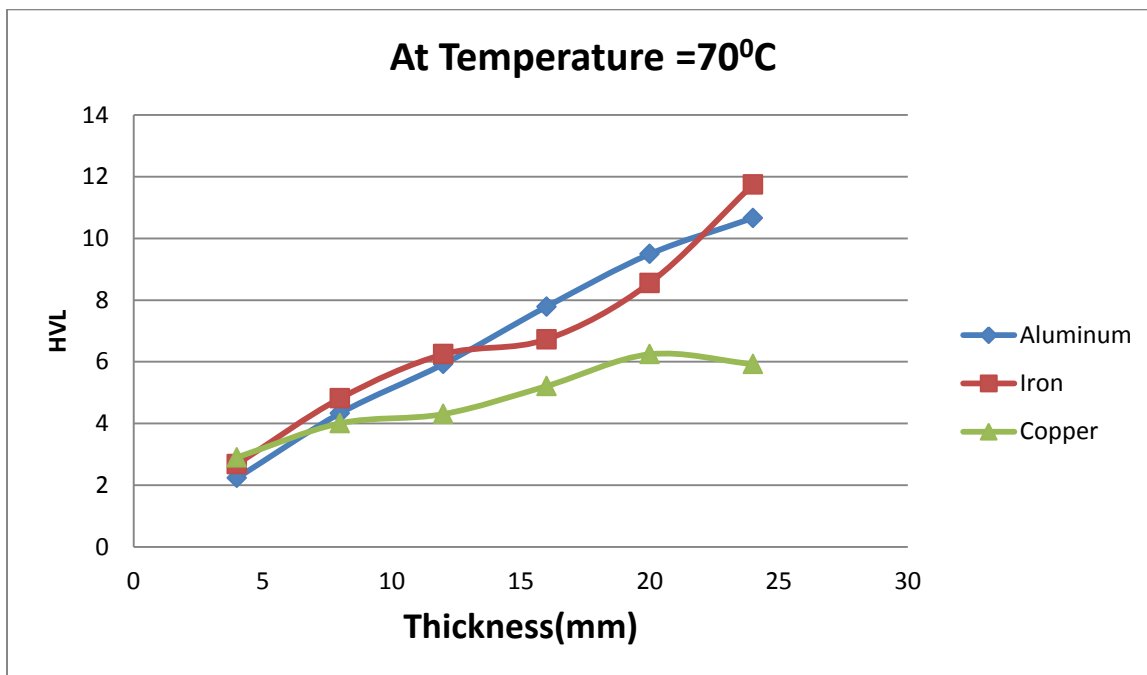


Figure (5-9-2): Comparison between the HVL and thickness of Aluminum, Iron, and Copper at temperature 70°C

5.3 Discussion:

The relation between count rate (I) and temperature (T) for Al in fig (5-1-1) shows exponential decrease as well as with thickness as shown in fig (5-2-1). This relation can be easily explained using non thermal equilibrium statistical laws. This relation may be attributed to the fact that increasing temperature increases the frequency of vibration of atoms which increases the collision rate with gamma photons thus decreases the emergent gamma radiation. These relations resembles the quantum relations for intensity obtained Rehab in her paper in fig. (3-7-2), where

$$I = I_0 e^{-T} \sin \pi T$$

Here in our work for thickness (x) one replace the temperature by (x) As far as:

$$I = I_0 e^{-\mu x}$$

The same explanation can hold for the change of count rate of iron (Fe) with thickness in fig. (5-2-2). Here in all these cases the curves resemble the part from (0-2) in fig. (3-7-2). However, the change of count rate with temperature for (Fe) in fig. (5-1-2) resembles the part of fig. (3-7-2) for (T) from (2-8).

However, the change of copper (Cu) count rate with temperature and thickness in figures (5-1-3) and (5-2-3) shows also decrease of count rate upon increasing temperature (T) and thickness (x). This can be explained using the same arguments that used for Al and Fe. The empirical relation resembles that of fig. (3-7-2) in the range (1-1.5).

The change in of attenuation coefficient with temperature of Al in fig. (5-5-1) for all thicknesses show increase in the temperature range (20-40) then gentle decrease after that but it's not as value as it was at room temperature. This may be due to the fact that the increase of temperature in the range (20-40) causes light elements to evaporate this increases intensity which increases attenuation coefficient which usually increases with density. This density decrease can be observed by Fourier Transformer Infrared (FTIR) Figs (5-10-1) and (5-10-2). However, further increase causes the metal to expand thus decrease density of atoms which in turn decreases attenuation coefficient

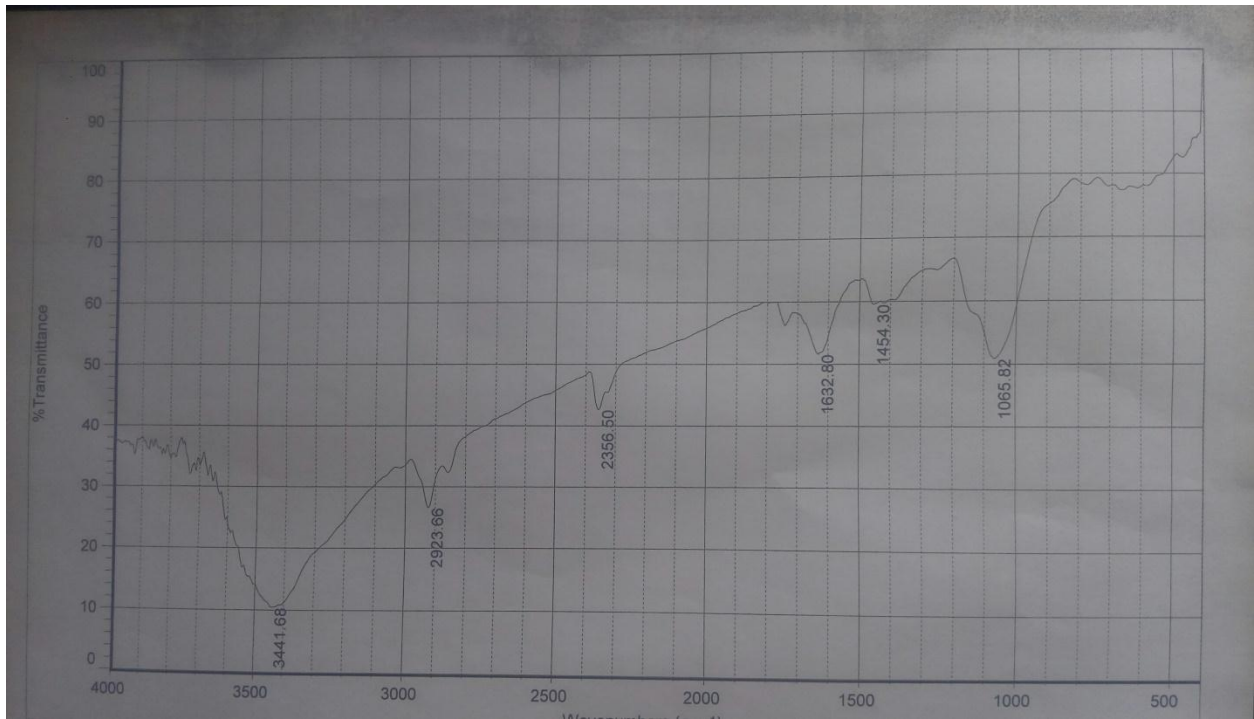


Figure (5-10-1): FTIR for Aluminum + Gum Before heating

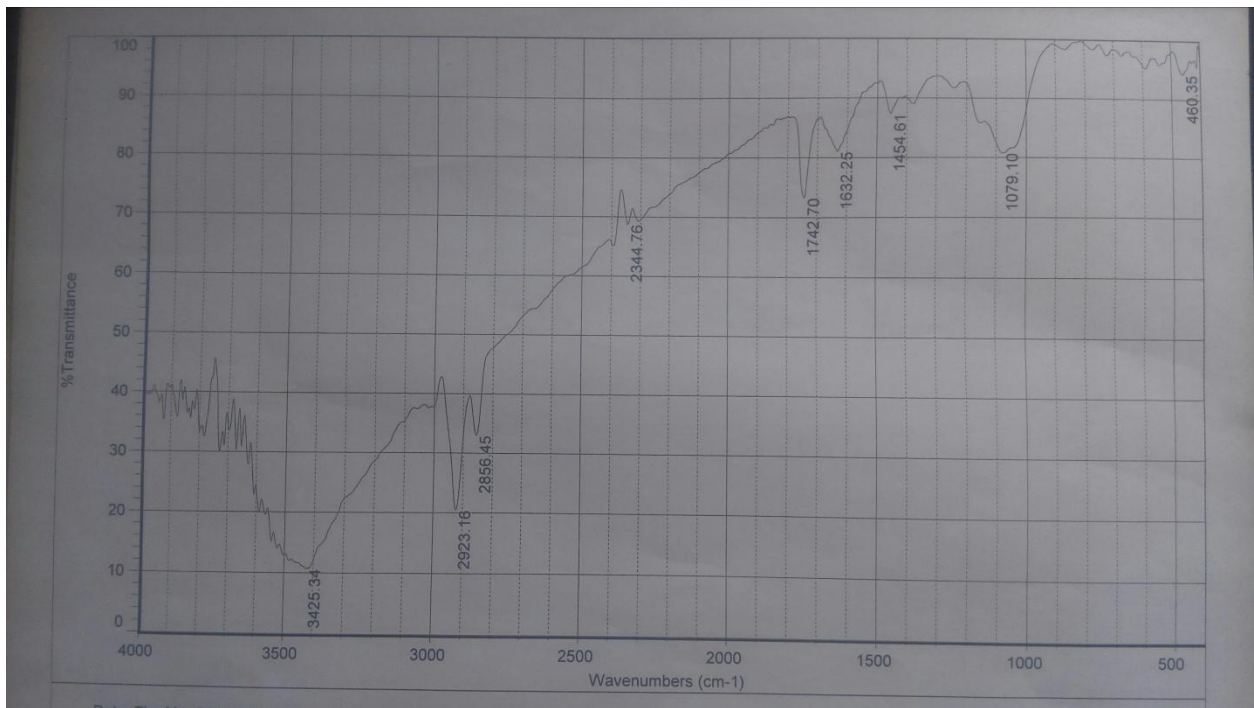


Figure (5-10-2): FTIR for Aluminum + Gum After heating

Fig. (5-5-2) shows that the attenuation coefficient of (Fe) decreases upon increasing the thickness of the samples increases the number of atoms that emit gamma photons, which increases the number and energy of the transmitted number of photons. This of course decrease attenuation coefficient. The change of the attenuation coefficient of iron (Fe) in fig. (5-4-2) for all thicknesses is almost constant. This means that the temperature change does not affect density or scattering probability. However, the attenuation coefficient for (Fe) decreases with thickness for all temperatures as shown in fig. (5-4-2), this can be explained using the same arguments that used for (Al). Also FTIR were made to Cu sample as shown in figs. (5-11-1) and (5-11-2).

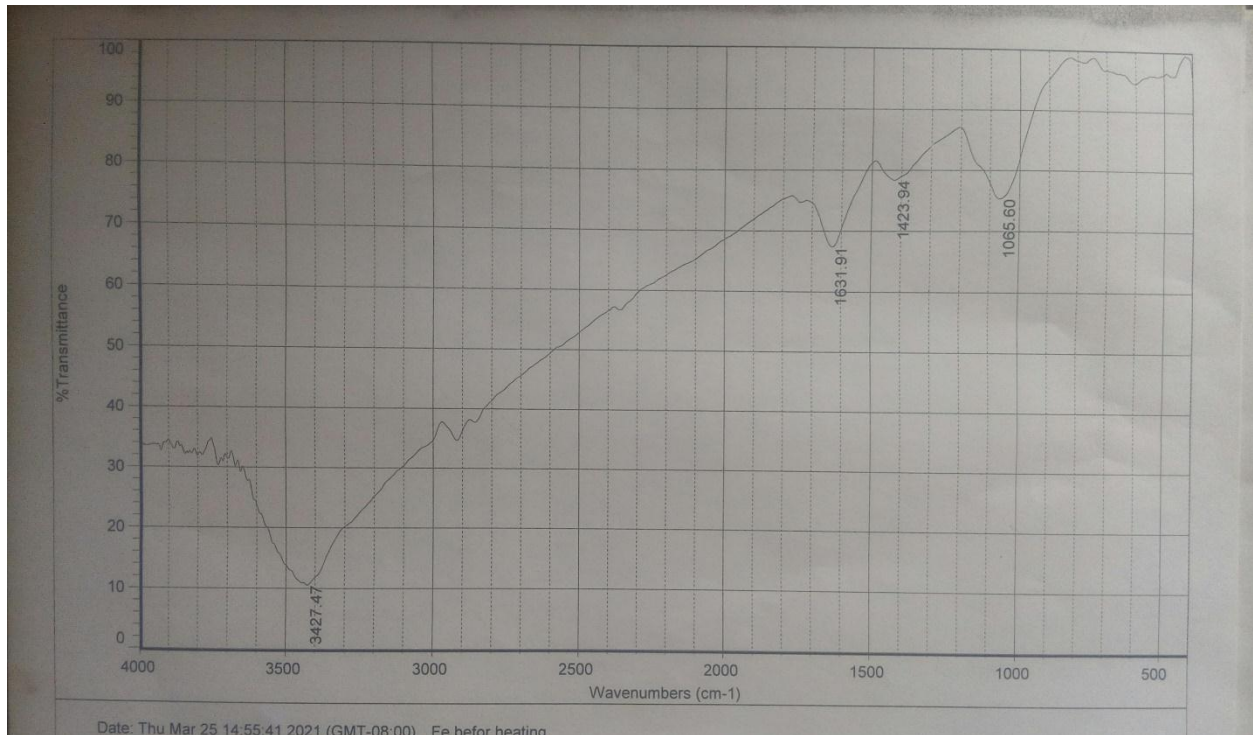


Figure (5-11-1): FTIR for Iron + Gum Before heating

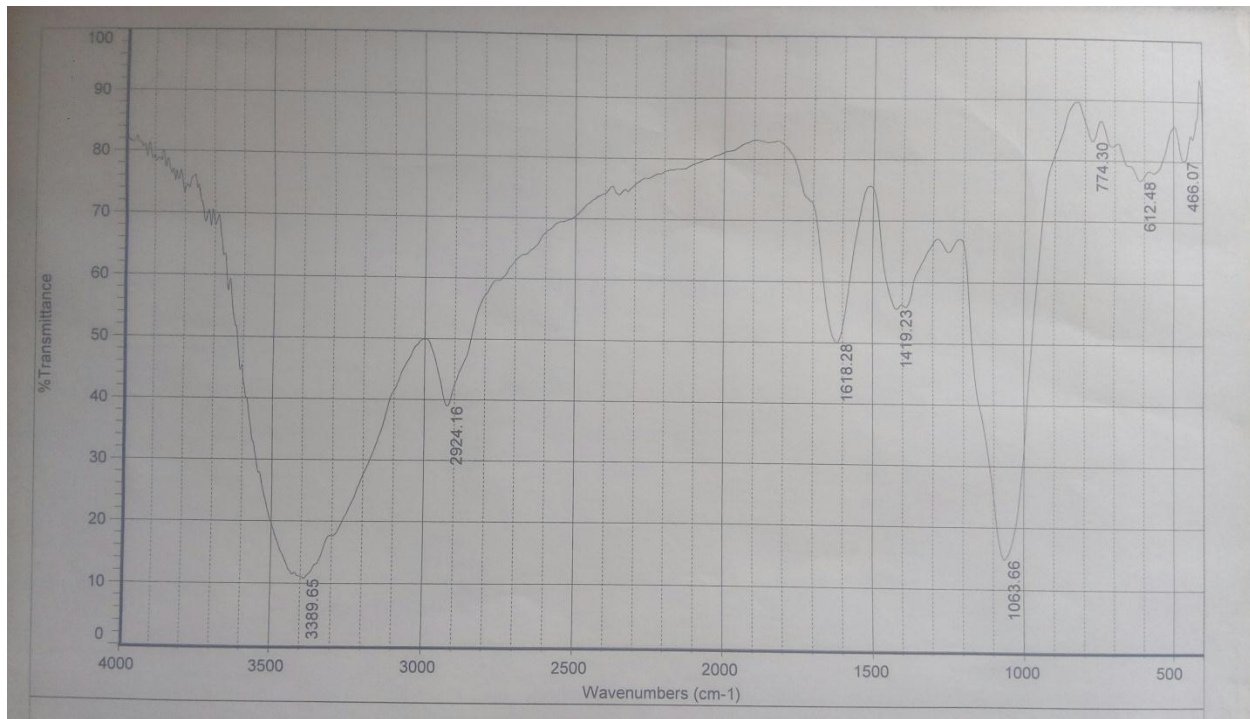


Figure (5-11-2): FTIR for Iron + Gum After heating

The change of attenuation coefficient of copper (Cu) with temperature in figure (5-5-3) shows that it decreases upon increasing temperature. Figure (5-4-3) for the change of attenuation coefficient of (Cu) with thickness, indicates also decrease of attenuation coefficient upon increasing the thickness. This can again explained as before. But fortunately these relations can be easily explained using non-equilibrium statistical laws derived from plasma and quantum equations. It is very interesting to note that. Like Al and Fe figs. (5-12-1) and (5-12-2) shows FTIR for Copper.

Fig. (5-3-1) shows the comparison between the count rate of (Al, Fe, and Cu) at room temperature with thicknesses we note the count rate of Al decrease from 3.3c/s to 0.98c/s, Fe decrease from 2.18c/s to 1.43, and Cu decrease from 4.26c/s to 0.98c/s. From these values we note that the decreasing of count rate for Cu is very sharp than Al and Fe. Fig. (5-3-2) shows the comparison between the count rate of (Al, Fe, and Cu) at 70⁰C with thicknesses we note the count rate of Al decrease from 1.45c/s to 0.98c/s, Fe decrease from 2.43c/s to 1.66, and Cu decrease from 7.63c/s to 1.9c/s. From these values we note that the decreasing of count rate for Cu is very high because Cu has lower specific heat, and lower density of electrons.

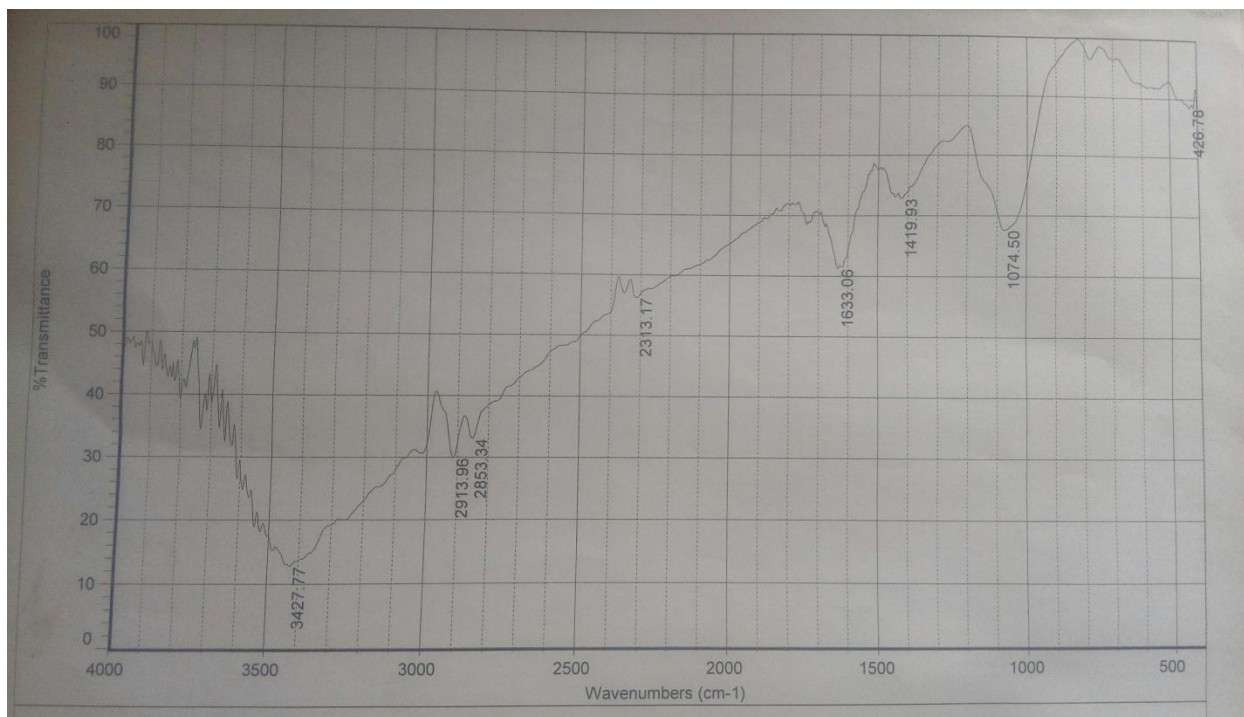


Figure (5-12-1): FTIR for Copper + Gum Before heating

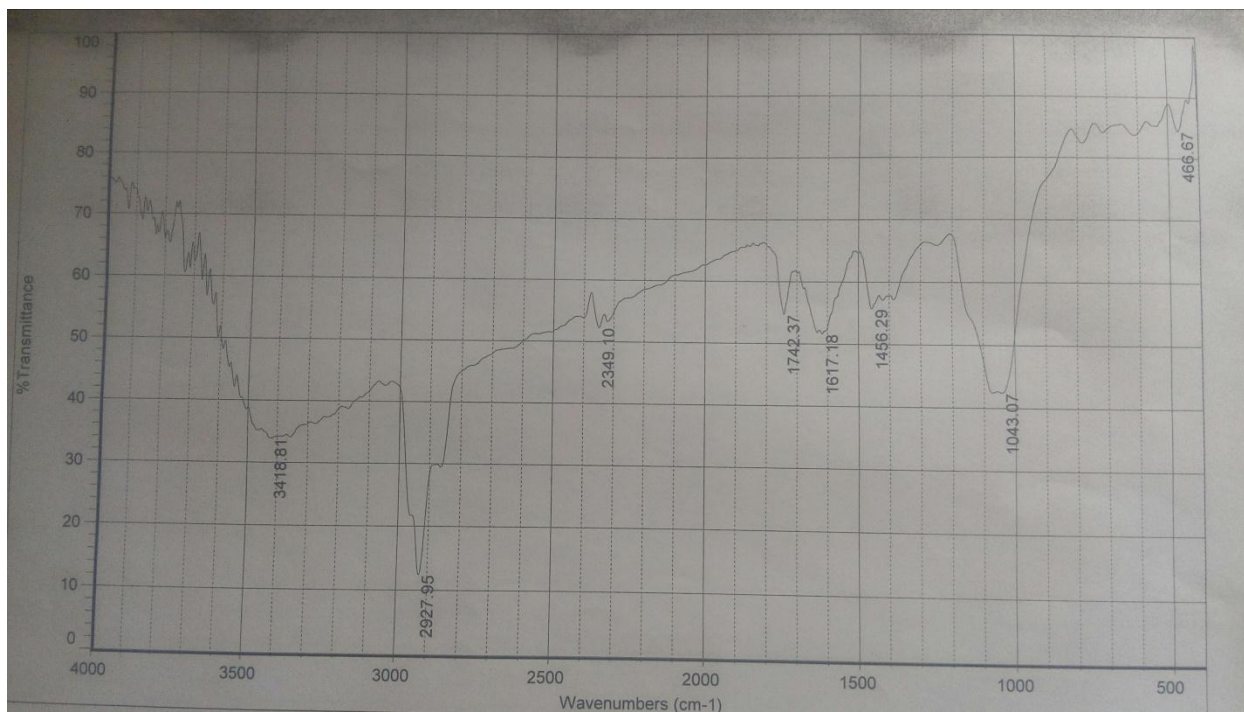


Figure (5-12-2): FTIR for Copper + Gum After heating

Fig. (5-6-1) shows comparison between the attenuation coefficients of Al, Fe, and Cu at room temperature, and we note that the attenuation coefficient of Al change from 0.146 to 0.311, Fe change from 0.287 to 0.065, and Cu change from 0.433 to 0.154. Attenuation coefficient of Cu is high than Al and Fe, and the manner of three element similar they decrease then a slight increase occur. Fig. (5-6-2) shows comparison between the attenuation coefficients of Al, Fe, and Cu at 70⁰C. Iron is almost unchanged because it has a small thermal conductivity and its heat expansion is slow compared to aluminum and copper. In addition, Fe and its compounds always tend to be more magnetic than optical and electrical and are easy to magnify.

In a similar way, figures (5-7-1), (5-7-2), (5-7-3), (5-9-1), and (5-9-2) can be explained for Half Value Layer (HVL) for three elements.

5.4 Conclusion:

The change of temperature of Al, Fe, and Cu samples which makes it in non-equilibrium state changes its attenuation coefficient with both temperature and thickness. The attenuation coefficient decreases and sometimes remains almost constant with slight decrease upon increasing temperature and thickness. Fortunately these changes can be described using non-equilibrium distribution laws derived from plasma and quantum laws for resistive medium.

References:

- [1] Turns SR, Pauley LL. Thermodynamics: Concepts and Applications: Cambridge University Press; 2020.
- [2] Franses EI. Thermodynamics with Chemical Engineering Applications: Cambridge University Press; 2014.
- [3] Schmidt A. Technical thermodynamics for engineers: Springer; 2019.
- [4] NARAYANAN KV. A TEXTBOOK OF CHEMICAL ENGINEERING THERMODYNAMICS: PHI Learning; 2013.
- [5] Casas-Vázquez J, Jou D. Temperature in non-equilibrium states: a review of open problems and current proposals. Reports on Progress in Physics. 2003;66(11):1937.
- [6] de Oliveira MJ. Equilibrium Thermodynamics: Springer Berlin Heidelberg; 2014.
- [7] Demirel Y. Nonequilibrium Thermodynamics: Transport and Rate Processes in Physical, Chemical and Biological Systems: Elsevier Science; 2013.
- [8] Mandl F. Statistical Physics: Wiley; 2013.
- [9] Kjelstrup S, Bedeaux D, Johannessen E, Gross J. Non-equilibrium Thermodynamics For Engineers (Second Edition): World Scientific Publishing Company; 2017.
- [10] Zia R, Shaw L, Schmittmann B, Aсталos R. Contrasts between equilibrium and non-equilibrium steady states: computer aided discoveries in simple lattice gases. Computer physics communications. 2000;127(1):23-31.
- [11] Ilangovan K. Nuclear Physics: MJP Publisher; 2019.
- [12] Singh K, Singh S, Dhaliwal A, Singh G. Gamma radiation shielding analysis of lead-flyash concretes. Applied Radiation and Isotopes. 2015;95:174-9.
- [13] Zeb J, Arshad W, Rashid A, Akhter P. Gamma shielding by aluminum (Al-shielder manual). Pakistan Institute of Nuclear Science and Technology; 2010.
- [14] Turchanin M, Agraval P, Nikolaenko I. Thermodynamics of alloys and phase equilibria in the copper-iron system. Journal of phase equilibria. 2003;24(4):307-19.
- [15] Childs PR. Practical temperature measurement: Elsevier; 2001.
- [16] Equity AOERT. College Physics Textbook Equity Edition Volume 2 of 3: Chapters 13 - 24: Lulu.com; 2016.
- [17] Davis PD, Parbrook GD, Kenny GN. Basic physics and measurement in anaesthesia: Butterworth-Heinemann; 2015.
- [18] Dass NDH. The Principles of Thermodynamics: Taylor & Francis; 2013.
- [19] Ventura G, Perfetti M. Thermal properties of solids at room and cryogenic temperatures: Springer; 2014.
- [20] Clark JOE. The Basics of Heat: Rosen Publishing Group; 2014.
- [21] Gupta S. Engineering thermodynamics: S. Chand Publishing; 2013.
- [22] Nag P. Engineering thermodynamics: Tata McGraw-Hill Education; 2013.
- [23] Tosun I. Thermodynamics: Principles And Applications: World Scientific Publishing Company; 2015.
- [24] Swendsen R. An introduction to statistical mechanics and thermodynamics: Oxford University Press, USA; 2020.
- [25] Borgnakke C, Sonntag RE. Fundamentals of Thermodynamics: Wiley; 2020.
- [26] Moran MJ, Shapiro HN, Boettner DD, Bailey MB. Fundamentals of Engineering Thermodynamics, 8th Edition: Wiley; 2014.
- [27] Greven A, Keller G, Warnecke G. Entropy: Princeton University Press; 2014.

- [28] Kreith F, Manglik RM. Principles of heat transfer: Cengage learning; 2016.
- [29] Rajput R. Engineering thermodynamics: A computer approach (si units version): Jones & Bartlett Publishers; 2009.
- [30] Karwa R. Heat and Mass Transfer: Springer Singapore; 2016.
- [31] Lienhard JH. A Heat Transfer Textbook: Fifth Edition: Dover Publications; 2019.
- [32] Bejan A. Convection heat transfer: John wiley & sons; 2013.
- [33] Reisel JR. Principles of Engineering Thermodynamics, SI Edition: Cengage Learning; 2015.
- [34] Shahzad A. Nuclear Medicine Physics: IntechOpen; 2019.
- [35] Osibote A. Ionizing and Non-ionizing Radiation: BoD–Books on Demand; 2020.
- [36] Rangacharyulu C. Physics of nuclear radiations: concepts, techniques and applications: Taylor & Francis; 2013.
- [37] Abd El-kader NM. A Study of the effect of gamma radiation on some alloy materials for use as dosimetry systems and its applications. 2013.
- [38] Carter V. Advanced Nuclear Physics. Global Media. 2009;First Edition.
- [39] MITTAL VK, VERMA RC, GUPTA SC. INTRODUCTION TO NUCLEAR AND PARTICLE PHYSICS, FOURTH EDITION: PHI Learning Pvt. Ltd.; 2018.
- [40] Bryan JC. Introduction to Nuclear Science: CRC Press; 2013.
- [41] Khan FM, Gibbons JP. Khan's the Physics of Radiation Therapy: Lippincott Williams & Wilkins; 2014.
- [42] Kuppusamy T. Basic Radiological Physics: Jaypee Brothers,Medical Publishers Pvt. Limited; 2017.
- [43] Chang DS, Lasley FD, Das IJ, Mendonca MS, Dynlacht JR. Basic Radiotherapy Physics and Biology: Springer International Publishing; 2014.
- [44] Martin JE. Physics for Radiation Protection: Wiley; 2013.
- [45] Srivastava PBB. Nuclear Physics: Rastogi Publications; 2011.
- [46] Podgorsak EB. Radiation Physics for Medical Physicists: Springer International Publishing; 2016.
- [47] Powsner RA, Palmer MR, Powsner ER. Essentials of Nuclear Medicine Physics and Instrumentation: Wiley; 2013.
- [48] AGRAWAL HM. NUCLEAR PHYSICS: PROBLEM-BASED APPROACH INCLUDING MATLAB: PHI Learning Pvt. Ltd.; 2016.
- [49] MacDonald CA. An Introduction to X-Ray Physics, Optics, and Applications: Princeton University Press; 2017.
- [50] Nikjoo H, Uehara S, Emfietzoglou D. Interaction of Radiation with Matter: CRC Press; 2016.
- [51] Jiráček D, Vítek F. Basics of Medical Physics: Charles University, Karolinum Press; 2018.
- [52] Singh H, Sasane A, Lodha R. Textbook of Radiology Physics: Jaypee Brothers,Medical Publishers Pvt. Limited; 2016.
- [53] Reda S. Gamma ray shielding by a new combination of aluminum, iron, copper and lead using MCNP5. Arab Journal of Nuclear Science and Applications. 2016;94(4):211-7.
- [54] HARBISON AMSA. An Introduction to Radiation Protection: Springer US; 2013.
- [55] Maqbool M. An Introduction to Medical Physics: Springer International Publishing; 2017.
- [56] Crouthamel CE, Adams F, Dams R. Applied gamma-ray spectrometry: Elsevier; 2013.
- [57] Akkurt I, Tekin H, Mesbahi A. Calculation of detection efficiency for the gamma detector using MCNPX. Acta Phys Pol A. 2015;128(2-B):332-4.

- [58] Tsoufanidis N, Landsberger S. Measurement and Detection of Radiation: CRC Press, Taylor & Francis Group; 2015.
- [59] Saha GB. Physics and Radiobiology of Nuclear Medicine: Springer New York; 2013.
- [60] Murray R, Holbert KE. Nuclear energy: an introduction to the concepts, systems, and applications of nuclear processes: Elsevier; 2014.
- [61] Nenoï M. Evolution of Ionizing Radiation Research: BoD–Books on Demand; 2015.
- [62] Leroy C, Rancoita P-G. Silicon solid state devices and radiation detection: World Scientific; 2012.
- [63] Lutz G, Klanner R. Solid State Detectors. Particle Physics Reference Library: Springer; 2020. p. 137-200.
- [64] Knoll GF. Radiation detection and measurement: John Wiley & Sons; 2010.
- [65] Gupta T. Radiation, ionization, and detection in nuclear medicine: Springer; 2013.
- [66] Pandey S, Pandey A, Deshmukh M, Shrivastava A. Role of Geiger Muller Counter in Modern Physics. Journal of Pure Applied and Industrial Physics. 2017;7(5):192-6.
- [67] Rehab Ibrahim Hamad Eisa MD, Abd Alla Khair, Suhair S. Makawy ,and Rawia Abd Elgani. Explanation of Intensity Spectral change of Bhutan, Carbon dioxide , Carbon Monoxide, Oxygen, Nitrogen Gases on the basic of Nun Equilibrium. IOSR Journal of Applied Physics (IOSR-JAP).
- [68] Eisa RIH. Interpretation of the Effect of Temperature on the Change of Spectra of Atmospheric Gases on the Basis of Modified Quantum Statistical Equations: Sudan University of Science and Technology; 2015.
- [69] Mohamed ME, Allah MDA, Fadol AAM, Rashed MM, Mahmoud HM, AbdAlgadir LM, et al. Quantum Heat Flow Model for Heat Flow in Some Nanotubes. American Scientific Research Journal for Engineering, Technology, and Sciences (ASRJETS). 2019;62(1):84-90.
- [70] Muhanad Elfadil Mohamed MD, A. Allah, Asim Ahamed Mohamed Fadol, Mohammed Margani, Hasaballa M. A. Mahmoud, Lutfi Mohammed Abd Algadir. Zoaloon Ahamed, Abd Elazeem Mohammed. Thermal Conductivity Coefficient on the Based of Phonon Model and Einstien Energy Relation for Nanomaterials. Global Journal of Engineering Science and Researches. 2019
- [71] Mubarak Dirar Abdallah AAA, Ali Suliman Mohamed, Abdalsakhi Suleman, Sawsan Ahamed Elhourri Ahamed. The effect of Annealing Temperature, Dopping Carbon Nanotubes with TiO₂, CuO, ZnO and MgO On Its Conductivity And Electrical Primitively. Global Journal of Engineering Science and Researches. 2019.
- [72] Azza Abdalwahab Abdallah ASM, Mubarak Dirar Abdallah, Abdalsakhi Suleman, Sawsan Ahamed Elhourri Ahamed. The Effect Of Annealing Temperature Change On Carbon Nanotubes Absorption and Refractive Index When Dopped with TiO₂, CuO, ZnO and MgO IJISSET- International Journal Of Innovative Science, Engineering, and Technology. 2019.
- [73] Yan Z, Guo L, Li Z, Yu Y, He Q. Effects of laser glazing on CMAS corrosion behavior of Y₂O₃ stabilized ZrO₂ thermal barrier coatings. Corrosion Science. 2019;157:450-61.
- [74] Mubarak Dirar Abdallah AADA, Abdelazeem Mohamed Ali, Sawsan Ahamed Elhourri Ahamed. The concept of Force For Thermodynamic Frictional System. Global Journal of Engineering Science and Researches. 2017.
- [75] Mubarak Dirar Abdallah AADA, Abdelazeem Mohamed Ali, Sawsan Ahamed Elhourri Ahamed. The Concept Of Energy For Thermodynamic Frictional System. IJISSET- International Journal Of Innovative Science, Engineering, and Technology. 2017.

- [76] Sivasankaran S, Alsabery A, Hashim I. Internal heat generation effect on transient natural convection in a nanofluid-saturated local thermal non-equilibrium porous inclined cavity. *Physica A: Statistical Mechanics and its Applications*. 2018;509:275-93.
- [77] Mirzayev M, Jabarov S, Asgerov E, Mehdiyeva R, Thabethe TT, Biira S, et al. X-ray diffraction and thermodynamics kinetics of SiB 6 under gamma irradiation dose. *Silicon*. 2019;11(5):2499-504.
- [78] Mirzayev M, Demir E, Mammadov K, Mehdiyeva R, Jabarov S, Tugrul AB, et al. Thermodynamics kinetics of boron carbide under gamma irradiation dose. *International Journal of Modern Physics B*. 2019;33(09):1950073.
- [79] Tunes MA, Greaves G, Kremmer TM, Vishnyakov VM, Edmondson PD, Donnelly SE, et al. Thermodynamics of an austenitic stainless steel (AISI-348) under in situ TEM heavy ion irradiation. *Acta Materialia*. 2019;179:360-71.
- [80] Hamid AMS. Development of Gamma-based Nondestructive Testing System for Thickness Measurement: Sudan University of Science and Technology; 2016.
- [81] Ahmed Mohamed Salih Hamid NAAE, Mubarak Dirar Abd-Alla, Asma M. Elhussien. DEVELOPMENT OF GAMMA-BASED NONDESTRUCTIVE TESTING SYSTEM FOR MATERIAL DISCRIMINATION. *INTERNATIONAL JOURNAL OF ENGINEERING SCIENCES & MANAGEMENT*. 2016.